Evaluation of the concentrating PVT systems MaReCo and Solar8

Erik Pihl
Cecilia Thapper

Handledare: Johan Nilsson

Key words
Solar energy, photovoltaic cell, solar collector, PVT hybrid, solar concentrator, Solar8, MaReCo

Layout: The authors
Cover: Erik Pihl
Cover photos: Erik Pihl and Göran Björkvist

Printed by KFS AB, Lund 2006

R EBD-R—06/13
Evaluation of the concentrating PVT hybrids MaReCo and Solar8
Department of Architecture and Built Environment, Division of Energy and Building Design, Lunds University, Lund

ISSN 1651-8136
ISBN 91-85147-18-4

Lund University, Lunds Institute of Technology
Department of Architecture and Built Environment
Division of Energy and Building Design
Box 118
221 00 LUND

Phone: 046 - 222 73 45
Fax: 046 - 222 47 19
E-mail: ebd@ebd.lth.se
Homepage: www.ebd.lth.se

Abstract

The European solar energy business faces the challenge of developing more cost-effective solar energy systems and one solution could be using concentrating hybrid PVT systems. Two such hybrids, the Swedish systems MaReCo and Solar8, are evaluated in this study.

MaReCo is a fixed concentrating system with a high angle of acceptance. Solar8 is a new system, which is under development. It is inspired by MaReCo, but has a lower angle of acceptance, which means a higher concentration, and is sun tracking. Both systems use water as cooling agent.

The purpose of this report is to evaluate the geometrical shape and simulate the electrical and thermal output of Solar8, in order to suggest improvements to the model. MaReCo has been evaluated in earlier reports, so the main purpose of the measurements in this project has been to get a reference to the results on Solar8, using both established and new measurement devices and techniques. The study is conducted at Lund Institute of Technology (LTH).

The simulated annual electrical output for a Solar8 system located in Lund, Sweden, based on the conducted measurements, is 42 $kWh \cdot m^{-2} \cdot yr^{-1}$ glazed area. For an ideal model using a PV module with 18% COP, the output would increase to 59 $kWh \cdot m^{-2} \cdot yr^{-1}$ glazed area and 813 $kWh \cdot m^{-2} \cdot yr^{-1}$ PV cell area. The simulated thermal output from the system is 330 $kWh \cdot m^{-2} \cdot yr^{-1}$ at 25°C working temperature. If the trough is instead operated at a working temperature of 50°C, the electric output would decrease with approximately 11% and the thermal output with 10%.

For Madrid, the simulated thermal output is 681 $kWh \cdot m^{-2} \cdot yr^{-1}$ glazed area and the electrical output would be 118 $kWh \cdot m^{-2} \cdot yr^{-1}$ glazed area and 1607 $kWh \cdot m^{-2} \cdot yr^{-1}$ cell area respectively, to compare with 257 $kWh \cdot m^{-2} \cdot yr^{-1}$ for a fixed flat module. This means that the PV cells deliver 6.3

times as much electric energy per area unit. For Lund, the equivalent value would be 5.4 times, which is due to the lower ratio of direct radiation in Northern Europe.

The study has shown that there still is much work to be done concerning the geometric design and the reflector surface, in order to increase the output. The components should also be made cheaper and economically more viable, and the producers must prove that they can meet the challenge of creating stabile, reliable systems with low demands of maintenance.

Concentrating PVT-systems show a potential to fill a larger share of the future solar energy market. They offer the possibility of lowering the costs, at the same time as they have less impact on the environment than flat PV-systems. With several European countries giving subsidies to solar energy, the possibility to introduce this new solar technology to the market is presently good.

Index

Nomenclature

A	Area	(m^2)
α	Angle of incidence	(°)
α_{abs}	Absorbed effect	(Wm^{-2})
c	Speed of light	(ms^{-1})
C	Concentration factor	(-)
E	Energy	(J)
E_{kin}	Ability to create kinetic energy	(J)
E_g	Energy band gap	(eV)
η	Efficiency	(-)
$\eta_{optical}$	Optical efficiency	(-)
η_{hybrid}	Hybrid efficiency	(-)
η_{pv}	Efficiency of the PV cell	(-)
FF	Fill factor	(-)
f	Frequency	(s^{-1})
h	Plank's constant	(Js)
h_{hybrid}	Height of trough	(m)
h_{abs}	Height of absorber or cell	(m)
G_d	Direct irradiation	(Wm^{-2})
G_{diff}	Diffuse irradiation	(Wm^{-2})
G_{total}	Total irradiation	(Wm^{-2})
$G_{surface}$	Irradiation on a certain surface	(Wm^{-2})
G_{annual}	Total annual irradiation on a surface	($kWhm^{-2}$)
I_{sc}	Short-circuit current	(A)
I	Current	(A)
I_{mp}	Current at P_{max}	(A)
λ	Wavelength	(m)
λ_l	Latitude	(°)
P	Power	(W)
P_{max}	Maximum power	(W)
Q	Annual electrical output	($kWhm^{-2}$)
QEext	External quantum efficiency	(%)
q	Quality factor of energy	(-)

T	Temperature	(K)
T_a	Temperature ambient	(K)
T_{abs}	Temperature absorber	(K)
τ	Transmission factor	(-)
V	Voltage	(V)
V_{oc}	Open-circuit voltage	(V)
V_{mp}	Voltage at P_{max}	(V)

For all cost estimates, the currency used is Swedish krona (kr).

Acknowledgement

This project has been made during Erik's master's course in environmental engineering at Lund Technical University (LTH) and Cecilia's master's course in physics at Lund University (LU). It has been made at the Division of Energy and Building Design (EBD) at LTH.

We would like to thank everyone who helped us during the course of this project with their time, effort and knowledge. We are especially grateful to our tutor Johan Nilsson and the division's own device inventor Håkan Håkansson, who have made many of the experiments possible. We also thank Arontis AB for offering us this master's project and Professor Björn Karlsson for granting us the possibility of conducting it at EBD. The help and advice from Bengt Perers, Helena Gajbert and Sylvester Hatwambo has been very valuable to us. Finally, the very best to everyone else at the Division of Energy and Building Design for making it a great working environment.

All experiments have been made together. The discussion and results as well as the introduction and abstract were written jointly.

Erik Pihl is the main editor of the chapters regarding the installation and concentration measurements and thermal simulations.

Cecilia Thapper is the main editor of the chapters regarding the theory and I-V measurements and electric simulations.

1 Introduction

1.1 Background

As the effects of climate change are becoming increasingly obvious and the global oil reserves seem to have reached their peak production, a change in the energy system is becoming necessary. Apart from increasing the efficiency in the energy use, developing alternative sources is a must. Renewables can play an important part in this process.

Several of the promising technologies for energy conversion from renewable sources, involves the use of solar radiation. Photovoltaic cells (PV) convert light directly into electricity, while solar collectors produce heat.

Concentrating systems offer a possibility of increasing the electric output from PV cells. The basic idea is that reflector materials are considerably less costly per area than the relatively expensive PV cells. In theory, replacing cell area with reflector materials will enable solar electricity at lower and more competitive costs.

With increased concentration, there will be an increased demand of effective cooling to keep the temperatures moderate and maintain cell efficiency. This can be done using air or water as cooling agent, and as a result, one can gain energy in the form of heat. Systems which give both solar electricity and heat are known as PVT hybrids.

The PV market has for a long time been driven by subsidies and with the high costs involved; this will probably continue to be the case at least for a close future. With the lack of feedstock silicon for the PV industry, countries are now almost competing to give the most

profitable subsidies and make solar energy an important part of their energy systems.

Since 2005, Sweden has had the so-called ROT support, which gives a 70% subsidy for PV installations on public buildings. For solar collectors, the subsidy gives up to 7500 kr for separate houses and maximum 25% of the investment cost for apartment buildings. (Boverket, 2000)

In 2003, renewables accounted for 6.6% of the total energy share in Spain and the target is to get this number up to 12% in 2010. To reach the goal, Spain offers generous subsidies, which include 50% of the total investment cost of solar heat, 263-553 cent euro/WP for PV instalment and tax benefits for people and companies who install in solar energy. (EREC)

In Germany, the pace has been set even higher than in Spain. The country is eager to increase the ratio of renewable energy, which only reached 2.8% in 2003 to 12.5% in 2010. The government offers both subsidies and favourable loans from the government controlled bank to encourage investments in solar energy. Despite still being the smallest electricity source, PV is currently exhibiting the highest growth rate among all. (EREC)

Sweden is keeping a front position in the solar research and development. The Ångström laboratory at Uppsala University is one of the leading research groups in PV thin film technology in the world and Lund University conducts research on concentrating PVT systems.

The concentrating PVT hybrids Solar8 and MaReCo, which are evaluated in this study, have both been developed in Sweden. MaReCo 2002 is a model developed by Vattenfall Utveckling AB and LTH. Solar8 is a project lead by Arontis AB, also in cooperation with LTH and the Solar 20-project.The study is conducted at Lund Institute of Technology (LTH), in cooperation with Arontis AB.

1.2 Objective

The main objective of this thesis is to evaluate and suggest improvements to the Solar8 PVT system, which is currently under

development. Also, a case study has been made to evaluate the technical and economic potentials of two different Solar8 installations.

During a preparatory phase of the project, experiments have been made on MaReCo to get references and gain experience in measurement techniques used for PVT systems.

1.3 Method

This project has been mainly experimental, which means that a lot of time has been spent preparing, conducting and analysing measurements.

The results have been acquired through both practical measurements and simulations. IV-characteristics have been measured for both MaReCo and Solar8. The Solar8 geometry has been studied using photographic ray tracing and laser analysis, and intensity distribution on the receiver has been measured using a rotating photo diode device. Simulations of the thermal and electrical output for Solar8 have been done using the program Winsun/TRNSED.

Literature and report studies as well as interviews have also been done in areas relevant to the project.

1.4 Limitations

The Solar 8 prototype was delivered in November, giving only a short time to conduct measurements. Because of this, the tests had to be conducted under less than ideal conditions and the most important measurements had to be prioritized in the few available sunny days. We therefore focused on evaluating the geometrical shape and making I-V and concentration measurements. Since the Solar8 prototype available only had a length of 1/10 of full trough length, thermal measurements were considered to give too uncertain results and therefore the output has only been simulated.

For MaReCo, I-V measurements were prioritized. Since we had access to a control rig, measurements were done at different temperatures. The

annual output was not simulated for MaReCo, since this has already been done in a previous master's thesis.

2 Theory

2.1 Sustainability in the energy sector

A few principle strategies, which could help making today's energy system more sustainable with less impact on the environment, are (Svenningsson, 2005):

- Decreasing the energy use through increased efficiency and lifestyle changes
- Replacing fossil fuels with renewable energy
- Replacing fossil fuels with nuclear energy
- Continuing the use of fossil fuels, but in extremely clean systems

When focusing on the energy demand rather than staring ourselves blind at one energy source or the other, technical possibilities can be found. For sustainability maybe the most important strategy is to have a diversity of energy sources to avoid a dependence on any specific one. This becomes especially important when using intermittent energy sources like sun and wind or non-renewable energy sources like fossil fuels.

Fossil fuels remain a finite resource and even with a technical fix, alternatives need to be developed, especially in the transport sector, which relies heavily on oil. Nuclear energy adds little to the climate change, which is a clear advantage, but has other environment and safety effects, which needs to be considered, as well as leaves us with the problem of storing the waste. Developing renewable energy sources and making them more accessible by finding ways to cut the costs, remains an important alternative.

At the same time as it is vital to choose energy sources which have minimum impact on the environment, it is also necessary to review how we use energy and make lifestyle changes to decrease the need. There are two main strategies for this. The first is saving energy by using energy efficient appliances in our homes, turn the light off when we are not in the room, and decrease our consumption to mention a few. The second one is to use energy with as low quality factor (see equation 2.1) as possible to meet the demand satisfactorily (Areskoug, 1999)

One way to stabilise and, if possible, to decrease the energy usage is to match the energy type used with the demands of the service or application. Energy can be rated both according to quantity (joule) and quality. The quality, q, of a certain amount of energy is a measure of how much kinetic energy, E_{kin}, that can be derived from it. It is calculated by

$$q = \frac{E_{kin}}{E} \tag{2.1}$$

In the equation, E is the total energy of the amount. Table 2.1 shows how the quality factor differs between different energy sources and energy types.

Table 2.1 Quality factor of different energy types and energy sources (Areskoug, 1999)

Energy source	Quality factor q at 300 K
Mechanical energy	1,00
Electrical energy	1,00
Sun irradiation	0,95
Chemical energy	0,85-0,90
Thermal energy at 285°C	0,46
Thermal energy at 70°C	0,13

For example, heating for buildings only requires energy of a low quality and can easily be done by using passive solar heating and good isolation together with thermal energy from active solar heating or geothermal energy to mention a few. Electric appliances like computers on the other hand require very high quality energy, like electric energy from PV cells. To be able to save electric energy, which is considerable harder

to provide than thermal energy, it is therefore recommended to try to avoid using this for services like heating.

2.2 Solar radiation

2.2.1 Irradiation

The irradiation is the amount of radiation energy that hits a surface per area and time unit. It is usually denoted with G and has the dimension W/m^2. Global irradiation is the total irradiation towards a horizontal surface. The irradiation can be separated into two types; direct irradiation G_d that is irradiated directly from the sun, and diffuse irradiation G_{diff} that consists of reflected or scattered light. The sum of these, the total irradiation, can be measured with a pyranometer.

Outside the atmosphere the annual average irradiation is 1360 W/m^2. Due to the effect of the atmosphere, the average irradiation at the earth's surface on a clear day is 1000 W/m^2 perpendicular to the sunrays. The total annual irradiation in Sweden reaches approximately 1000 kWh/m^2,yr and for the areas close to the equator the equivalent value is 2500 kWh/m^2,yr. (Areskoug, 1999)

The irradiation on a surface is dependent on the angle of incidence. It varies as the cosine of the angle, which means it decreases only marginally for a few degrees deviation from the perpendicular angle to the surface, but a lot at big angles.

$$G_{surface} = G \cdot \cos\alpha \tag{2.2}$$

In the equation, G represents the irradiation on a plane perpendicular to the irradiation and α is the angle of incidence.

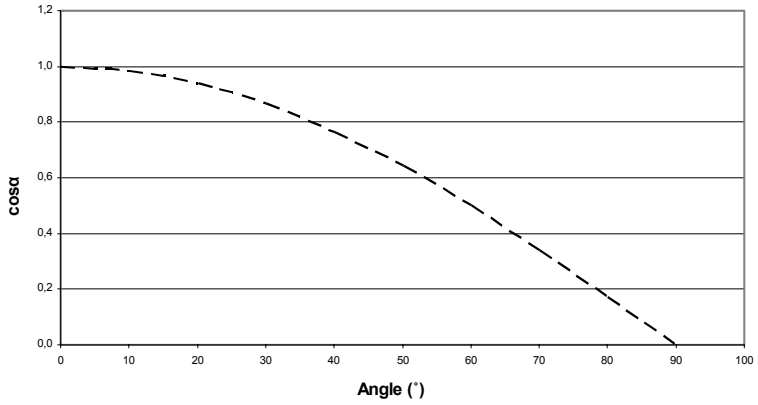

Figure 2.1 Cosine dependency

2.2.2 Solar elevation

At the equator the solar elevation is 90° at noon on the day of vernal equinox and on the northern hemisphere the angle is 90°-λ_1, where λ_1 is the latitude of the location. For Lund, Sweden, that roughly means 34°. At summer solstice it increases to 56° due to the Earth's inclination. In April and August, the highest solar elevation in Southern Sweden reaches around 46° and in October/February it decreases to 23°. In December, it barely reaches over 10°. (Areskoug, 1999)

2.3 The PV cell

2.3.1 Electrical characteristics of silicon PV cells

A simple way of picturing a typical 100-cm^2 silicone PV cell is by comparing it to battery that produces a voltage of around 0,5V and delivers a current proportional to the sunlight intensity. More needs to be known about the PV cell behaviour when connected to different electric loads to be able to understand and use it effectively, though. There are two extreme points, which are the base for the electrical behaviour of a certain PV cell. The first is when the circuit is open and the current is at its minimum and the voltage is at its maximum. This is known as open circuit voltage (V_{oc}). The second is when the resistance is zero and the current reaches its maximum. This is known as short

circuit current (I_{sc}). When the resistance is varied between the two points, the current and the voltage varies according to Ohm law (Boyle, 1996):

$$V = R \cdot I \tag{2.3}$$

If further measurements are done at different temperatures and irradiations, more information on the PV cells electrical behaviour is found. The resistance which is optimal for one irradiation might be far from suitable at another irradiation, which explains why even simple experiments with PV cells can be difficult to carry out with a satisfactory result. The potential decreases linearly with an increased temperature and the current is directly proportional to the irradiation. This explains why the power of the PV cell increases with high irradiation and low cell temperature and why the maximum power occurs on the bend of the IV-curve. The power is calculated by multiplying the voltage with the current:

$$P = V \cdot I \tag{2.4}$$

The result can be studied in an I-V curve, which is characteristic for a certain PV cell. An example of an I-V curve is shown in figure 2.2.

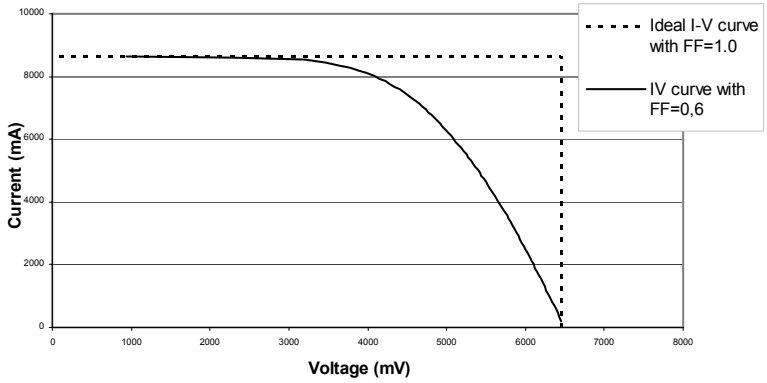

Figure 2.2 Example of I-V curves with different fill factors.

The quality of a PV cell can be defined by the fill factor, *FF* (Wennerberg et al):

$$FF = \frac{V_{mp} I_{mp}}{V_{OC} I_{SC}} \tag{2.5}$$

The better the cell, the sharper the corner of the I-V curve will be. In the same way, a very inclined curve indicates a poor cell. The fill factor decreases with an increased temperature.

A photovoltaic cell is basically a diode. If the material is excited by for instance sun exposure, electrons will start to move across the material. If a load is connected, current will start to flow in the circuit. The diode model for a PV cell can be described by:

$$I = I_L - I_0\left(e^{\frac{qV}{kT}} - 1\right) \tag{2.6}$$

In the equation, I_L is the light induced current and T the absolute temperature in the material. I_o is the dark saturation current through the diode, meaning the current leakage in absence of light. I_o is a measurement of the quality of the material. It decreases with increased quality and increases with the temperature. The diode behaviour can be described further by including a shunt resistance and a series resistance (Wennerberg et al, 1998)

The temperature of the PV cell is decided by a number of factors such as wind velocity, irradiance, outdoor temperature etcetera and it influences both the current and the voltage. An increased temperature helps to increase the current since the energy gap will become smaller and an increased number of electrons will be activated. However, the major impact will be on the voltage, which decreases with an increased temperature. The theoretical values for the temperature dependence of silicon are (Wenham et al):

$$\frac{I}{I_{sc}}\frac{dI_{sc}}{dT} = +0.0006/°C \tag{2.7}$$

$$\frac{dV_{oc}}{dt} = -2mV/°C \tag{2.8}$$

$$\frac{1}{FF}\frac{d(FF)}{dT} = -0.0015/°C \tag{2.9}$$

$$\frac{1}{P_m}\frac{dP_m}{dT} \approx -(0.004 \text{ to } 0.005)/\,^{\circ}C \qquad (2.10)$$

One other factor, which affects the efficiency of the PV cell is its series resistance, since a high resistance causes a drop in the fill factor (Wennerberg et al).

2.3.2 Efficiency of a PV cell

The maximum theoretical conversion efficiency in a single junction silicon PV cell (see chapter 2.3.5) has been calculated to about 30% and the highest efficiency reached in large commercially silicon PV cells is about 21.5%, while multi junction cells, which are well suited for concentrating systems, have reached as high as 32% COP (co efficiency of performance) (Green et al). Reasons for why the large cell is mentioned are that it is closer to what could be produced commercially than many other lab cells. The reasons why commercial cells have a lower efficiency than lab cells include that it is difficult to mass produce PV cells with as high accuracy as specialized labs have and that laboratory cells are usually not glazed or laminated.

The efficiency of a PV cell is also limited by optical and electrical factors. The optical losses are specific and constant in size for a certain PV cell. For the electrical losses, the power losses increase with higher currents and the recombination losses increase with lower currents. (Areskoug, 1999)

Optical losses (Areskoug, 1999):

- Reflection on the surface
- Shadowing from the metal grid
- Limited absorption of radiation due to photons with lower energy than the band gap, or with higher energy that cannot be utilized

Electrical losses (Areskoug, 1999):

- Power losses in the inner resistance in the PV material
- Current losses due to recombination of electrons and holes

To reduce the optical losses in a PV module in its turn, it is for instance possible to use low-iron glass with antireflection coating.

2.3.3 Construction of a solar cell

A crystalline silicon PV cell consists of two layers of dissimilar semiconducting materials, where the thin upper layer has been n-doped and the thicker lower layer has been p-doped, creating a p-n junction. To be able to exert current from the PV cell, a thin layer of metal is placed under the semiconductor and a metal grid placed on top of the cell. Since it is vital that the sunlight can reach the silicon, the metal on top of the cell shall preferably cover a small area, and shadowing of the silicon shall be avoided as much as possible. (Boyle, 1996). This is explained further in the following chapters.

2.3.4 Semiconductors and doping

In essence, the PV cell consists of a semiconductor material, mainly silicon, which can generate electricity by absorbing the energy from light. For the electric current to flow free, energy carriers need to be created and they have to be given enough energy. Both these conditions can be met as the PV cell is exposed to light. A third condition is that the free carriers need to be separated to become available for the external circuit. This is done by an inner potential that is characteristic for the p-n junction in a semiconductor. (Boyle, 1996)

Although other materials are used, the most common semiconductor material used in PV cells is silicon (Si). Solid silicon is produced by sand. After extraction, it is melted and then slowly cooled down. The silicon then forms into diamond structure crystals, which is typical for the elements of the IV group in the periodic table. This means that every atom is surrounded by its four nearest neighbours in a tetrahedral configuration, sharing two electrons with each one creating a stable shell. When all electrons are bonded in this way, silicon is a very poor conductor, since electricity is just a flow of electrons. The intrinsic carrier concentration of Si is 1.5×10^{10} cm^{-3} at 300 K, which is not nearly as much as required to produce enough current for practical semiconductor devices. This can be helped by the method of doping, which increases the concentration of intrinsic carriers in the material. (Ibach et al, 2003)

Doping of a semiconductor means that electrically active impurities are added to the material. These impurities raise the concentration of free electrons or free holes, depending on the characteristics of the impurity,

by donating electrons to the conduction band (*donors*) or by accepting them from the valence band (*acceptors*). To create a donor in a silicon lattice, a silicon atom with its four valence electrons and the configuration $3s^2 3p^2$ is replaced by an element, which atoms have five valence electrons and thus the electron configuration $s^2 p^3$. (Ibach et al, 2003) The method of introducing an impurity with higher number valence electrons is called n-doping. Phosphorus (P) is commonly used for n-doping of silicon, but also arsenic (As) and antimony (Sb) can be used. The doped material possesses a surplus of free electrons.
Similarly, if a valence-three impurity is added to the silicon lattice, an acceptor is created. The element used for this purpose has the configuration sp^3. This type of doping is called p-doping and it creates a deficit of free electrons in the material. The missing electrons are called holes. A common element to use for p-doping of silicon is boron (B), but aluminium (Al), gallium (Ga) and indium (In) are also used. (Boyle, 1996)

2.3.5 p-n junctions

One of the most important building blocks in semiconductor devices is the so-called p-n junction. The p-junction is basically the foundation for the microelectronic industry and the key element in PV cells. To create a p-n junction, silicon is n-doped and p-doped on one respectively.

Both doped semiconductor materials would be electrically uncharged held separately at low temperatures since the atoms added are neutral, but the doped material can conduct electricity better than the pure semiconductor. In the n-doped material, the excess electron can move freely between the atoms in the silicon crystal structure. Similarly, the hole in the p-doped material can be seen as a missing electron in the crystal structure. The hole can be filled by another electron, which leaves a new hole behind and causes a new electron to fill it. In this way, the hole can travel though the material and lead current. The hole is equivalent to a positively charged particle. (Areskoug, 1999)

In the junction between the p-doped and the n-doped layers, electrons will move across to the p-doped side to fill up the holes. This leads to that the area on both sides of the junction will eventually lack both free electrons and empty holes. This creates a barrier between the negatively charged p-doped side and the positively charged n-doped side, called

the depletion region. Equilibrium occurs when the diffusion of electrons is equivalent to the repulsion of electrons from the p-side to the n-side. (Areskoug, 1999)

It is this barrier an electric field is created, which can separate the electrons and the holes produced by the sunlight and which also gives rise to a voltage difference between the two layers. (Boyle, 1996)

2.3.6 Band structure of semiconductors

According to quantum theory, the conducting characteristics of a material are described by its band structure. According to this, each atom has a certain number of defined energy levels in which the electrons will lie. Which of these bands the electrons will lie in is related to the quantity of energy they possess. The electrons that normally keep the atom together lie in the valence band. If the electron acquires energy that is equal to or larger than the defined band gap or energy gap (E_g), it can move to the conduction band and be free to dissociate though the material and conduct electricity. The band gap is measured in electron volts. (Boyle, 1996)

The photons from the sunlight can provide the electrons in a material with enough energy to move up to the conduction band. The photons will have different energy depending on the wavelength of the light and only those with energy at least equal to E_g can excite the electrons to the conduction band. Any excess energy or energy from photons with a lower energy than E_g, will be dissipated as heat to the surroundings. This explains why PV cells cannot be 100% efficient in converting the energy from the solar radiation to electrical energy. (Boyle, 1996)

The energy gap between the valence and the conduction bands is temperature dependent, due to thermal expansion of the lattice parameter and lattice vibrations. The relation is linear for room temperatures and exponential at very low temperatures. (Boyle, 1996)

Table 2.2 The temperature dependence of silicon's energy gap (Ibach et al 2003)

	$E_g(T=0K),[eV]$	$E_g(T=300K),[eV]$
Si	1.17	1.12

2.3.7 Spectra

A PV cell cannot use all incoming photon energy to create electricity. For an electron to be excited past the energy gap, the photon needs to have an energy which equals or exceeds the height of the band gap, which is characteristic for the semiconductor used. For Si, the energy gap E_g = *1,1 eV*. Silicon has a so-called indirect band gap which means that the maximum of the valance band and the minimum of the conduction band lie in different k points in the reciprocal room. Because of this, optical transmissions across the band gap can not take place without excited phonons to keep the momentum. (Materialfysik, 2006). The photon energy is decided by its frequency f and Plank's constant h with $h = 6{,}6 \cdot 10^{-34}$ Js. (Areskoug, 1999)

$$E = h \cdot f \tag{2.11}$$

The frequency of the photon wave behaviour is related to the wavelength by:

$$f = \frac{c}{\lambda} \tag{2.12}$$

This gives

$$\begin{aligned} &\frac{hc}{\lambda} = E = E_g \Rightarrow \\ &\lambda = \frac{hc}{E_g} = \frac{6{,}6 \cdot 10^{-34} \cdot 3{,}0 \cdot 10^{8}}{1{,}1 \cdot 1{,}6 \cdot 10^{-19}} m = 1{,}1 \mu m \end{aligned} \tag{2.13}$$

The energy of the photon is inversely proportional to the wavelength, which means that only photons with a wavelength shorter than 1.1 µm can excite the electrons in silicon-based semiconductor. 1.1 µm, represents infra-red light in the spectrum. The maximum intensity of the solar spectrum is found at a wavelength of 0.5 µm, which still means most electrons have a higher energy than necessary to overcome the band gap. Photons with higher energy than E_g cannot be used fully either, though, as they will give off their excess energy as heat to the surroundings. Photons with energy less than E_g also give off their energy as heat. (Areskoug, 1999)

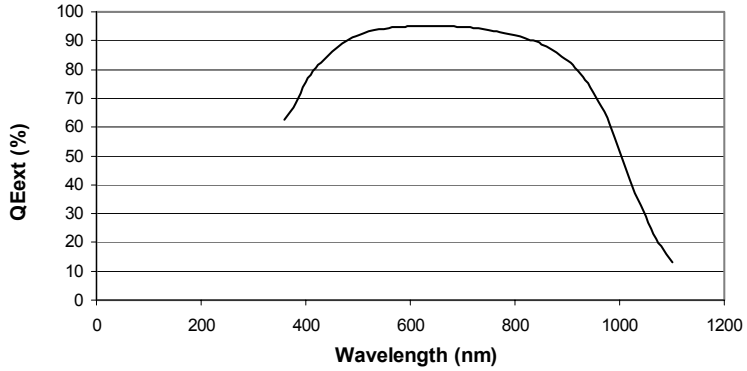

Figure 2.3 The spectral sensitivity of the PV cells used in Solar 8. (NAREC, 2005)

The production data from the manufacturer of the PV cell used in the Solar8 model, illustrates the silicon sensitivity for the spectra in figure 2.3.

2.3.8 Different types of PV cells

There are several types of PV cells available on the market. The most common ones are the crystalline silicon cells, of which the monocrystalline PV cell is also the most effective. This type of silicon cells are very expensive though, since the cost of manufacturing the pure silicon is high due to a labour and energy intensive production process, the so called Czochralski process. Another factor influencing the high cost is that the extremely pure electronic-grade silicon, which was previously used since the silicon to the PV industry mainly came from plants making electronic semiconductors, is of unnecessarily high quality. The possibility of using lower-quality solar-grade silicon has enabled the production of cheaper PV cells without more than a marginal reduction in the efficiency. Other approaches to reduce the cost of PV cells include producing PV cells using polycrystalline silicon and developing amorphous silicon and other thin film alternatives. (Boyle, 1996)

Photovoltaic cells function well at high intensities, but for PV cells used in concentrating systems, an effective cooling is vital, as well as there is a risk of resistive losses. Special high performance modules with high voltage and low series resistance are well suited for demanding

concentrating systems. Multi junction cells, which can reach higher efficiencies than single junction cells are also a good alternative to use in concentrating systems.

The resistive losses in the cells are due to the high intensities in the concentrator and they are proportional to the square of the module current. Ways to solve this problem is done by making smaller cells and modules, to decrease the current and to have more top metal grids on the cell to improve the electrical conductivity. The cells used in Solar8 are an example of this (Wennerberg et al, 1998).

2.4 Solar thermal energy

2.4.1 Construction of a solar collector

A solar collector, which converts energy from sunlight into heat in air or water, is an essential part of all active solar heating. They are often mounted on the roof of a building and produce low temperature heat to be used for domestic purposes or swimming pools. (Boyle, 1996)

The construction of a solar water heater is very basic, with a solar panel and water channels, which run from the panels to a storage tank. The solar panel consists of a black absorber plate, which absorbs heat from the sunlight and heat up the water pipes and the fluid in them. The water circuit is often made a completely closed system to allow the possibility of adding non-freezing agents like glycol during the cold part of the year without risking polluting the water.

A pump is used to circulate the water. A higher flow rate, gives a lower temperature on the water, but small heat losses. This can be suitable choice for heating the water to an outdoor swimming pool. A lower flow rate, which gives higher water temperatures, but more heat losses on the other hand, is more suitable for domestic purposes and systems that involve heat tanks. For stored water, it's important to heat it above 55°C to avoid *Legionella* infection. (Boyle, 1996/Areskoug, 2003)

Using concentrators is a possibility of increasing the heating capacity in a solar water heater, by increasing the intensity of the irradiation.

2.4.2 Efficiency of a solar collector

The efficiency of a solar collector as a function of the temperature difference between the absorber and the surroundings is defined as (Areskoug, 1999):

$$\eta = \tau \cdot \alpha - \frac{U}{G_{surface}} \cdot \left(T_{abs} - T_{amb}\right) \tag{2.14}$$

The equation shows that the efficiency decreases with an increased working temperature, which is due to increased heat losses. The transmission through the glass, τ, is directly proportional to the efficiency, as is the absorbed powe α. The U-value defines the collector's heat losses per square meter and Kelvin and is the sum of the losses through the front glass and the back isolation. $G_{surface}$ is the perpendicular irradiation to the glass. The glazing of the solar panel is an important factor since it both influences the transmission and the *U*-value. (Areskoug, 1999)

2.4.3 Absorption and selective surfaces

When radiation hits matter, it will be reflected, absorbed or transmitted. According to the energy principle, the sum of these three will always be one. For non-transparent material like the absorber on the solar panel, the transmittance is zero and thus the reflection and the absorption will equal 1. Different materials have different properties, which define how well they absorb and reflect light and other types of radiation. Due to the material atomic structure and the height of the energy bands, it will absorb radiation of the same wavelengths as it will emit radiation. This is defined in Kirchoff's heat law and means that materials with a high inclination to absorb radiation also have a high inclination of emitting heat. A black surface, with high absorption will also have a high emittance. For a solar collector, this is not a good characteristic, since it means much of the heat will be lost.

According to the Wien Displacement Law, which says that the temperature of a surface is inversely proportional to the maximum wavelength it emits, the maximum in the energy distribution of the radiation from a body at 350K is almost 20 times higher than from the sun with a surface temperature of 6000K. This, combined with the fact

that almost 95% of the radiation energy is found in the span $0{,}5\lambda_{max}<\lambda<5\lambda_{max}$, means that the spectra for incoming and outgoing radiation are almost entirely separated. Using this, it is possible to construct a selective surface. It absorbs in the wavelengths of visible light, but emit poorly in the wavelengths of infrared light (Areskoug, 2003).

In principle this means that it could be possible to construct a selective surface that absorbs 100% of the incoming radiation and emits close to 0% of the radiation at the same temperature. This type of material does not exist in reality, but metal oxides and some other metal compounds have suitable properties for an absorber. In solar collectors, black chrome, which consists of chrome and nickel oxides, is widely used. (Areskoug, 1999)

2.5 PVT hybrids/concentrators

PVT hybrids refer to solar energy systems that give both heat and electricity. The most common PVT hybrids are flat systems where the PV cells function both as electric receivers and thermal absorbers, and water channels behind the receiver help cooling down the PV cells by heating up water. Since the PV cells are sensitive to overheating and give a higher output at low working temperatures, a hybrid construction where PV and cooling is combined can improve the electric output.

Using concentrators to increase the electric output from a PV cell array can have big economic advantages in terms of lowering the cost of PV electricity. This can be done using lenses and reflecting mirrors. By decreasing the required cell area for production of electricity environmental gains can also be made, since PV production is very energy demanding and is responsible for different kinds of pollution, including heavy metals and radioactive radon gas. An ecological Life Cycle Assessment (LCA) has been conducted for the MaReCo in connection with this thesis (Appendix B). The results show that concentrating systems can produce electricity at the same, or in some aspects even less environmental impact than flat PV systems. Since the concentrating systems also deliver heat, environmental impact per unit energy delivered should be less than for regular PV-systems.

Concentrating the light on the cells means a possibility of increasing the electric output, but it also means an obvious risk for high temperatures. For a concentrating collector, it is therefore of great importance that the cooling is very effective. For MaReCo and Solar8, water has been considered the most suitable cooling medium.

The acceptance angle of a concentrator defines the angle in which the irradiation will reach the receiver and the concentrating factor describes how much the incoming light on the receiver is multiplied in the concentrator compared to a flat module. The intensity can be distributed over the whole surface or appear as a band on the array.

The concentration factor of a concentrating PVT system is calculated by the equation:

$$C = \frac{h_{hybrid}}{h_{abs}} \tag{2.15}$$

h_{hybrid} represents the height of the glass and h_{abs} the height of the absorber or PV cell. If the absorber has cells on both sides, the height of the absorber is multiplied by 2. A large concentrating factor is a result of a low acceptance angle in the concentrator and for systems with a high acceptance angle; the concentration factor will be lower. The maximum possible concentration for a system can be calculated from (Nilsson, 2005):

$$C = \frac{1}{\sin\theta} \tag{2.16}$$

where θ is half the acceptance angle. This means that high concentrating systems are often suitable to be solar tracking, while low concentrating systems benefit from a high acceptance angle and can be made fixed. Since it is mainly direct irradiation that will be reflected in the concentrator, concentrating systems are benefited by being used in locations with a high percentage of direct irradiation compared to diffuse irradiation.

The optical efficiency of the concentrator can be calculated with the equation;

$$\eta_{optical} = \frac{I_{SC,concentrator}}{C \cdot I_{SC,flat}} \tag{2.17}$$

where C is the concentrating factor and I_{SC} represents the short circuit current for the panel with and without concentrator.

The electrical efficiency of the hybrid model and the PV cell in the concentrator is;

$$\eta_{PV} = \frac{P_{mp}}{G_{surface} \cdot A_{PV}} \tag{2.18}$$

$$\eta_{glass} = \frac{P_{mp}}{G_{surface} \cdot A_{glass}} \tag{2.19}$$

$G_{surface}$ is the irradiation perpendicular to the surface of the glass.

The research on concentrating PVT hybrids done at Lund University in Sweden focuses on asymmetric parabolic shaped reflector troughs with a combined receiver/absorber in the trough. They are built as fixed systems with a high angle of acceptance.

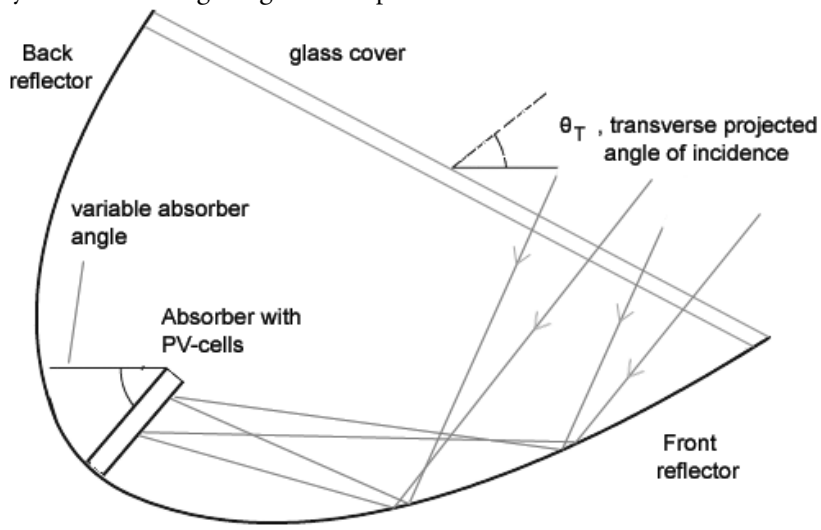

Figure 2.4 *The MaReCo fixed concentrating parabola. Ray tracing shows how incoming light at different angles of incidence reflects and hits the absorber.*

2.6 Solar tracking systems

PV modules and solar collectors are usually mounted in fixed arrays facing south in the Northern hemisphere. The angle the system is tilted from the horizontal plane is depending on the location of the park. A fixed system is stable and requires little maintenance if the right materials are chosen, which makes it suitable for many applications. Seasonal tilting to adjust to the solar elevation is a cheap and easy way of increasing the electric and thermal output from a fixed system.

Using a tracking system gives a possibility to increase the electric output and use the PV cells to a maximum. This is both because more sunlight will hit the receiver and because a higher percentage of the direct sunlight will hit the glass at a low angle of incidence, which means less transmission losses. For a flat panel, one axis tracking can increase the electric output with up to 20% compared to a fixed system and two axis tracking can give an increase of up to 40% (Wenham et al) in southern locations.

For concentrating systems, it is difficult to compare how much the output increases with solar tracking, since it is built to be either tracking or fixed from the beginning and has an angle of acceptance according to that.

At the same time as a tracking system is a possibility of increasing the electric output from the PV system, the construction and the maintenance of a tracking unit is more than that of a fixed system. Therefore, this needs to be carefully considered when building the model. While the PV cells are long-life, have low maintenance and can easily stand undamaged for 20 years, there are more factors, which can fail in a tracking system.

3 Equipment

MaReCo and Solar8 are built using the same principle components: A high-reflection parabolic reflector that concentrates light on a receiver, on which solar cells are mounted. The cells are water-cooled by a copper pipe (MaReCo) or an aluminium profile (Solar8) which runs between the panels, in which water flows. While cooling the cell the water is heated, hence the system also operates as a solar heater. In both systems, the front of the concentrator is covered by a low-iron, non-reflective glazing, offering both protection from the weather and minimizing heat losses.

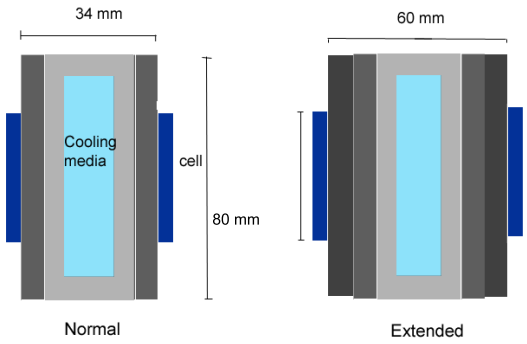

Figure 3.1 *Cross section picture of the Solar8 absorber with the two experimental designs. There are PV cells on each side of the absorber.*

MaReCo 2002 is a model developed by Vattenfall Utveckling AB and LTH. Solar8 is a project lead by Arontis, also in cooperation with LTH.

3.1 MaReCo 2002:1 - Fixed PVT system

MaReCo 2002:1 (MaReCo) is a fixed system with a high angle of acceptance, which allows it to produce electricity during a big part of the year. The glass front is tilted with a 30° angle and the power peaks at 0°, which represents a solar height of 60°.

The concept of MaReCo is to use low-cost, commercially available PV cells to keep the production costs low. Three models of MaReCo were evaluated in Alexander Fahlström's master thesis (Fahlström, 2002). MaReCo 2002:1 is one of these three models. According to his results, MaReCo has a maximum electric output of 55 kWh/m^2,yr and a thermal output of 300 kWh/m^2,yr, both at 25°C.

The MaReCo trough used for the experiments measures 1.96x0.65 m^2. The PV module consists of 12 square shaped PV cells connected in series, each being 12.5x12.5 cm^2 and is facing the front reflector. The concentration factor of MaReCo, meaning the ratio between the glass surface and the height of the absorber, is 3.53 times. The glass used on the MaReCo trough during the measurements had a transmission of 85% at normal incidence.

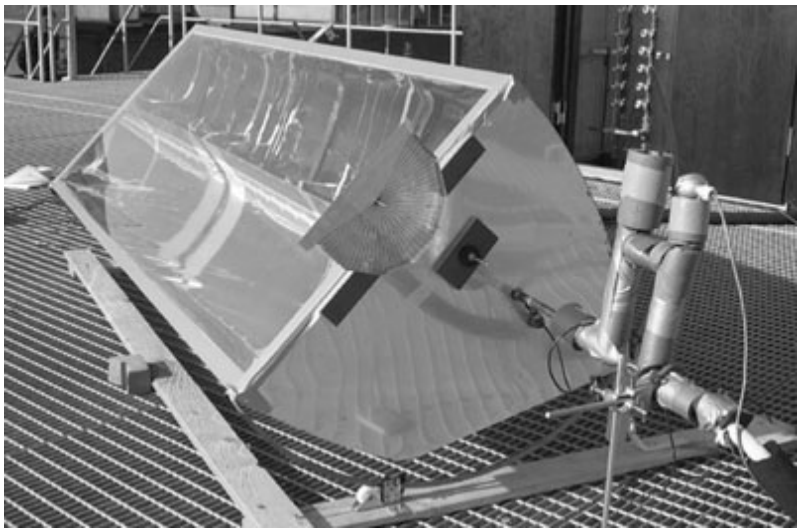

Figure 3.2 MaReCo 2002:1 on the EBD laboratory solar roof

3.2 Solar8 – 1 axis tracking PVT system

Solar8 is a new system, which is under development. It is inspired by MaReCo, but has a higher level of concentration and is sun tracking. The system consists of two separate parabolic reflectors and an absorber in the middle, which has one PV panel on both sides. The geometrical concentration of Solar8 is 10. The low-iron, low-reflective glass used on the trough will have a transmission of 97%. The measurements of the experimental trough are 0.5x0.92 m^2 and the cells are 4.6x11.6 cm^2. The panel used has 4 cells on each side and the absorber is 3.4 cm thick. The absorber can be extended by 1.3 cm on each side, which means it will be 6.0 cm thick.

Figure 3.3 The Solar8 trough used in the experiments

The Solar8 is built to be a one axis tracking system, with the axis in a east-western orientation and with the trough facing south. The suntracking will follow the suns vertical movement, the solar elevation. It will be controlled by a climate file, which allows the trough to always be at the ultimate angle of incidence towards the sun. It has a retractable arm that tilts the collector to follow the suns vertical movement. A motor is used to control the arms movement according to the climate file.

3.3 Other equipment

Pyranometer 1:
Hukseflux Thermal Sensors
Type: LP02
Serial No: 40093
Sensitivity: 15.88 µV/Wm^{-2}

Pyranometer 2:
Kipp & Zonen
Type: CM5
Serial No: 752510
Sensitivity: 10.77 µV/Wm^{-2}
(calibrated July 4th 05)

Figure 3.4 Pyranometer 1, Hukseflux

Photo diode multiplexer/PhMux
In essence, the photo diode multiplexer consists of a CMOS analogue multiplexer from Maxim and an array of 32 photo diodes. It is used to measure the intensity of the concentrated light on the PV cells. Each photo diode measures 3 x 3 mm^2. The inner electric resistance in the multiplexer is 100 Ω. Each diode is reversely biased by 5 V.

Due to electrical loads, in addition with high temperatures on the receiver and from solar radiation, the resistance in the multiplexer became too high, which caused the PhMux to cut the high values of the intensity. For this reason, PhMux was rebuilt by adding a 1 Ω resistance over each photo diode and replacing the thin wires with a braided copper wire.

PhMux is built by Håkan Håkansson at the Division of Energy and Building Design, Lund Institute of Technology.

Rotating photo diode device
The RPDD consists of a 3 x 3 mm^2 photo diode, which is covered by an aluminium frame with a circular opening measuring 1 mm in diameter. The photo diode and the frame are mounted on a rotating arm connected to a motor and a potentiometer. The arm can be rotated, manually or by using the motor, to move the position of the photo diode in a vertical bow across the PV cell. The potentiometer

determines the angle and using this, the logger calculates the perpendicular distance of the photo diode from the centre of the receiver.

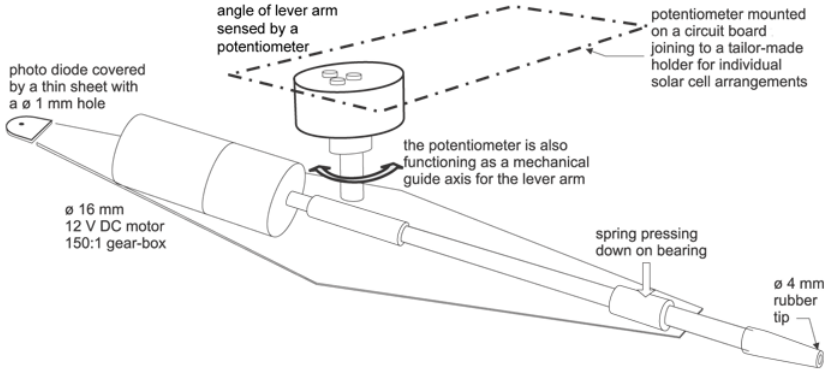

Figure 3.5 Schematic drawing of the RPDD. (Picture by Håkan Håkansson)

The rotating photo diode device is built by Håkan Håkansson at the Division of Energy and Building Design, Lund Institute of Technology.

Logger 1
Campbell Science
Model: CR10
Logger 2
Campbell Science
Model: CR10
Logger 3
Campbell Science
Model: CR1000

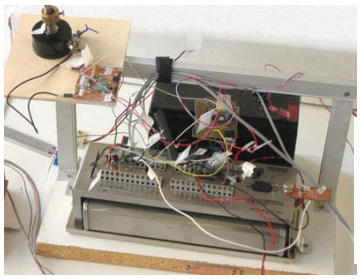

Figure 3.6 Logger 1, rigged for measurement of concentration

Logger 1 and 2 were used for concentration, thermal and dark I-V measurements. Logger 3 was used for temperature measurements on the PV cell surface, the aluminium profile and the copper pipe.

IV measurements

IV measurer 1: is built by Vattenfall Utveckling AB, Älvkarleby and programmed by Stefan Larsson.

IV measurer 2: is built by Håkan Håkansson at the Division of Energy and Building Design, Lund Institute of Technology.

Thermometer: Technoterm
Type: Pt100
Model: 7300

Thermo couples

The thermo couples, which were used for measuring the temperatures of the cell surface, the aluminium profile and the copper pipe on MaReCo were made by Håkan Håkansson at the Division of Energy and Building Design, Lund Institute of Technology.

4 Measurements and results

The cross-section picture of Solar 8 in figure 4.A explains how negative and positive angles of incidence and upper and lower parabola are defined in the measurements.

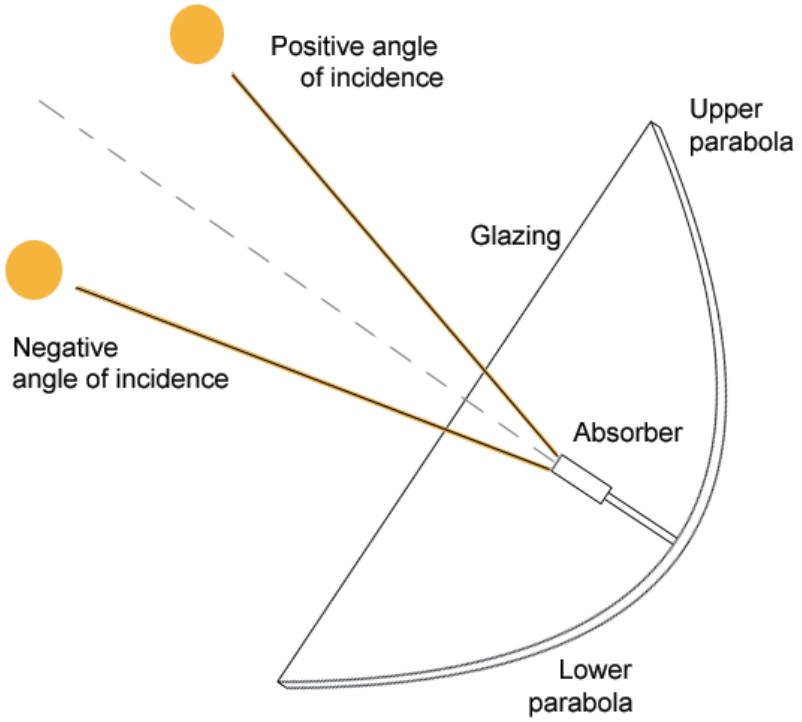

Figure 4.A *Cross-section of Solar8, showing definitions used in the measurements.*

4.1 I-V characteristics

4.1.1 Steady-state IV-curves - MaReCo

The IV-measurements done on MaReCo includes measurements at several different temperatures and angles of incidence. The angle was changed by rotating the trough and fixing it at given angles. Before collecting data for the I-V curves, though, the trough was left standing for a few minutes, to let the temperature, voltage and current reach a "steady state". In order to evaluate our measurements and determine what would be a sufficient adjustment time after changing the angle of incidence, a series of rapid measurements of the IV-characteristics were performed at three different changes of angles.

The test was conducted as following: The trough was fixed at a certain angle and left for approximately 15 minutes, in order to reach steady values. One reference measurement was done, before rapidly changing the angle 20 degrees up or down. At the new angle, a first I-V measurement was conducted within a few seconds, followed by measurements every 30 seconds, up to 6-7 minutes after start. The reason why we chose a 20 degree difference is because the reflection pattern and position on the module changes a lot in those degrees which means a big difference in the intensity.

The results were analysed graphically by plotting the IV-curves from each time series in the same graph, and evaluating at what time the IV-curves could be said to be stable. The results would show if sufficient adjustment time was used, and if the normal measurement procedure would provide representative results.

4.1.2 Result from steady state I-V curves - MaReCo

As the graph in figure 4.1 clearly shows, the IV characteristics adjust almost instantly after rotating the trough to the new angle of incidence. The rotation from -20 to 0 degrees angle of incidence means an increased intensity on the cells and higher power, which can be seen in the graph. Although the major change happens within the first few seconds after changing the angle, small adjustments take place within the next few minutes. Following the increased intensity and therefore increased temperature on the panel, the I-V characteristics show a small

increase in the current and a small decrease in the voltage during the first minutes.

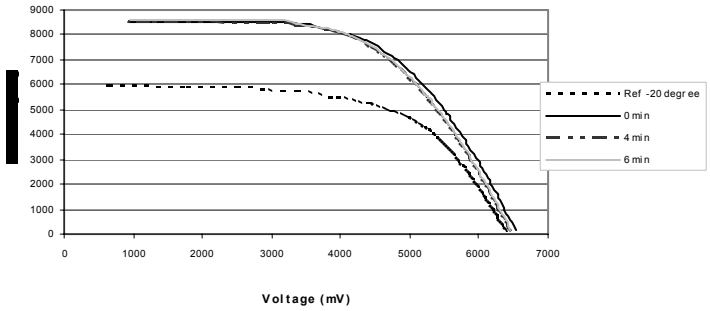

Figure 4.1 *The time it takes to reach a semi-steady state for the I-V measurement after rotating the trough from -20 degree to 0 degree angle of incidence at 1000 W/m^2 total irradiance.*

The result after 4 min and 6 min are almost overlapping in the graph. The conclusion of this, is that there is an instant reaction to the change in light intensity, but the gradual temperature change which occurs within the following minutes will also cause the I-V characteristics to adjust slightly. Waiting six minutes between each measurement at a new angle in the following experiments seems to be sufficient according to the result.

4.1.3 Measurement of IV-characteristics - MaReCo

I-V data was also collected for MaReCo to determine the hybrid's I-V characteristics due to the angle of incidence and the temperature, respectively.

To study the trough's dependence on the angle of incidence - and the solar elevation since MaReCo is a fixed system – I-V measurements were done at different angles of incidence ranging from -55° to 15°. This represents 5° to 75° solar elevation. The result was studied as a graph over the corresponding I-V curves for each angle as well as graph showing how the maximum power and the fill factor changes as a function of the angle of incidence.

For the temperature dependence measurements, the IV-characteristics were measured at three different angles and at three different operating temperatures. The temperature of the water in the system was fixed at

25°C, 42.5°C and 60°C to simulate different cases and the temperature of the cells was measured by a thermal sensor and logged simultaneously. To ensure that all the water in the system had reached the right temperature, the temperature was set one hour before starting each series. IV data was then collected at three different angles, 0°, -20° and -40° angle of incidence on the glass. According to the steady state measurement, the trough was allowed to adjust for minimum six minutes at each angle to stabilize.

It is important to note that the temperature chosen for the inlet water as it left the heater does not necessarily correspond to the temperature which passing through the trough. Because of this, two Pt100 sensors, were logging the temperature of the water before entering and when it left the trough. The temperature of the cell surface, pipes and aluminium profile was also logged. The temperature referred to in the results, represents the average temperature of the water passing through the trough.

4.1.4 Results of measurement of IV characteristics – MaReCo

As figure 4.2 clearly shows, the open-circuit voltage of the PV module is highly dependent on the surface temperature. The voltage falls linearly with an increased temperature and it is also possible to detect a small increase in the current with a higher surface temperature. The stagnation in the voltage due to increased temperature is 1.8 mV/°C per cell, which is close to the theoretical value.

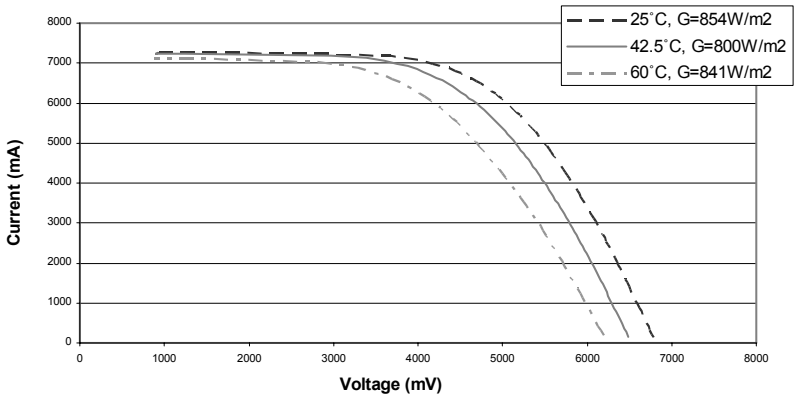

Figure 4.2 *The I-V characteristics dependence on cell temperature on MaReCo at 1000 W/m^2 total irradiance*

There are small deviations in the current, which can be a result of different ratios between the direct and diffuse irradiation at the time of the three measurements as well as an uneven temperature across the cell surface. The measurements took several hours, since the water temperature had to be changed, and by the last measurement on 60°C, the clear blue sky from the morning had turned somewhat hazy.

Figure 4.3-5 shows how the I-V characteristics, the fill factor and the maximum power of MaReCo vary with the angle of incidence.

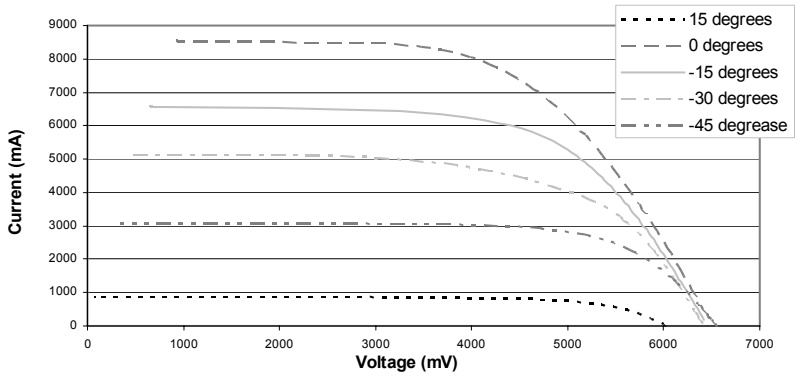

Figure 4.3 *I-V characteristics dependence on angle of incidence on MaReCo at 1000 W/m^2 total irradiance*

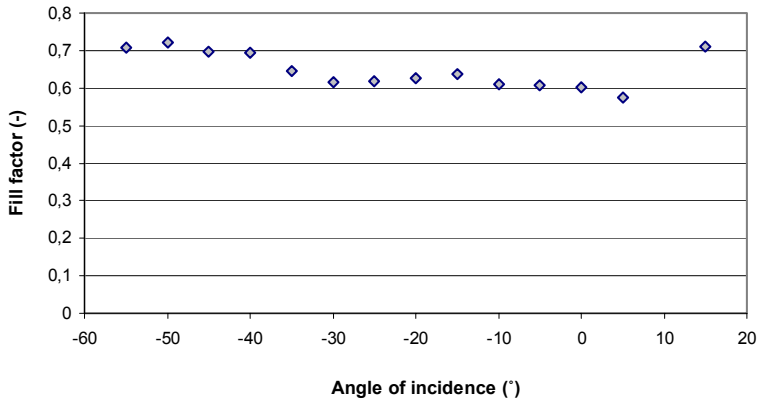

Figure 4.4 *The fill factor for MaReCo at different angles of incidence with water temperature 42.5°C*

The measured fill factor for MaReCo varies a bit in the graph. The fill factor increases with a low current, which explains the shape of the

graph, with the lower fill factors within the acceptance angles. The average value of the fill factor for MaReCo for the work angles can be said to be about 0.62 in the measurements, which is slightly less than previous measurements done on MaReCo. This can because that the earlier measurements have been done at lower temperatures and because there has been a natural stagnation in the cells.

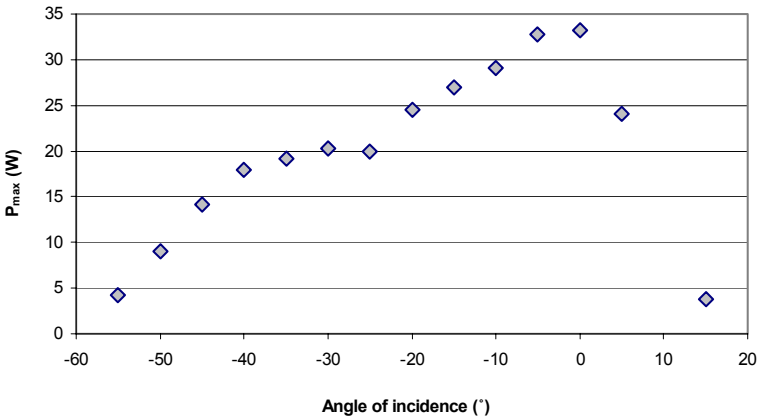

Figure 4.5 *P_{max} dependence of the angle of incidence on MaReCo with water temperature 42.5°C at 1000 W/m2 total irradiance.*

From the graph of P_{max} as a function of the angle of incidence on MaReCo it can clearly be seen that the power peaks at a solar elevation of 60°, which represents a 0° angle of incidence on the trough. The angle of acceptance is high, reaching as much as 45°. This makes MaReCo suitable as a fixed concentrator system. The exact angle of the trough can be adjusted dependent on location to optimize the output.

4.1.5 Measurement of IV-characteristics – Solar 8

The Solar 8 trough used was delivered without any PV module; therefore, a panel had to be constructed by Håkan Håkansson at the research division using PV cells from NAREC. The PV cells used were lab cells and the panel was constructed without glass or laminate. Two modules were made to have one in reserve, but the one used in the measurements presented in this project has four cells. The hybrid was not glazed during the measurements, which needs to be compensated for later in the calculations.

The I-V characteristics were measured for one reflector at a time, which means that only one side of the absorber, was covered with PV cells. Measurements were done both with the standard absorber (34 mm thick) and with a thicker absorber (60 mm thick), to be able to evaluate the construction further. This is described in chapter 4.3.

The absorber was filled with water to cool the system, but there was no flow. The measurements were conducted outdoors in November and with the low outdoor temperatures, the absorber construction itself was able to keep the cell temperature stable at a relatively low temperature. The cell temperature was measured with a Pt100 thermometer.

The trough was rotated to different angles of incidence and the IV-characteristics were measured at each angle. The results are presented as IV-curves and a graph, which describes how the maximum power changes for the different angles.

4.1.6 Results of measurement of I-V characteristics – Solar8

Figure 4.6-8 shows the results from the I-V measurements of Solar8. As can be seen from the graphs, Solar 8 has an angle of acceptance of approximately 10°, even though the relatively high outputs are within a 6° span. This clearly shows that the model is suited for solar tracking, which is also the purpose. A small acceptance angle enables a higher concentration and therefore helps to justify the investment cost of high efficiency PV cells.

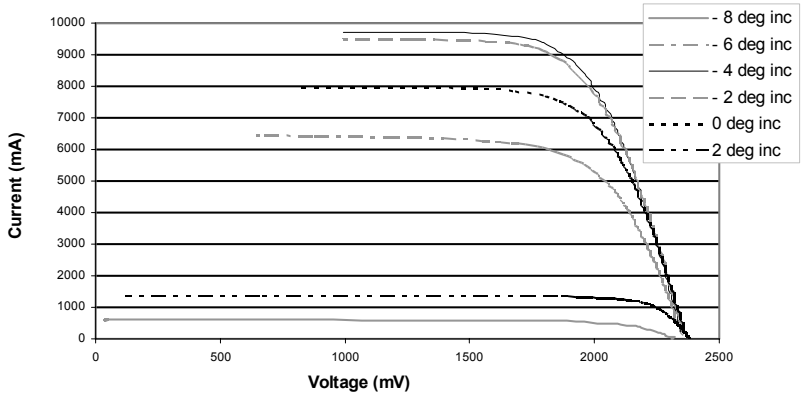

Figure 4.6 I-V characteristics dependence on angle of incidence on Solar8 at 1000 W/m2 total irradiance

The fill factor for Solar8 is shown in figure 4.7. As can be seen, it is relatively stable within the angle of acceptance with a *FF* of about 0.74, with peak values reaching as high as 0.82 at angles with low current. This is quite a lot better than MaReCo, which has an average working fill factor of about 0.62 and is because the cell quality differs.

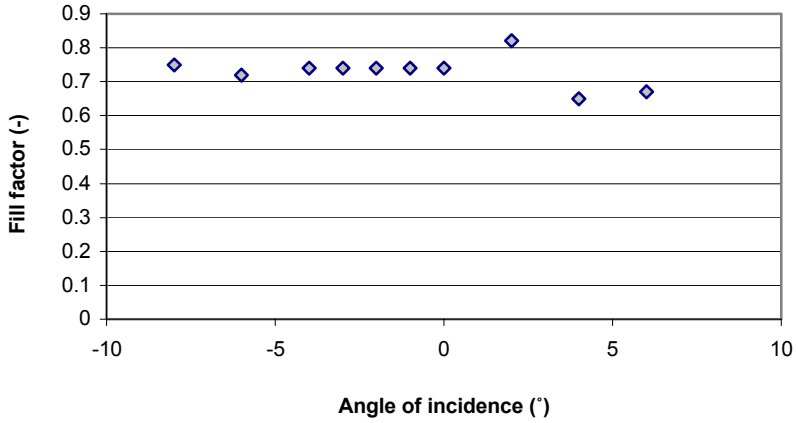

Figure 4.7 The fill factor for Solar8 at different angles of incidence

The high values in the graph, especially at 2° could be a result of that the I-V series is too short, i.e. that the values used in the calculations are not really the open-circuit voltage and the short-circuit current for the specific angle of incidence (see equation 2.5).

As can be seen in figure 4.8 Solar 8 has the highest P_{max} at -4 degrees angle of incidence according to the measurements. The maximum power at 0° is 17% lower than P_{max} at -4°, which is rather much. This means that if the the trough is programmed to follow the sun with a zero angle of incidence relative to the glass surface, the maximum power produced from one of the modules can be as much as 17 % lower than if it would have its peak power at this angle. Taking both panels into account, the net result shown from these measurements indicates that P_{max} would reach 28.12 W at zero degrees (since both reflectors give the same power), which is equivalent to a 4.34 times multiplication of the power when the cells are directed perpendicularly to the incoming sunlight without using any concentrators. If the trough would instead be programmed to maintain a 4°/-4° angle of incidence, P_{max} will reach only 17.54 W though, since the output for 4° is so small. This is equivalent to a concentration factor of 2.71 for the power, which is very low seen to the system and the PV cells used.

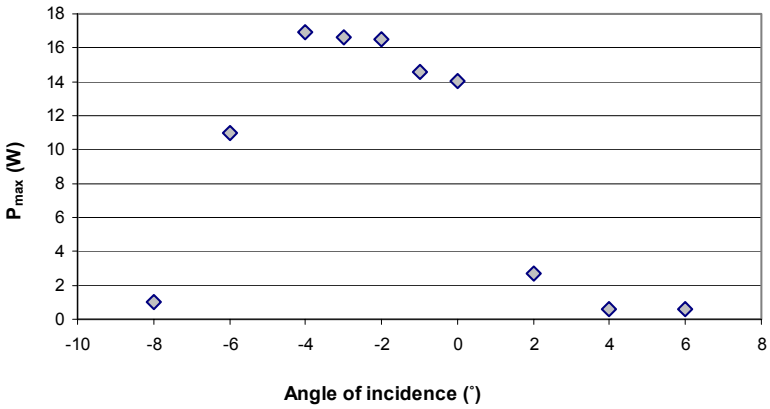

Figure 4.8 *P_{max} dependence of the angle of incidence on Solar 8 at 25°C surface temperature and a total irradiance of 1000 W/m2.*

There are a number of factors, which could have influenced the result of the measurement. It was expected that the power would peak at 0° angle of incidence, since the trough has been designed to be a solar tracking unit. This could have two different explanations. First of all, the angle was measured manually with a hand-made graduated arc and it is possible that there is a small deviation between the registered angle and the actual angle of incidence towards the sun. This could be valid for an error of up to 2%. Furthermore, the shape of the trough used for the experiments is not exactly symmetrical. This is mainly because that the wood support, which holds the reflector, has deformed the parabola slightly and makes one side a bit higher than the other. The angle was consistently measured on the left-hand side of the trough seen from the front, but the difference in angle of incidence between the right hand side and the left hand side due to the effect of the stand, was approximately 1°. Added together, this could explain a deviation in the angle of incidence representing the different P_{max}.

Construction flaws in the reflector, discussed further in chapter 4.3, can explain the relatively low electrical output from the hybrid further. Another reason is that the PV module has a low efficiency compared to what the efficiency of the PV cells used. This is because the PV cells were delivered separately and the module was hand-made on site at the division to be able to carry out the measurements. For commercial production, this problem has to be eliminated when the modules are laminated.

4.1.7 Dark I-V/One-diode behaviour of the PV cell – Solar8

The PV cells diode behaviour can be studied further through a Dark-IV measurement. The measurements carried out during this experiment were done at different temperatures and shows how the cells are affected by the temperature difference. According to the Ideal Diode Law, current changes with the voltage and temperature. By studying the results from the diode I-V curves taken at different temperatures, we can confirm that our measurements give a reasonable result on the voltage stagnation due to temperature influence.

When performing the measurements, it is important that the system is kept stable. The load is varied manually by using metal wires with known resistances. The logger waits 1/100 s before the measurement is taken to ensure stability. Because of the high currents in the circuit, two field effect transistors are used to avoid the system from being overheated. This way, cooling does not become a problem but is solved automatically. An external battery is connected across the circuit to function as a control unit for the output value of the potential.

The temperature of the water passing through the trough was registered by the logger and the temperature of the PV cell surface was measured using a Pt100 thermometer.

4.1.8 Results of the dark I-V measurements – Solar8

From the results of the dark I-V measurements, it can be seen that there is an apparent fall in the potential as the temperature of the cells increase, which is expected.

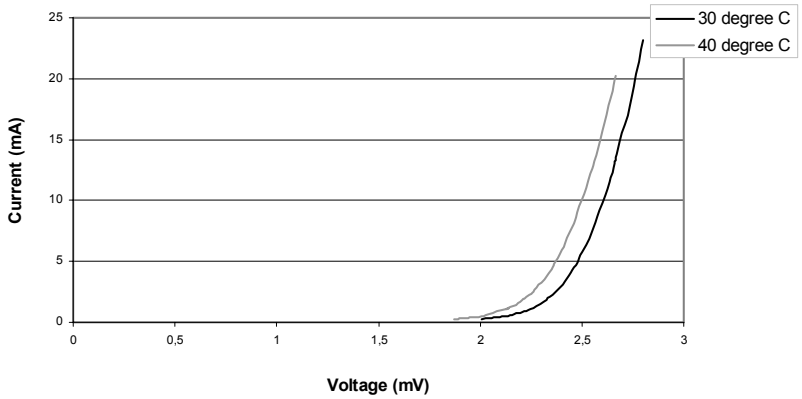

Figure 4.9 *Dark I-V characteristics of the PV cell depending on the surface temperature.*

Taken the data from the measurement and calculating how much the potential drops per °C, we get -3,5mV/°C, which is considerably higher than the -2mV/°C, which is the theoretically excepted value. This can partly be due to errors in the temperature measurement, since it was difficult to place the thermometer in exact line with the surface. This might have let some air in between, which would give lower temperature. Furthermore, the temperature might not have been stable throughout the cell material, especially at the high water temperatures where there were more heat losses to the surroundings. To get a better value, more measurements should have been done to rule out any mistake in the experiment itself, but there was not sufficient time within this project.

4.2 Concentration/intensity measurements

The trough consists of a parabolic shaped reflector material which concentrates the irradiation from the sun to the photovoltaic cells. Depending on the construction, in some angles of incidence, the cells will also be hit by direct sunlight. Apart from this, diffuse irradiation adds to the total irradiation on the cells. Examining how the concentration varies dependent on angle of incidence provides information regarding the shape of the reflector and placement of the absorber. For a concentrating hybrid system this is vital information to be able to approximate the efficiency of the system.

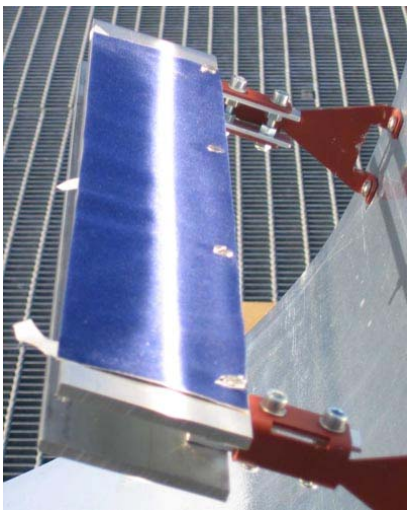

Figure 4.10 An absorber with velvet covering, showing an example of intensity distribution.

The aim of this experimental study was to determine the level of concentration on the absorber. The results show how well spread the concentrated light is on the absorber, which is vital information, as high concentration levels decrease efficiency. From the results, it is also possible to calculate the optical efficiency, $\eta_{optical}$, which is a key figure in evaluating reflector geometry. Figure 4.10 shows how much of the incoming sunlight that reflects and hits the absorber.

4.2.1 Measurements

Initial measurements were conducted using the multiplexer array (PhMux). As a reference, the same measurements were done with the photo diode device (RPDD). These different measurements were compared, and the result can be seen in figure 4.11. The results show

clearly a relevant difference between the results of the two equipments used. Obviously, the multiplexer array had difficulties handling high levels of concentration and the values were cut off. As a result of this comparison, it was decided that only the RPDD would be used to measure concentration on the Solar 8 collector.

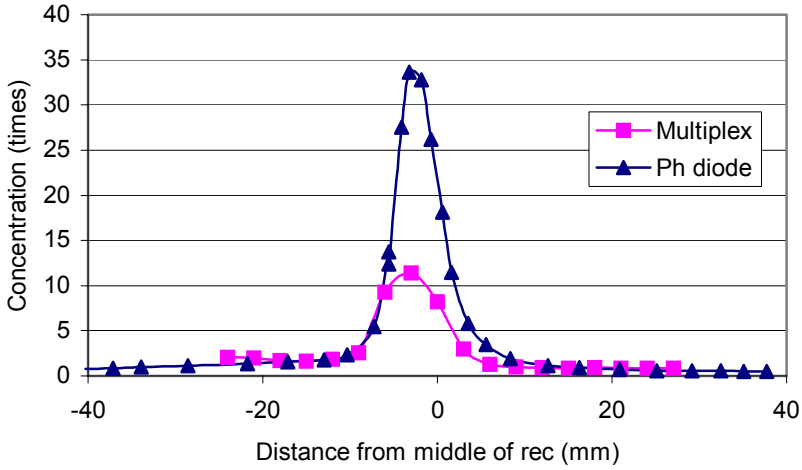

Figure 4.11 *Comparison between two different measurements of concentration, conducted with multiplexer and photo diode respectively, on the Solar 8 collector at 0 degree angle of incidence. Standard absorber.*

Measurements were conducted on the MaReCo using the multiplexer array. As the results proved to be incorrect, they are not presented in this thesis. The multiplexer was reconstructed and developed during the project time, but was not ready to be used for any further measurements in this thesis.

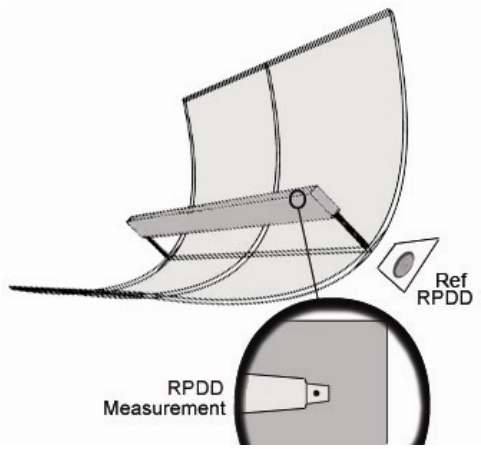

Figure 4.12 *Concentration measurement with the RPDD, on the absorber and reference in direct sunlight*

The photo diode of the RPDD, mounted on the rotating arm, was moved transversally over the surface

of the absorber and measured the intensity at each point. Before and after every series of measurements, the photo diode was held perpendicularly towards the sun, as a reference to measure the intensity of the incoming sunlight.

As secondary and tertiary references, a reference diode and a pyranometer were used. While taking reference measurements with the RPDD, these were partially shadowed, in order to determine the diffuse factor in the sunlight. They could also tell if large variations in incident light occurred during measurements on the absorber.

4.2.2 Calculations

4.2.2.1 Calculation of concentration factor over the absorber

The concentration values were calculated as non-dimensional proportions, between the intensity of the incoming sunlight and the concentrated light that hit the absorber. The concentration at every point on the absorber surface was calculated as the intensity at the given point, divided by the mean value of the intensities of the references before and after the measurement.

4.2.2.2 Calculation of mean concentration

The mean concentration was calculated over the absorber and the cells, respectively. The mean concentrations, derived from measurements, are called C_{meas}.

When calculating mean concentration over the absorber, the first point was ca -40 mm and the last point ca +40 mm (distance from centre). When calculating concentration over the cells, the first point was ca -20 mm and the last +20 mm (distance from centre).

4.2.2.3 Calculation of optical efficiency

The full width of the glazed surface is 0.46 m for a half reflector parabola. The incident light on this surface is meant to hit the 0.040 m wide cell surface for the construction to be optimal. The cells are in fact slightly broader, but it is preferred that the intensity focuses in the area

between the metal contacts of the cells. This means, that if all the incoming sunlight was reflected and hit the cells, the mean concentration would be 11.5 times. As the absorber has a width of 0.080 m, the mean concentration on the entire absorber would be 5.75 times as a theoretical maximum.
Not all incident light is reflected and hits the absorber or cell area. By comparing the mean concentration factors derived from measurements (C_{meas}), with the ideal concentration factors mentioned above (C_{theo}), the optical efficiency can be approximated. This can be expressed as:

$$\eta_{optical} = \frac{C_{meas}}{C_{theo}} \tag{4.1}$$

4.2.3 Results

4.2.3.1 Dependence on angle of incidence

Figure 4.13 shows how the concentration spreads over the absorber, and varies with different angles of incidence. Note that cell area is between -20 and +20 mm from absorber centreline. Measurements are conducted at weather conditions with approximately 94 % direct sunlight and with a 60 mm thick absorber, meaning a 13 mm extension on each side. Figure 4.14 also shows effects of varying angles of incidence, but without absorber extension.

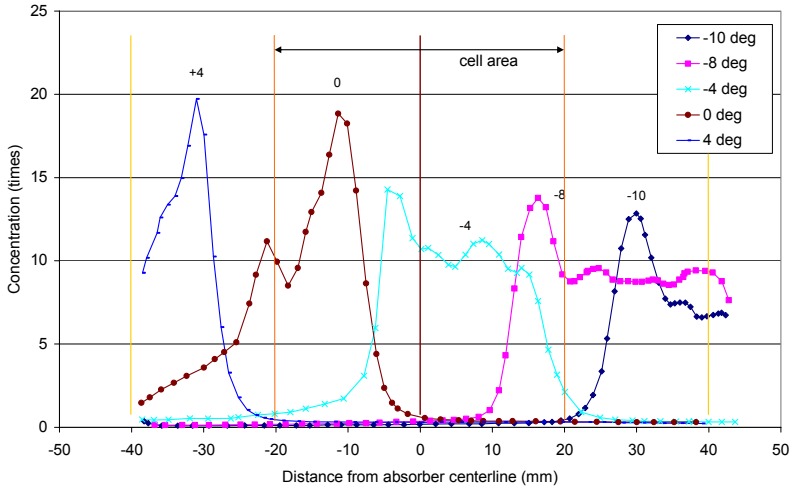

Figure 4.13 *Concentration on the Solar8 absorber (upper, middle), at variable angles of incidence. 60 mm thick absorber.*

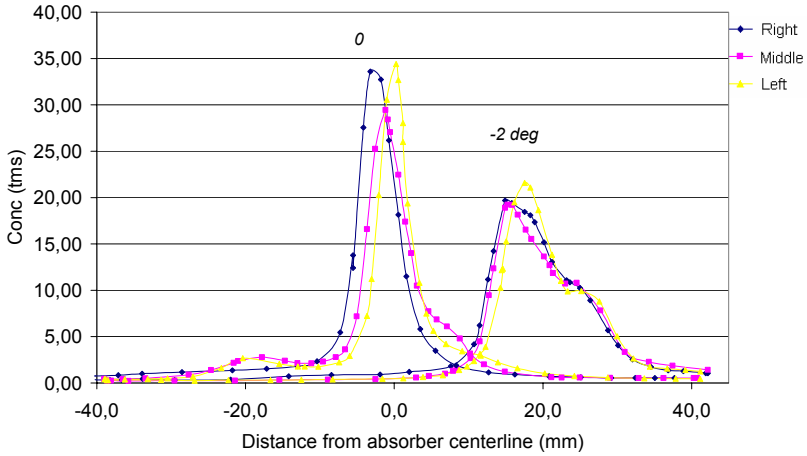

Figure 4.14 *Concentration at different sides of the Solar8 absorber, upper, at varying angles of incidence: -2° and 0°, respectively. Curves for varying locations on the absorber; on the edges (right and left) and in the middle. Standard absorber.*

The results show that a few degrees variation in angle of incidence has a big effect on the concentration levels and how the light is distributed over the cells and absorber. This effect is extra pronounced without extension on the absorber.

4.2.3.2 Effect of absorber extension

Figure 4.15 shows concentration levels for Solar 8 at 70% direct sunlight, with and without extension. 13 mm extension (on both sides) means that the absorber is totally 60 mm thick instead of the standard 34 mm.

As can be seen from figure 4.15, and when comparing figure 4.13 with figure 4.14, the peak concentration levels are also significantly higher in the case without extension. This is because the extension moves the absorber surface away from the focal point.

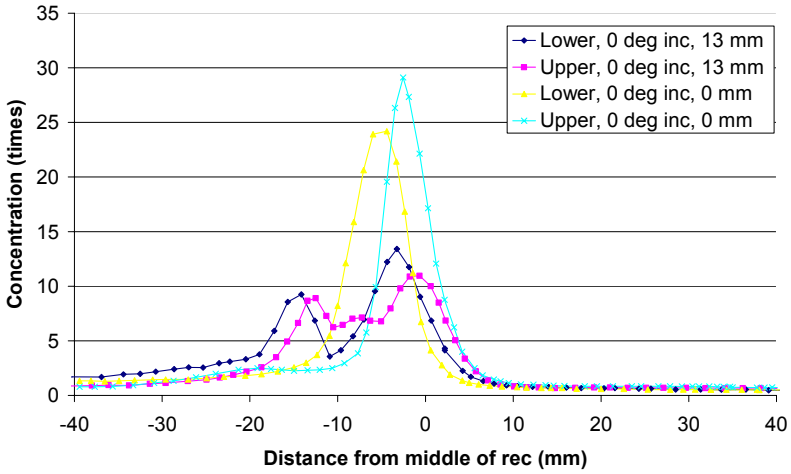

Figure 4.15 *Solar8, concentration on absorber at 0° angle of incidence, with standard absorber (0mm extension) and thick absorber (13mm extension)*

4.2.3.3 Mean concentration and optical efficiency

Figure 4.16 shows the calculated mean concentration for the Solar8, with 94% direct sunlight and at varying angles of incidence.

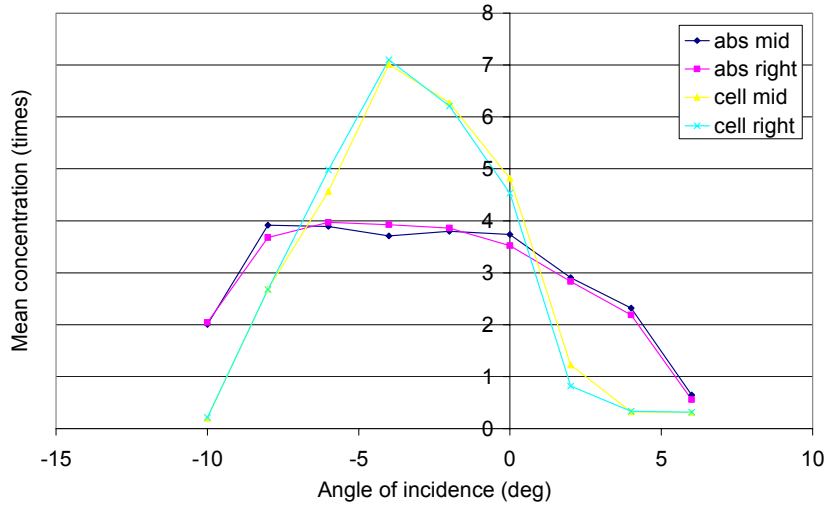

Figure 4.16 *Mean concentration at varying angles of incidence (upper, middle), 60 mm thick absorber.*

Results are shown C_{meas} for both the absorber and cells. Also, results for both the centre and the edge of the absorber are presented. The figure shows how quickly the mean concentration over the cells decreases when the angle of incidence moves away from the optimum, hence decreasing optical efficiency. The mean concentration and optical efficiency over the total absorber is much more stable, and does not show an absolute maximum at the same angle of incidence than what can be seen for the cells.

Table 4.1 Mean concentrations and optical efficiencies for the Solar 8 system. Values represent the results for optimal angle of incidence.

	70 % direct light		*94 % direct light*	
	Mean conc (times)	Optical eff (-)	Mean conc (times)	Optical eff (-)
Cells	5.81	0.51	7.1	0.62
Absorber	3.49	0.61	3.9	0.68

The Solar8 trough reaches its highest mean concentration at -4° angle of incidence. This means that the parabolic shape is not optimal, at least not for an absorber with extension.

The optical efficiency barely reaches 70% at best case. Probably, this is partly due to reflected light missing the cells, because the absorber has an extension. The greatest losses can be traced to the reflector, because of absorbed light and rays reflected wrongly by the diffusing surface or by scratches on the reflector. The optical efficiency could be improved by changing parabola geometry, using a reflector with higher reflectance and by careful handling that avoids all damage of the reflector surface. If the reflector material is changed to one with better reflectance it is important, though, to make sure that it possesses the same or better mechanical properties. If not, the losses because of faults in reflector shape will be greater than the gains of better reflectance.

Sources of errors in the concentration measurements are because of scratches and flaws in the reflector, characteristics of the photo diode and difficulties in measuring incident light, specifically the diffuse fraction. The photo diode has a different spectrum sensitivity than solar cells. Also, the aluminium frame can prevent the rays, incoming at low angles, from reaching the diode.

The values for mean concentration and optical efficiency are relatively high in the case for 70% direct light, compared to the case with more direct light, which seems odd. In our models, and as can be seen in figure 4.13, Solar8 can utilize very little diffuse light; therefore the values should be almost proportional to the level of direct light. Our results are probably due to high irradiation from the hazy area of the sky close to the sun, which has not been shadowed when reference measurements of diffuse light were done; hence the proportion of light in Solar8's angle of acceptance has been underestimated.

4.3 Evaluating the reflector shape of Solar8

The I-V and concentration measurements have indicated that the Solar8 trough is not exactly symmetrical. This and the general design of the trough are evaluated further in this chapter.

4.3.1.1 Optical analysis by ray tracing

By putting a screen with a row of horizontal slits on top of the trough in a plane perpendicular to the sun and holding a piece of cardboard on the side of the trough, a ray pattern will occur on the cardboard and visualise the path of the rays. The ray pattern is photographed and the analysis will show where on the receiver the focal point is. It also shows which part of the parabola that reflects light to the focal point and receiver. By studying how much light is reflected on to the receiver, the reflector shape can be evaluated.

Figure 4.17 *An example of optical ray tracing on Solar8, with 0° angle of incidence and a 60 mm thick absorber (Photo by Håkan Håkansson)*

4.3.1.2 Results from optical ray tracing

The picture from the ray tracing in figure 4.17 illustrates the principle of the concentrator quite clearly. More detailed ray tracing can be done using a computer, but even the photo tells us a lot about the reflector and imperfections in the specific mounting. In the photo, it is possible to see that the light is effectively reflected toward the absorber. The distribution of the concentration can be examined further by using a laser source (4.3.2.1).

4.3.1.3 Mapping the diversion from focus for incoming light by using a laser source

With use of a laser beam, the reflection of the parabola can be evaluated. The method studies the reflection of discrete beams of light – with an incidence angle parallel to the receiver – incoming at different positions on the reflector.

A rod with a rectangular cross section was placed on top of the trough and perpendicular to the receiver. A laser source was placed on a sliding sled on the rod and was adjusted so the light shone parallel with the receiver. A scale was fitted to the rod and zero was marked at the point where the laser was in the same plane as the receiver. This procedure was repeated for each series of measurements done.

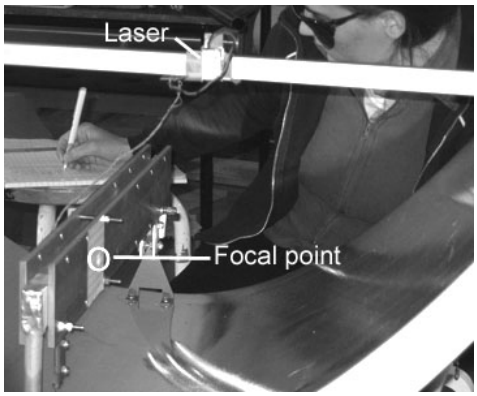

Figure 4.18 Setup of the laser analysis (Photo by Håkan Håkansson)

When the laser was moved away from the receiver by sliding it towards the edge of the reflector, the beam was reflected and made a "spot" as it hit the receiver. The position of the focus and the spread of the spot could be studied by fitting another scale vertically on the receiver. For each measurement, the laser was moved one cm away from the receiver, and the position of the focus, height and width of the spot was

registered. The outgoing laser beam was elliptic with the approximate measurements of 3.5 x 4 mm^2.

Measurements were done at three positions at each side along the receiver; 15 cm from the left and right end respectively and in the middle (25 cm from the ends). For the left and middle position, additional measurements were done after altering the receiver by making it 13 mm thicker on each side.

4.3.1.4 Results from laser analysis

The results of the laser measurements can be seen in figure 4.19.

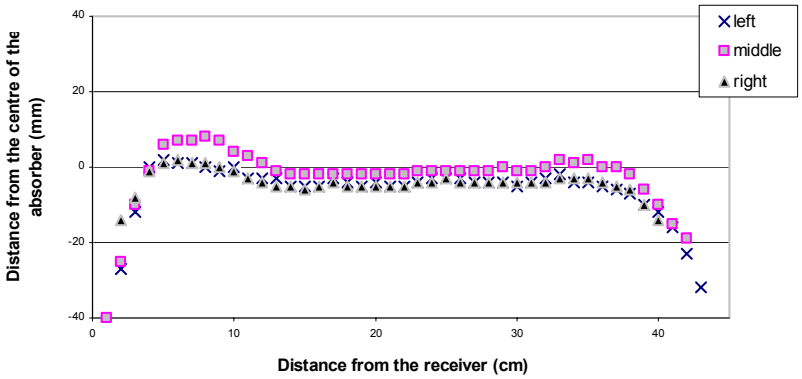

Figure 4.19 *The position of the focal point from light reflected at different parts on the upper parabola.*

As can be seen in the graph, the light is distributed over the lower half of the absorber at 0° angle of incidence. Scratches and buckles in the reflector material, could be responsible for some errors in the measurement. That could explain some of the extreme values, but mostly influenced the results by blurring the laser point. It's interesting to see that despite that the trough was hung up on to trestles to minimize the distorting effect of the stand; the result still differs significantly across the reflector material. This most likely affected the other measurements done on the trough, but should be possible to fix in new models by using a better stand and protecting the trough well during transportation. One other factor, which could have influenced the results, is that it was difficult to know if the laser was pointed exactly vertical during the measurements. This means that the position of the laser on the absorber could have moved slightly during the measurements.

It can clearly be seen that the focal point of the reflector ends up below the centre point of the absorber for most of the measurements. Considering that the PV cells are only 46 mm wide with as little as 40 mm PV in between the metal grids, it is very important that the concentration hits the cell. The absorber should therefore be moved a few millimetres downwards to increase the radiation on the cells. In the case of the thicker absorber (60 mm) in figure 4.20, the absorber needs to be installed even lower.

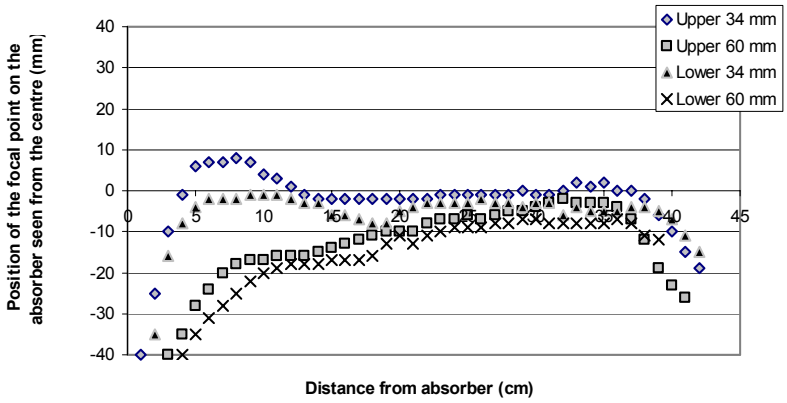

Figure 4.20 *The focal point of light reflected from different parts on the upper and lower parabola comparing the stand absorber (34 mm) with a thicker absorber (60mm).*

Even if the absorber is moved downwards, there will be parts of the reflecting light, which will not be used. There are parts of the reflector which are dead zones, meaning that they do not reflect any light to the absorber. When making the new prototypes and later the retail model of Solar8, the geometry should be corrected to include these dead parts or exclude them to cut the building cost.

It is though important to remember that the light from the middle part of the reflector, which we utilize according to the graph, is more worth than the light reflected from the bottom of the trough, which we see to the left in the graph. This light will hit the cells with a high angle of incidence, which means we will not be able to use it as effectively.

5 Simulations and Calculations

5.1 Winsun

Winsun is a program built from TRNSED/TRNSYS, developed and used at LTH. The version used for the simulations in this project is WINSUN0509. It has been added a component by Bengt Perers (EBD, LTH) to be able to simulate sun-tracking systems as Solar8.

Climatic data are hourly values for a normal year. It represents an average year derived from Metonorm climate files for a certain location over several years, to make it more accurate and minimize the effect of extreme climate variations.

5.2 Annual thermal exchange

Experimental thermal measurements on Solar 8 have not been conducted, because a full-scale prototype not was accessible. Therefore, the annual performance had to be retrieved through simulations. Input values are based on results from measurements of concentration.

The program Winsun was used for the simulations. The simulated model was a one-axis sun-tracking trough with the axis placed horizontally in a west-east alignment. Input values for the simulations are presented in table 5.1. Diffuse and Heat loss factor are estimates. The efficiency for the hybrid, expressed as absorbed light per glazed area, is calculated with the following expression:

$$\eta_{glass} = \eta_{optical} \cdot \frac{4}{5} \cdot \tau = 0.68 \cdot \frac{4}{5} \cdot 0.96 = 0.52 \quad (5.1)$$

The term $4/5$ is used because the absorber is only four meters long in a five meter trough. τ is the glass transmittance. $\eta_{optical}$ is derived from the measurements of concentration (table 4.17).

Table 5.1 Input values for annual heat-exchange simulations in Winsun0509.

η_{hybrid} (-)	Diffuse factor (-)	Heat loss ($W/m^2_{glass} \cdot K$)
0.52	**0.10**	**0.5**

The results from the simulations are presented in table 5.2.

Table 5.2 Results of the thermal output simulations.

Water temp.	*Lund*, ***Sweden***, thermal output (kWh/m^2,yr)	*Munich,* ***Germany*** thermal output (kWh/m^2,yr)	*Madrid,* ***Spain*** thermal output (kWh/m^2,yr)
90°C	**251**	**272**	**566**
70°C	**273**	**296**	**599**
60°C	**284**	**308**	**616**
50°C	**297**	**321**	**634**
25°C	**330**	**358**	**681**

Comparing the results with the annual thermal output for MaReCo which was simulated in Fahlström's thesis, we can see that Solar8 has a slightly higher output. At 25°C, MaReCo gives approximately 300 kWh/m^2,yr, which is 9 % less than the simulated output for Solar8.

5.3 Annual electric exchange

After calculating the maximum power for different angles of incidence from the results of the I-V measurements, the efficiency and annual electrical output per glazed area and per cell area can be calculated for Solar8. By comparing it with a reference measurement for a flat panel and with the earlier published results on MaReCo, information is given on the concentration and output for both hybrids. The optical efficiency of Solar8 can be calculated using the short-circuit currents derived from the I-V measurements and the concentration factor, according to equation 2.17.

$$\eta_{optical} = \frac{I_{SC,concentrator}}{C \cdot I_{SC,flat}} = \frac{9736mA}{10 \cdot 1495mA} = 0.65$$

In the equation, the currents are given for the total irradiation of 1000 W/m^2. Some key data for Solar8 collected from the measurements are given in table 5.3.

Table 5.3 Concentration and optical efficiency for the unglazed Solar8

Factor	(-)
I_{sc} concentration	6.5
P_{max} concentration	6.3
Decrease factor for the FF	0.97
Geometrical concentration	10
Optical efficiency	0.65

To calculate the efficiency of the concentrating hybrid model, the following equation can be used:

$$\eta_{hybrid} = \frac{P_{\max}}{G_{total}\left(0.9 \cdot \cos\alpha + \frac{0.1}{C}\right) \cdot A} \tag{5.2}$$

In the equation, A is the area of the glass and α the angle of incidence. It has been assumed that 10% of the total irradiation is diffuse. By

dividing the diffuse irradiation with the concentration factor, we get an approximation of how much diffuse light that reaches the absorber. The trough has a low angle of acceptance and unlike the direct radiation; only a small portion of the diffuse light will be reflected towards the receiver in the trough. For simplicity, it is possible to make a good approximation of the efficiency of the hybrid using only the direct irradiation. This will give a slightly lower value of the annual output, but it will only differ a few percent. Furthermore, the measured power and irradiation is used in the equation, which means that reflection losses are accounted for.

The efficiency of a flat panel can be calculated using the same equation, but with the concentration factor set to 1, since a flat panel can use both the direct and diffuse irradiation.

Considering the possible sources of error in the measurement and the possibility to adjust the production mistakes in the trough, P_{max} used in the simulations represents the maximum value measured. For our series, the highest P_{max} occurred at –4°, but in the simulations, it is assumed that the trough can give the same output from both sides at 0° angle of incidence.

Knowing the efficiency of the PVT hybrid and the total direct annual irradiation on the trough, an approximation of the annual electrical output can be calculated from the equation:

$$Q = \eta_{hybrid} \cdot \tau \cdot G_{d,annual} \tag{5.3}$$

The equation includes only the direct irradiation, since the concentrators mainly reflect direct light efficiently to the receiver. Depending on the acceptance angle of the concentrator, different portions of diffuse irradiation will be used, but it will only account for a few percent. Normally, the diffuse light can therefore be neglected in the calculations and still give a good approximation of the annual output. The annual irradiation used in the calculations is the same as we use for the thermal simulations in Winsun.

The simulated annual electrical exchange for Solar8 based on the measurements performed in for this thesis, is presented in table 5.4. Winsun0509, which is presented in chapter 4.1, was used for the simulations.

The on-site welded panel for Solar8 was found to have an efficiency of 12.8 % and since the measurements were performed with an unglazed trough, the efficiency was multiplied with the transmission 0.97 to give 12.4 %. In the Solar8 troughs, there will be two four meter PV cell modules in each five meter trough. This is to minimize the effect from shadowing and decrease the investment cost.

Table 5:4 Annual electric exchange, simulated from results of the experimentally used Solar8 panel with an efficiency of 12.8%

Location	Lund	
	Hybrid	**Flat panel**
Q (kWh/m^2,yr)	42	106

As can be seen in table 5.4, the hybrid only gives 40% of the output that a fixed module at a 30° slope would give per m^2, but seen to the PV cell area, Solar8 gives 577 kWh/m2,yr, which is 5.4 times more electricity than the fixed module. Since PV cells account for an extensive part of the investment cost in the hybrid, this means that the electricity can be delivered at a lower cost, though.

The PV cells used have an efficiency of 18% normally and with the condition that the panels are industrially made with high accuracy, the optimal annual exchange of the trough would increase significantly. The simulated annual exchange for the Solar8 trough using a PV *module* with an efficiency of 18% and reference values from a fixed panel for different locations in Europe are shown in table 5.5.

Table 5:5 Annual electrical output per glazed area and PV cell area for the solar tracking Solar8 at different locations, assuming 18% module efficiency and 97% glass transmission.

Location	**Annual electrical output per hybrid glass area (kWH/m^2,yr)**	**Reference for fixed PV module at 30°/20°/15°**
Lund	59	150
Munich	65	163
Madrid	118	257

Studying the results closer, it is possible to see that the output compared with a fixed panel is higher in Southern Europe compared to Sweden. This is due to the ratio of direct and diffuse irradiation, since concentrating systems mainly reflect direct light. While the output per

PV cell area only multiplies 5.4 times in Lund, Sweden, it increases by a factor 6.3 for the same system located in Madrid, since it will give 1607 kWh/m2,yr per PV cell area installed in the hybrid.

The calculations are based on measurements performed at 25°C surface temperatures. This could be valid if the thermal heat is used instantly in swimming pools, which does not require any storage. It is though likely to assume that the hybrid will be operated at higher temperatures for systems, which require storage. At a cell operating temperature of 65°C, the annual electrical output would decrease by 16-20% totally according to equation 2.10.

The maximum electrical output for the MaReCo 2002 model is 55 kWh/m^2,yr, which is considerably more than the 42 kWh/m^2,yr the Solar8 trough used in the experiments give. Fahlström's simulations were done for a instalment in the Uppsala region and not Lund, but since the days will be slightly longer during the summer in Uppsala, which is north of Lund, the total irradiation will even out over the year.

If we look at the outputs from Solar8 using a PV module with 18% efficiency, which is closer to the planned model, Solar8 will give approximately 7% higher electric output per m^2 than MaReCo. Though, it should be noted that if MaReCo is glazed with a low-iron glass with anti-reflection coating instead, it will produce slightly more electricity than Solar8. The PV cell area installed in Solar8 is much smaller than the cell area in MaReCo, though, and the small PV area in Solar8 might enable the investment in high efficiency cells. The total cost should still not exceed the investment cost of MaReCo per glass area.

6 Solar8 System Design

As a finishing part of this thesis, the design of possible Solar8 systems was studied, and costs were calculated. The goal was to find locations for possible installations, determine which systems were needed for utilization of the generated heat and electricity, and the economic conditions. Two site locations were studied; a small-scale installation at LTH (Lund, Sweden) and a large-scale installation at *Korpen* (Visby, Sweden).

6.1 Reference projects

A number of reference projects were studied in order to evaluate the costs of installation. Because Solar8 delivers heat *and* electricity, both solar heating and PV-systems had to be studied.

6.1.1 Gårdsten

In the residential area Gårdsten (Göteborg, Sweden) solar heat collectors have been placed on the rooftop of 6-story buildings, with storage tanks in the basements. Each installation has 235 m^2 solar collector area, and the storage capacity is 18-20 m^3 per system (approx 80 litres/$m^2_{coll.area}$) (Dalenbäck, 2006). The collectors deliver about 400 kWh/m^2,yr.

Three of the installations were finished in 2000, another three in 2004. For the first three, the cost was calculated to 5700 kr/m^2, whereof the collectors themselves cost 2000 kr/m^2. For the last three, the cost was 8500 kr/m^2. The calculations are a bit uncertain, especially as the increase in cost between the years exceeds the general entrepreneur index. The collectors' contribution to the cost for the 2004 systems is not stated.

6.1.2 Malmö

Two systems in the city of Malmö (Sweden) are references for the PV-systems. Both are grid-connected and built within the last one or two years. The first installation is at the "ecological area" Augustenborg, a 91 m^2, 11 kW_p system, mainly with poly-crystalline cells (Nilsson, 2006). Poly-crystalline cells are sold at a price of roughly 3500 kr/m^2 (Exoheat 2006), but the figure is uncertain as prices varies much at different occasions and for different retailers. The total investment was at 950,000 kr.

The second installation is at the Technological Museum of Malmö. It features 125 m^2 mono-crystalline cells on the facade and 390 m^2 poly-crystalline cells on the rooftop (Nilsson 2006). Total installed power is 64.8 kW_p. Mono-crystalline cells are sold for 4500-5000 kr/m^2 (Exoheat, 2006) and for poly-crystalline cells the same price can be used, as mentioned earlier, 3500 kr/m^2. The installation at the museum totals 3,500,000 kr, and the price includes insurance costs etc.

6.2 The sites

At the initiation of this project, it was already quite clear that the aim was to install one full-scale Solar 8 prototype at LTH. Another site, a location for a large-scale commercial installation, with good conditions for solar energy, had to be thoughtfully selected. Visby on the island of Gotland was identified as one location with ideal conditions in terms of sunlight, at least with a Swedish viewpoint. Strömstad and the Island of Tjörn, both on the Swedish west coast were also studied, but finally the best site was selected to be a building in Visby. The Visby site and LTH are both public buildings, which enables subsidies of 70% through the ROT-support for PV installation on public buildings.

6.2.1 LTH

Figure 6.1: The EBD laboratory in Lund

The installation at LTH, Lund Institute of Technology is a possible prototype: one single Solar8 trough placed on the EBD laboratory solar roof. The laboratory is a one story, solitary building with a flat roof, custom-built for solar collectors. The building houses several large storage tanks and piping systems connecting the roof with the tanks. This means that there already is a "plug and play"-system.

6.2.2 Korpen

Korpen is a large medical care centre in Visby. It consists of several buildings, but the focus of this study has been a location of the collectors on the flat rooftop of the large main building.

Existing heating system consists of a heat-exchanger connected to the district heating. Energy is supplied by the company Gotlands Energi.

The heating demand in the building varies between over 300 MWh/month in mid-winter, to slightly less than 50 MWh/month in July-August (Gotlands kommun, 2005). Electrical demand shows less variation, it was between 95 and 130 MWh/month for 2005, the least being used in June-July.

6.3 System

The system design for the two sites would differ substantially, because of different conditions and as a natural effect of the varying sizes.

6.3.1 LTH

The collector would be connected to an existing storage tank, hence the installation costs can be held more moderate. All that is required for installation are pipes, for connection of the trough to the buildings piping system, and an inverter and controller, for connection to the main electrical grid.

6.3.2 Korpen

For Korpen, two different heat systems are presented. One possibility is to connect the solar heating directly to the district heating. This means that the solar circuit, by connection to a heat exchanger, heats the district heating return water and delivers forward water to the district heating grid. Most of this "solar district heating" will be used within the building. Systems that operate like this can be bought as complete modules, meaning minimal installation cost. The proposed system in this study is the "Solfjärrvärmecentral SFV" from Exoheat AB. A system scheme is presented in Appendix A. This is a cheap and simple system, but the required high temperature means lower heat and electrical output.

Figure 6.2 *The Korpen main building in Visby with a part of the collector installation (Picture by Göran Björkvist , photomontage by Erik Pihl).*

The other possibility is a system with lower temperatures. Cold water is heated by two heat exchangers, one connected to the district heating, the other connected to a storage tank. The storage tank, in turn, is heated by solar energy. A proposed scheme can be viewed in Appendix A. Calculations have been made proposing two models of this system, one running on hot solar temperatures: "system 2a" (65°C), and one with lower solar temperatures: "system 2b" (50°C). Since the annual

thermal output for the installation is in parity with the monthly load for the building in mid-summer, it is feasible to suggest that the heating demand at almost all times will be larger than the collected solar heating. Therefore, storage tank sizes can be held small, decreasing tank costs. The reference installation (chapter 6.1.1) needed 80 $l/m^2_{coll.area}$, and with output per m^2 being less than ¾ in the Solar8 system compared to the Gårdsten system, the Solar8 installation should not need more tank storage volume than 40 $l/m^2_{coll.area}$. According to this, the storage volume would be 7.36 $m^3 \approx 8\ m^3$.

Table 6.1 Suggested system design for the installations at the two sites.

LTH		*Korpen*	
Collector		Collectors	
Solar collector	***1 (5m) Solar8 trough***	**Solar collectors**	***40 (5m) Solar8 troughs***
Electric system		Electric system	
Inverter	**Steca Grid 300W**	**Inverter**	***Ex:*** **3 x SB 5000W + 1 SB 3000W**
Controller	**Steca Guard**	**Controller**	***No recommendation***
Heat system		Heat system	**Alternative #1**
Piping	**Existing piping + extra tubing**	**Connection to district heating**	**Sun district heating terminal, SFV 250**
Storage Tank	**Existing tank**	**Piping**	***Depends on details in site characteristics***
			Alternative #2
		Storage tanks	**8 m^3**
		Piping	***Depends on details in site characteristics***

6.4 System performance

There is a noticeable difference in the system performance between the two sites, although not drastically. Lund has approx 1700 hours of sunlight and 1000 kWh/m^2 irradiation a standard year, to compare

with Visby which has approx 1900 hours and 1050 kWh/m^2 a standard year (SMHI, 1961-1990 (1),(2)). Climate data files for Lund have been available for WinSun simulation, but unfortunately not files for Visby. To cope with this, electrical and heat output has been calculated for Lund, and multiplied with the factor 1050/1000 for the Visby case.

Electric output, as calculated in chapter 4.3 is 59 kWh/m^2 for a system with full performance, situated in Lund. The output will decrease with rising temperatures, as stated in chapter 2.3.8. Output of heat, as hot water, has been calculated using WinSun0509, as described in chapter 4.1. The figures used for these calculations are the results presented in chapter 4.2. For system 2, tank losses of 5% have been assumed.

For the system delivering thermal energy at district heating temperatures, there is a need to operate at different temperatures, since forward temperatures differ from 75°C in mid-summer to 110°C in midwinter. Simulations with temperatures varying stepwise with season in the range 80-120°C has showed results very similar (<1% difference) to the results for 90°C operating temperatures. For simplicity, therefore, results for steady 90°C operating temperature have been used.

Table 6.2 Thermal and electrical output from Solar 8 system at different sites and operating temperatures.

	LTH, **Lund** (kWh/m^2,yr)	Korpen, **Visby** (kWh/m^2,yr)	Korpen, **Visby** *incl 5% tank losses* (kWh/m^2,yr)
Electric output at 50°C	**53**	**56**	**-**
Electric output at 65°C	**51**	**53**	**-**
Electric output at 90°C	**46**	**48**	**-**
Thermal output, 90°C	**251**	**264**	**-**
Thermal output, 65°C	**280**	**290**	**279**
Thermal output, 50°C	**297**	**312**	**296**

6.5 Economic conditions

6.5.1 LTH

6.5.1.1 Collectors

The trough is a prototype, and as such it will be costly. The price is an estimate, after discussing with the producer and given the condition that the pay-back times not should be unrealistic.

6.5.1.2 Electric system

The electric system is proposed to be a simple system from Steca. The university has bought the same kind of system earlier and costs are estimated with those as a reference.

6.5.1.3 Thermal system

Most of the system is already in place, all that is needed is simple piping. Costs are estimated to be 1000 kr.

6.5.2 Korpen

6.5.2.1 Collectors

Korpen would be a much larger installation than that at LTH, significantly decreasing unit costs. The collector costs are an estimate, showing what price levels would be reasonable.

6.5.2.2 Electric system

In order to evaluate the costs of the electric system, the reference projects from Malmö (chapter 6.1.2) were used. Since electric output per m^2 is different for the Solar 8 system compared to these installations, the cost per peak power is of most interest.

The first reference project (chapter 6.1.2) had a system cost of 631,500 kr, cell costs excluded, for 11kW_p. This equals ca 57,400 kr/kW_p. The

second project had a cost of 1,541,250 for 64.8 kW_p, if cell costs are excluded (assuming 4750 kr/m^2 for mono-crystalline cells). System cost would be 23,800 kr/kW_p.

The Solar8 troughs produce approximately 100 kW_p/m^2, meaning 40 troughs reach a top power of ~18.5 kW. The electric system cost for the Solar8 installation is assumed to be the mean value of the above references, ca 40,000 kr/kW_p. In this cost maintenance, insurances etc are included.

6.5.2.3 Thermal system

Two different systems are proposed, one producing energy at district-heating temperatures, the other with two alternatives: temperatures at 65 °C or 50 °C, respectively. The first system is a "plug and play" solution with few extra costs apart from the SFV terminal, which would cost in the range 250,000 – 300,000 kr (Exoheat 2006).

System alternative 2 involves (a) storage tank(s), and the Gårdsten installations (chapter 6.1.1) are a reference case. Though, as mentioned in chapter 6.3.2, tank volumes can be significantly smaller than in the reference case. The Gårdsten installation cost approximately 3700 – 6500 kr/m^2, when collector costs are not included. Mean value is 5100 kr. As the required tank volumes and system capacity is less per m^2 for Solar 8, the system costs are also lower. If the cost per m^2 is assumed to be 40% lower, the figure 3000kr/m^2 is reached.

6.5.3 Calculations

Calculations were done using a model with discrete steps of single years, and with different interest rates. The model presupposes an initial investment, being paid off with the annual energy savings. Savings, which can also be viewed as income, are likely to increase with time because of inflation and rising energy prices. The Swedish Riksbank's (Bank of Sweden) goal is to keep the inflation at a steady 2±1% (Riksbanken, 2006). The annual increase in income is presented as "income increase".

Reference price for district heating is 0.55 kr/kWh and for electricity 0.90 kr/kWh. These are estimated with current long-term prices at Gotlands Energi (delivers energy to Korpen) as a base (Gotlands Energi

2006-02-13 and 2006-02-23). The figures are rough and uncertain, though, as they most certainly will change during the coming 20 years.

As a reference case, the pay-back time was studied for a scenario with quickly rising energy prices. In the scenario, the energy prices rose instantly to 0.75 kr/kWh (heat) and 1.5 kr/kWh (electricity), and experienced no further growth in value (e.g. only normal inflation rate: 2%).

All input data concerning collector performance is presented in table 6.3.

6.5.4 Results

The input values for system performance and component costs, and the results in key figures such as yearly savings and total investment cost, are presented in table 6.3.

Table 6.3 Input values and key figures for investment analysis

	Income			**Investment**				
	Heat	Electricity	Energy savings	Collectors	Heat system	El. system	Subsidy	Tot. Invest
	kWh/yr	kWh/yr	kr/yr	kr	kr	kr	% subs.	kr
LTH	1288	244	**928**	40,000	1000	4000	70	**13,500**
Korpen								
System 1	48,493	8832	**34,666**	1,200,000	300,000	720,000	70	**666,000**
system 2a	51,336	9752	**37,012**	1,200,000	600,000	720,000	70	**756,000**
system 2b	54,464	10,304	**39,229**	1,200,000	600,000	720,000	70	**756,000**

The results, expressed as pay-back times for the alternative installations and at different interest and income increase rates, are presented in table 6.4. The “income increase” is, as earlier mentioned, an estimate of monetary income (e.g. savings) increase because of inflation (2%) and real energy price increase. The “pay-back time” is at the normal energy prices mentioned in chapter 6.5.3, and “P-B time at price 0.75;1.5” means pay-back time at the higher energy prices mentioned in the same chapter.

Table 6.4 Results of the (economic) cost estimate

	Interest rate %	Income increase %	Pay-back time years	P-B time at price 0.75;1.5 Years
LTH	5	2	20	12
	7	2	28	15
	5	4	17	
	7	4	21	
Korpen				
System 1	5	2	30	18
System 1	7	2	*inf*	24
System 1	5	4	23	
System 1	7	4	31	
system 2a	5	2	33	19
system 2a	7	2	*inf*	26
system 2a	5	4	24	
system 2a	7	4	34	
system 2b	5	2	30	18
system 2b	7	2	*inf*	24
system 2b	5	4	23	
system 2b	7	4	31	

6.5.4.1 LTH

The installation at LTH is surprisingly economical, being a prototype system. Although, one must consider that several costs are not included. For example, the heat system used is considered "free" as it is already in place, but one might instead consider it fair that the Solar 8 system pays its price for the capacity it uses. Also, the time spent by scientists or staff to install the system is not considered in this study, but it is at the other hand difficult to estimate. Yet, even if these extra costs were taken into account, the installation may still prove economically viable.

6.5.4.2 Korpen

Both the district heating-connected and the storage tank system are interesting, the choice should be carefully decided after investigating more in detail what the systems would actually cost. The higher the cost is for the electrical system, the better choice would system alternative 2 be, as the output is higher but the electrical system cost is the same as for alternative 1. Note also that if the pay-back time is the same for both systems, alternative 2 is (at least theoretically) a better investment since it delivers more energy after paid back and the second-hand value for the system is greater. The choice between system alternative 2a and 2b depends on temperature requirements.

The installation at Korpen is just barely economically viable. It is characterized by low district heating costs and high electrical installation costs. That electric installation costs are high is, though, also true for any other PV-system. If the installation shall be economically sound, the interest rate should not exceed 5%. Public Solar8-systems cannot be sold under these conditions to a price above 30,000 kr/trough, unless other costs can be drastically reduced. Maintenance needs to be included on some degree in that price, which means that the need for service and repairs must be kept very low. This will be a great challenge for the manufacturer.

The effect of solar cell degradation and other age-induced losses of efficiency has not been considered in this project but should not be forgotten, as it will likely effect the economic conditions. On the other hand, it is also likely that energy prices in Sweden will rise drastically in the near future, which would improve the economic situation for solar systems as Solar 8. There should also be possibilities to find cheaper electric systems. The electric system chosen for Korpen is approximately five times higher per peak power than the system for the LTH installation, even though the LTH installation is much smaller, which indicates that cheaper systems should be available.

7 Conclusions and Discussion

The measurements and simulations show that the tested model of Solar8 gives an annual electric output of 42 kWh/m^2 glass and 577 kWh/m^2 PV cell area at 25°C operating temperature for an installation in Lund. The equivalent thermal output is 330 kWh/m^2 glass. The PV module only had an efficiency of 12.8% though, which is lower than expected. A fixed flat module having the same PV cells would give 106 kWh/m^2, which means that output per PV cell area increases with a factor 5.4.

If using high efficiency photovoltaic cells as planned and making sure that the modules are produced with high accuracy to maintain good module efficiency, the simulated electric output for a Solar8 trough with a module efficiency of 18% would increase to 59 kWh/m^2 glass and 813 kWh/m^2 per PV cell area. With an operating temperature of 65°C, both the electric and the thermal outputs are expected to decrease with 15-20%.

Compared to MaReCo, the electric output is 7% higher for the Solar8 trough using the high-efficient module and the thermal output is 9% higher. The fill factor for Solar8 cells is 0.74 within the angle of acceptance, while the measurements show that the fill factor for the MaReCo cells is 0.62. One factor which is in MaReCo's favour, though, is that ordinary window glass was used for the measurements, while Solar8 was simulated with a 0.97 transmission glazing. If MaReCo is instead equipped with a low-iron glass with anti-reflection coating, the output could increase at least 10% and it would give a higher output per hybrid area than Solar8. The photovoltaic cell area installed in Solar8, is considerable smaller than the PV area installed in MaReCo, though, which is important considering that the cells are the most expensive parts in the model. The NAREC cells used in Solar8 are

not yet available commercially, which makes it difficult compare the cost of the electricity from each hybrid.
One interesting observation from the simulations, is that the high ratio of direct irradiation in Southern Europe helps to increase the electric output per PV cell area in the Solar8 hybrid to 6.3 times in Spain compared to 5.4 times in Sweden. Concentrators clearly benefit from being used in areas with more direct irradiation and similar locations are therefore better suited for high-investment models like Solar8.

Due to the small-scale prototype used in the measurements, it was not possible to conduct reliable thermal measurements on Solar8, so the profile and heat transfer through the absorber have not been evaluated. It is important that the manufacturer follows this up so the thermal output, and hence the cooling of the PV module works optimally.

All the measurements done on Solar8 show that the prototype was asymmetrical and did not have the exact supposed shape which affected the results. The main reason for this is that the wood stand built to support the reflector distorts the shape quite a bit. The geometrical evaluation of Solar8 also suggests that the absorber should be moved slightly downwards in the trough to make use of more of the reflected light. The laser analysis shows that the reflector in itself is not optimally shaped and must be corrected a bit. It is very important that the reflector is made with high accuracy. There needs to be a way of guaranteeing that all troughs that are installed have a reflector with the right shape. The possibility of inventing a tool that verifies the shape of the parabola should be considered.

Using concentrating solar hybrids can be the key to reduce the cost of solar energy, and considering how PV cells are manufactured today, it presents a more environmentally friendly alternative to flat PV systems. While a lot of activity and development in the renewable field happens in laboratories around the world, it is also important to make the products and technologies available. MaReCo is a research product which has managed to reach the market, if yet in a limited scale. With Solar8 on the other hand, the objective has been clear from the beginning. The hybrid is solemnly developed to become a commercial product.

The model shows a potential of becoming a commercially available concentrating system soon, but improvements have to be made to the model before releasing it. It is also utterly important that the company

can provide guarantees that the system's solar tracking system will function satisfactorily. Because of the tracking system, there will be more mechanic stress on the components, which can cause them to break and the motor, which runs the tracking, can fail. Because of the low acceptance angle of the trough, any malfunction in the tracking can reduce the output significantly and thereby ruin the cost estimates. The company needs to have a clear strategy on how to fix and follow up any failures in the machinery already when they sell the systems, so the customers get a guarantee that the system they put up will work for 15-20 years minimum. The cost of service, repair and spare parts, needs to be transparent from the beginning.

The big challenge for the manufacturers of Solar8 is therefore to prove that they can produce the troughs at a low manufacturing cost, with high reliability and high efficiency.

References

Literature and reports

Areskoug, M. (1999), *Miljöfysik*, p 73-137, 186-224. Studentlitteratur, Sweden, ISBN 91-44-91-44-01114-8

Boverket (2000), *Förordning (2000:287) om statligt bidrag till investeringar i solvärme*, Miljö- och samhällsbyggnadsdepartementet.

Boyle, G. (red) (1996), *Renewable Energy*, p 41-59, 98-110. Oxford University Press, UK, ISBN 0-19-856451-1

European Renewable Energy Council (2004), *Renewable Energy Policy Review – Germany*, Belgium

European Renewable Energy Council (2004), *Renewable Energy Policy Review – Spain*, Belgium

Fahlström, A. (2002), *MaReCo, en koncentrerande solhybrid för el och värme*, p 9, 55-63. Lund University, Sweden, ISRN LUTADL/TABK-5025-SE

Gajbert, H. (2002), *Koncentrerande solenergihybrider for byggnadsintegrering*, p 73. Lund University, Sweden, ISRN LUTADL/TABK-5026-SE

Gotlands kommun, Tekniska Förvaltningen (Gotland Municipality Technical Administration) (2006), *Förbrukningsrapport Fastighetsbas*, förvaltningsenhet 01178, byggnad 01; measured values for Korpen building 01 energy use 2003-2005.

Green, M.A, Emery, K., King, D.L., Igari, S. & Warta, W. (2005:13), *Solar cell efficiency tables (Version 26)*. Progress in Photovoltaics, John Wiley & Sons, Ltd.

Ibach, H. & Lüth, H. (2003), *Solid-State Physics*, p 391-457. Springer-Verlag, Germany, ISBN 3-540-43870-X

Nilsson, J. (2005), *Optical Design and Characterization of Solar Concentrators for Photovoltaics*, p 21, 29. Lund University, ISBN 91-85147-15-X

SMHI (Swedish Meteorological and Hydrological Institute), *Solskenstid året*; mean values for years 1961-1990; solar map for Swedish average annual sun times (1)

SMHI (Swedish Meteorological and Hydrological Institute), *Globalinstrålning året*; mean values for years 1961-1990; solar map for Swedish average annual sun radiation (2)

Wenham, S.R., Green, M.A. & Watt, M.E., *Applied Photovoltaics*, p 25-41, 109-111. Centre for Photovoltaic Devices and Systems, University of New South Wales, Australia, ISBN0-86758-909-4

Wennerberg, J., Stolt, L. (1998), *Fördjupad analys av teknisk-fysikaliska krav på solceller för koncentrerande system*, p. Uppsala University, Sweden

Personal communication and lectures

Dalenbäck, Jan-Olof, Ass. Professor (2006-01-20); Installationsteknik (Building Services Engineering), Chalmers University of Technology, Göteborg; Mail contact

Jansson, Oscar (2006-02-22); Exoheat; telephone contact

Gotlands Energi (2006-02-23), telephone contact

Nilsson, Martin (jan 2006), Project leader; Malmö Stad Stadsfastigheter (Malmö City Estates); mail contact

Svenningsson, Per (2005-11-08); *Energy and environment*, Lecture, AMES, Lund University

Internet

Exoheat, 2006-02-17:
http://www.exoheat.com

Gotlands Energi, 2006-02-13: www.gotlandsenergi.se

Materialfysik, 2006-02-26:
www.materialfysik.se

Riksbanken, 2006-02-24:
http://www.riksbank.se/templates/Page.aspx?id=11017

Appendix A

Thermal designs for the Korpen installation

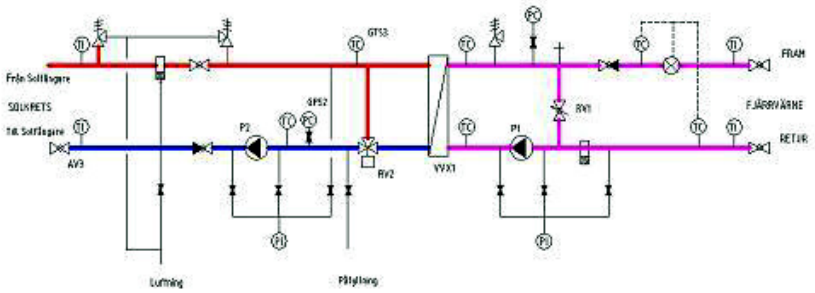

Figure A.1 *Scheme for the district heating sun terminal (SFV 50), picture by Exoheat.*

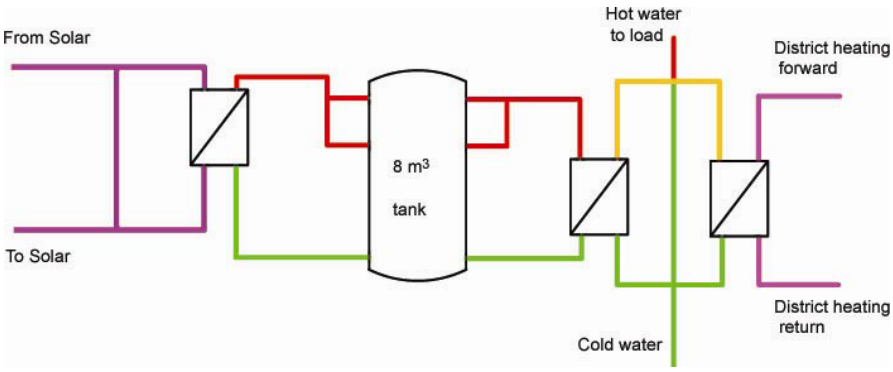

Figure A.2 *Principle scheme for the proposed thermal system alternative 2.*

Appendix B

Ecological Life Cycle Assessment on MaReCo

Abstract

This Ecological Life Cycle Assessment (LCA) is meant to show the environmental impact of a MaReCo trough from the cradle to the grave. The LCA is conducted at LTH, partially as a component in the master's thesis by Pihl and Thapper, partially at the Division Environmental and Energy Systems Studies, within an LCA course.

The functional unit of the study is a 6 meter wide trough. Included components are mono-crystalline PV-cells, an aluminium absorber, copper pipes, a steel reflector, low-iron glazing, concrete stands and a Teflon film. The figures for material recycling used: aluminium 85%, copper 30%, steel 20%, PV-cells 0%, Teflon 100%, glass 0% and concrete 0% (though 100% re-used).

The results show that PV-cells are responsible for the greatest environmental impact of the components in almost all aspects. Copper pipes can also be accounted for a great deal of pollution. The other major components have less impact, although not negligible. Teflon can produce some toxic substances at combustion, but impact in other environmental categories has not been possible to determine.

The trough uses 9,900 MJ of energy during its lifetime and produces 16,700 MJ electricity and 48,500 MJ thermal energy. The energy pay-back time is 3.8 years. Total green house gas emissions for a trough during its life time are 300 kg CO_2-equivalents.

The environmental impact of a trough should be able to decrease significantly. The European ecological LCA on PV suggests that impact from PV-cells could decrease by roughly 50% in a close future, if a

couple of simple measures were taken by manufacturers and users. This would mean that the environmental impact of a MaReCo trough could decrease significantly, green house gas emissions for instance with about 33%. An important measure to decrease the trough's impact on the environment would be to make sure that the used materials were recycled to a much higher degree. This is especially important for the copper pipes, the glass and the aluminium absorber. Another recommendation is to use steel stands instead of concrete.

The MaReCo trough gives roughly the same environmental impact as a flat PV module without reflectors and cooling, for the same amount of electrical energy. But MaReCo also produces a great deal of thermal energy. Therefore, it seems concentrating hybrids such as MaReCo have an ecological advantage compared to normal flat PV-systems.

Sammanfattning

Denna LCA syftar till att visa på miljöpåverkan av solhybridsystemet MaReCo från vagga till grav. MaReCo, en produkt framtagen av Vattenfall Utveckling AB och som nu ägs av Logosol, är ett koncentrerande solhybridsystem som ger både el (via celler) och värme.

Studiens funktionella enhet är 1 MaReCo-tråg med 6 meters längd. Ingående komponenter som studeras är solceller, receiver (aluminiumprofil), kopparrör, reflektorplåt, glas, betongstativ och teflonfilm. Följande återvinningsgrader antas för materialen: Aluminium 85%, koppar 30%, reflektorplåt 20%, solceller 0%, teflon ~100%, glas 0%, betong 0% (men 100% *återanvändning*).

Resultaten visar att solcellerna står för den största miljöpåverkan inom nästan alla miljöeffektkategorier. Även kopparrören står för en stor del av miljöpåverkan. Glas och betongstativ har medelstor påverkan, och reflektor, gavlar samt receiver står för ganska liten del. Utsläppen av växthusgaser under ett trågs livscykel är ca 300 kg CO_2-ekvivalenter. Under livscykeln använder tråget 9900 MJ energi och producerar 16 700 MJ el samt 48 500 MJ värme. Energi-paybacktiden är ca 3.8 år.

Trågets miljöpåverkan bör kunna förbättras avsevärt. En halvering av miljöpåverkan från solceller, enligt förslag från ECLIPSE, skulle innebära att hela trågets miljöpåverkan minskade, växthusgasutsläppen exempelvis med ca 33%. En anledning till att kopparrören har stor miljöpåverkan i denna LCA är att återvinningsgraden är liten, endast 30%. Återvinningsgrader har stor betydelse, i synnerhet för kompontentsystemen kopparrör, glas och aluminiumreceiver, därför är det viktigt att se till att så mycket som möjligt av komponenterna återvinns. En annan möjlig förbättring är att byta betongstativen mot stålfötter.

Att använda MaReCo ger ungefär lika mycket miljöpåverkan som om man använt motsvarande solceller, monterade utan reflektorer och kylning, för att få samma mängd el. Men MaReCo ger *dessutom* trippla mängden värme. MaReCo förefaller alltså ha en miljömässig fördel gentemot vanliga plana PV-system.

Innehåll

1. Mål och omfattning

1.1. Syfte och målgrupp

Denna studie skall beskriva och kvantifiera miljöpåverkan av solhybriden MaReCo under dess livscykel, utifrån livscykelanalys enligt ISO 14040-14043. Studiens syfte är att visa på den miljöpåverkan som produkten har i olika faser i livscykeln och för de olika komponenter som ingår i produkten. Denna LCA utförs som del av en kurs på LTH och omfattningen är begränsad. Studien är varken tillräckligt bred eller djup för att kunna användas för certifieringsändamål eller mot allmänheten.

Meningen är att resultaten skall kunna underlätta och förbättra miljöarbetet, vid utveckling av produkten och inför eventuell massproduktion av den. Studien skall visa vilka aspekter i livscykeln som har stor påverkan på miljön och energianvändning, så att fortsatt utveckling av produkten och produktionsprocesser skall kunna ta hänsyn till detta. Studien skall även möjliggöra jämförelse med alternativa energisystems miljöpåverkan, i de fall LCA finns enkelt tillgängliga för dessa. Främsta målgrupp är inblandade företag, forskare och produktutvecklare, men studien skall även kunna fungera som en språngbräda för efterföljande LCA på samma eller likartade produkt/-er.

1.2. Övergripande förklaring av produkt och system

Solceller, PV (*photovoltaics*) är en lovande teknik för energiomvandling i framtiden, men är fortfarande för dyr för att vara lönsam (utan bidrag). Framför allt är kostnaden för själva cellerna hög. Principen för ett MaReCo-system är att använda billiga reflektorer och öka solinstrålningen på de dyra cellerna, varmed man avsevärt kan förbättra cellekonomin. Cellerna behöver dock skyddas från överhettning, vilket görs genom aktiv kylning med en vattenslinga, som i en vanlig solfångare. Kylningen av cellerna och den receiver de är monterade på, innebär också uppvärmning av vatten, på samma sätt som i en solfångare. Systemet ger alltså både värme och el, och kallas därför ett *solhybridsystem*, internationellt förkortat *PVT*.

Systemet MaReCo har tagits fram av Vattenfall Utveckling AB och en kommersialisering av produkten utreds nu av Priono AB, vilka har tagit över utvecklingen av dito.

En MaReCo-hybridsolfångare består av en lång parabolisk reflektor i aluminiumbelagd stålplåt, byggd kring en receiver av aluminium med solceller monterade på. Receivern är fäst på kopparrör, vilka leder kylvatten. De delar av receivern som inte är täckt av solceller, målas med en högabsorberande färg för att fånga upp maximalt med solstrålning. Runt receivern spänns ett tält av teflonfilm upp, för att ytterligare minska värmeförlusterna. Framtill på solfångaren finns en anti-reflexbehandlad glasskiva. En solfångarenhet med reflektor, receiver, glas och tillbehör kallas i texten ett *tråg*.

1.3. Omfattning, funktionell enhet och systemgränser

1.3.1. Studiens omfattning

Studien beskriver miljöpåverkan för ett MaReCo-trågs hela livscykel, från råvaruutvinning till resthantering.

MaReCo byggs i flera delar, som sedan monteras ihop på plats. Det är därför naturligt att i tillverkningsskedet studera varje komponent för sig, och först se solfångaren som en helhet under användningsfasen. Monteringen av solfångaren kräver främst mankraft, vilken antas ha liten miljöpåverkan men stor osäkerhet och stora lokala skillnader. Denna fas av livscykeln har därför inte beaktats.

Till hybridsolfångaren behövs system för att ta till vara el och värmeenergi. Systemen dimensioneras efter hur många solfångare som används, men kvoten energisystem/solfångare (avseende miljöpåverkan) blir sannolikt mindre med fler solfångare (större ackumulatortankar, t ex, ger mer volym per insats tankmaterial). Eftersom systemens storlek bestäms av kunden och kan variera, är det svårt att veta hur stor påverkan dessa system får. Detta, tillsammans med det faktum att energisystemen är väldigt komplicerade och skulle åtminstone tredubbla LCA:ns omfattning, gör att de inte beaktas i studien. Det finns även en pedagogisk poäng med detta: MaReCo-trågen kan ersätta solceller och solfångare, och då är energiupptagnings- och lagringssystemen samma men själva solcell- och solfångarmodulerna byts ut. För en jämförelse

med systemets närmsta alternativ/konkurrenter är det alltså tillräckligt att se miljöpåverkan av enbart den del av systemet som gör den aktiva solenergiuppfångningen.

1.3.2. Funktionell enhet

Den funktionella enheten för denna studie är **ett MaReCo-tråg** (se beskrivning kap 2).

Under svenska förhållanden uppskattas tråget ge 50 kWh/m^2 elektricitet och 145 kWh/m^2 värme (vid 50°C) per år[1]. Med en bredd på 0.62 m och längden 6 m så motsvarar ett tråg 3.72 m^2 solfångaryta, vilket innebär att årsutbytet blir **186 kWh el** och **539 kWh värme**. Det är dessa energimängder (och kvaliteter) som man bör utgå ifrån vid jämförelser med andra system.

1.3.3. Systemgränser

De delsystem som ingår i studien visas i fig 1.1.

På grund av begränsningar i studiens möjliga omfattningar måste en del delsystem räknas bort. Det finns en mängd komponenter som ingår till liten del i konstruktionen. Dessa är skruvar, fogar, målning av selektiv yta samt kablar och kommer ej att beaktas i denna studie.

De geografiska gränserna är svårdefinierade. MaReCo kan komma att både säljas och tillverkas på flera olika håll i världen. Tänkbara marknader är förutom Sverige de subventionerade marknaderna i Tyskland och Spanien, och även länder som Australien och USA kan vara intressanta. Att trågen tillverkas i flera delar, som inte behöver passera genom samma fabrik, gör att tillverkningen kan bli vida utspridd. Tillverkning av solceller sker på ett fåtal fabriker i världen, men kopparrör och glas skulle kunna tillverkas på många olika håll. I denna studie har valts att utgå ifrån de tillverkare som tidigare anlitats eller som just nu planeras att anlitas. Detta ger hög säkerhet och bättre möjligheter att få tag på pålitliga data. Försäljningsområdet begränsas av praktiska skäl till Sverige. I denna LCA används ett ”base case” där

[1] Helgesson m fl, 2004 (2)

tråget placeras i Malmö (markfast), och transportsträckor beräknas utifrån detta.

Tidsmässigt så skall hela livscykeln tas med. Den börjar vid råvaruutvinning (el. återvinning) och slutar vid sluthantering. Livslängden antas vara densamma som brukar vara normalt för solceller, dvs 25 år. För att systemet skall vara ekonomiskt bärbart så skall skötseln under drift vara minimal och i princip begränsa sig till sällsynta tillfällen av glasputs. Negativ miljöpåverkan under driftsfasen anses vara försumbar. Däremot har systemet en stor ”positiv miljöpåverkan” under driftsfas, i och med att det ger nyttig energi och kan ersätta andra energisystem.

Gränsen mot andra produkters livscykler sätts så att miljöpåverkan av produktionskapitals tillverkning, uppvärmning av lokaler, anställdas resor och liknande försummas. Detta för att de inte bedömts ha stor påverkan och för att studien skall avgränsas till en rimlig omfattning. Som tidigare nämnts så försummas miljöpåverkan av monteringsfasen.

Avgränsningen mot natursystem börjar när jungfrulig råvara hämtas ut jordskorpan, och slutar när materialet sprids i naturen och inte har en toxisk eller annan störande effekt. Glas och metall som slutar i sin ”grav” anses vara ”inert” mot natursystemen.

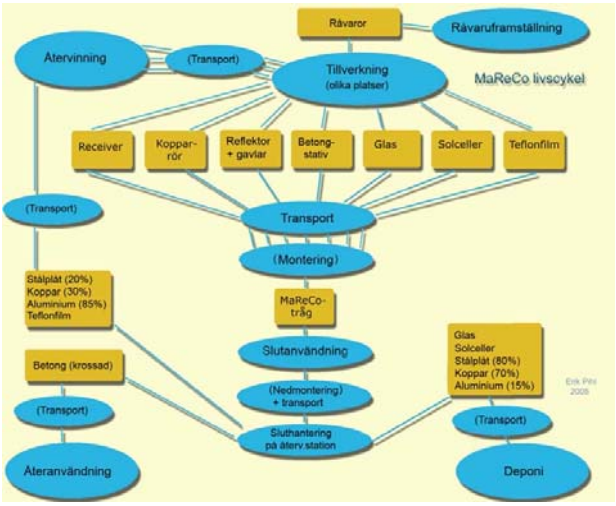

Fig 1.1. Ett MaReCo-trågs livscykel.

1.4.1. Datainsamling och datakvalitet

MaReCo-systemet innehåller en blandning av gammal beprövad, mogen teknik, och teknik som upplever stark utveckling. Starkast utveckling av komponenterna har själva solcellerna, medan stålplåt, glas och kopparör kan betraktas som mogen teknik med relativt liten utveckling. Den princip som valts för insamling av data avseende ålder är att den inte bör vara mer än 5 år gammal, men att extra kraft skall läggas på att hitta information kring PV som inte är mer än 1-2 år gammal. Vid daTabellrist kan upp till 10 år gammal data accepteras för system som kan anses ”mogna”, i de fallen skall detta motiveras.

Äldsta data som används är LCI-data för stål, aluminium och koppar som är nästan 10 år gammal, d v s det äldsta som godtas. Dessa LCI-data används eftersom det är den bästa information som gått att få tag på och eftersom processerna vid tillverkningen inte kan anses ha förändrats dramatiskt de senaste åren

Studien är framåtblickande och till dess att systemet verkligen börjar tillverkas så hinner mycket utvecklas, inte minst inom PV-branschen. För att kunna ta hänsyn till detta så skall studien inrikta sig mot att hämta data från de bästa tillgängliga processerna, snarare än från dagens standardprocesser. Oavsett val av princip så är dock osäkerheten kring processer stor, på grund av den hastigt föränderliga PV-industrin.

1.4.2. Allokeringsprinciper

Den allokeringsprincip som skall vara genomgående för studien är fysisk allokering. Detta eftersom mycket av tillverkning främst är råvaru- och energikrävande och man ganska enkelt kan allokera efter bruk av detta. Studien innehåller dock LCI-data för flera ingående komponenter, och i fall de av väl motiverade anledningar använder andra allokeringsprinciper så innebär det att avvikelser kommer göras från huvudprincipen.

1.4.3. Generella antaganden

Återvinnings- och återanvändningsgrader som antas för de ingående materialen i denna LCA anges i tabell 1.1.

I de flesta tillverkningsprocesserna används el. För komponentsystemen solceller, betong och glas ingår utsläpp från elproduktion i LCI-data, för koppar, aluminium och stålplåt behöver utsläpp från elproduktion beräknas separat, och förs sedan tillbaka till den enskilda komponenten och belastar dess miljödata. I de flesta fall används svensk medelel. Vid beräkning av denna utgås ifrån data från IVL[2].

En viss del norsk medelel, blandad med främst UCPTE-el, används för tillverkning av aluminium. För miljöpåverkan av denna används data från LCA för aluminium[3].

Material	Återvinning (%)	Återanvändning (%)	Deponi (%)
Aluminium	85	0	15
Koppar	30	0	70
Stålplåt	20	0	80
Betong	0	~100	0
Glas	0	0	~100%
Solceller	0	0	~100%
Teflon	~100	0	0

Tabell 1.1. Återvinnings- och återanvändningsgrader som antas för de ingående materialen

2. Beskrivning av MaReCo

Exakt vilken typ av MaReCo som kommer att masstillverkas än ännu inte helt bestämt. Denna studie utgår från en sorts tråg som tagits fram av Vattenfall Utveckling AB 2001-2003[4]. Trågets längd är enligt

[2] IVL, 2001

[3] Sunér, 1996

[4] Helgesson m fl, 2003

rapporten 6 meter, bredden 62 cm (se figur 2.1). Trågen i Vattenfalls projekt saknar dock solceller, men i denna studie räknas med att solceller finns monterade på receivern.

Fig 2.1. Ett MaReCo-tråg. Källa: Helgesson m fl, 2003

2.2. Ingående delar

2.2.1. Solceller

Solcellerna som använts för MaReCo är polykristallina eller enkristallina och tillverkas av GPV[5]. I denna LCA har antagits att enkristallina celler används. Cellerna har storleken 125 mm x 125 mm och för ett tråg där solceller sitter på både fram- och baksida används ca 80 st. Sammanlagda arean blir då 1.25 m^2/FE.

Solceller görs av kisel, av en sort som kallas ”*metallurgical-grade silicon*” och som renas med tekniker som liknar dem inom elektronikindustrin [6]. Kislet får ”växa” till en ”*ingot*” vilken skärs till många 0.25 – 0.35 mm tjocka ”*wafers*”. Wafers *dopas* sedan för att få rätt halvledaregenskaper och när ledarband för elektricitet

Fig 2.2. Solceller på receiver. Källa: Författaren

[5] Karlsson, 2005

[6] Frankl m fl, 2004

satts till är de färdiga *celler*. Därefter sätts flera celler tillsammans till en modul.

LCI-data för solceller baseras på en omfattande LCA från EU:s ECLIPSE-projekt[7]. För studien har använts data som är allmän för celltillverkningsprocesser. Äldst data är från 2001, yngst från 2003. FE är 1 kWh elektrisk energi. Studien utgår från ett base case, som är en takinstallation i Italien. De studerade cellerna har 13% verkningsgrad (=130 W_p/m^2), elproduktionen är 1413 kWh/kW_p,år , cellernas livslängd antas vara 25 år. Detta ger att cellernas elproduktion (i base case) under en livslängd är 4592 kWh/m^2, vilket betyder att FE kan översättas till: $1/4592 = FE = 2.18 \cdot 10^{-4}$ m^2.

Studien är från vagga till grav. Ingen
återvinning har hittills utförts på solceller, därför har denna behandling inte beaktats i LCA:n. Deponi förutsätts. Transportdata är för base case i LCA:n specifik för en anläggning i Italien, därför borde de räknas om att passa för grundfallet i Malmö. Eftersom det emellertid inte specificeras vilka transportdata som kan hänföras till transport till/från uppställningsplats, och transportpåverkan i allt väsentligt är mycket liten i jämförelse med övrig livscykelpåverkan (fr a vid tillverkning), så görs dock ej denna omräkning.

2.2.2. Reflektor och gavlar

Reflektorplåten är av typen Dobel, plastbelagd alumiumfolie laminerad på stålplåt, som görs av SSAB laminated steel och SSAB-tunnplåt[8]. Gavlarna antas vara av samma material. Plåten har dimensionerna 6 m · 1.10 m, med tjockleken 0.5 mm. Gavlarna beräknas vara 1.1 m^2. Filmen som lamineras på plåten består av tre lager: 20 µm PET-plast, 9 µm Al, 23 µm PET. Plåten har en sammanlagd densitet[9] på 7800 kg/m^3, vilket ger en totalvikt per tråg på ca 30 kg/FE.

För miljödata utgås ifrån miljödatablad, vilket är den miljöinformation som går att få från SSAB[10,11]. Databladet är drygt fem år gammalt, men

[7] Frankl m fl, 2004

[8] Larsson, 2005

[9] SSAB, 1999 (1)

[10] SSAB, 1999

anses kunna användas. Detta eftersom tekniken är mogen. Vissa LCI-data hämtas från en LCA för stålplåt, som är specifik för SSAB Tunnplåt[12].

Stålplåten tillverkas i Finspång eller Borlänge och lamineringen görs i Ronneby[13]. Plåten görs av 20% återvunnen och 80 % jungfrulig råvara. I den vanligaste processen så har fästmedel tillsatts på plåtplåten redan vid tillverkning, och vid laminering så förs plåt och plastfilm ihop och hettas upp, varpå fästmedlet aktiveras. I lamineringsprocessen frisätts lösningsmedel. Ångorna tas om hand genom förbränning vid 700°C och 99% av lösningsmedlen förbränns fullständigt. Innan lamineringen så tvättas plåten. Speciella reningsanordningar tar hand om tvättvätskorna och minimerar utsläpp av metaller, fasta partiklar mm.

Filmen är en specialfilm som tagits fram för denna reflekterande plåt. Miljödata på filmen har inte gått att få tag på.

Energi till processerna kommer i huvudsak från gasol (70%) och el (30%)[14]. Värme från förbränningen av lösningsmedel används för att minska användningen av LP-gas.

2.2.3. Glas

Glaset är av en speciell anti-reflexbehandlad typ med låg järnhalt, som tillverkas av Sunarc[15]. Det är specialdesignat för att släppa igenom ca 5 procentenheter mer ljus än vanligt glas med låg järnhalt[16]. Glasskivan (egentligen flera sammansatta glasskivor) har dimensionerna 6 m · 0.62 m = 3.72 m^2/FE. Glasskivan som används är 3-4 mm tjock.

Tyvärr har inte specifik data kunnat fås från Sunarc. Därför har en LCA för avancerad fönsterteknik[17], gjord inom ramen för EU-projektet

[11] SSAB, 2005 (2)

[12] Sunér, 1996

[13] SSAB, 1999 (1)

[14] SSAB, 1999 (1)

[15] Byström, 2005

[16] Sunarc, 2005

[17] Citherlet m fl, 2000

IMAGE, utgåtts ifrån. LCA:n är för hela fönster och i de data som presenteras för glasdelen av ett fönster, så innefattas även gaser i mellanrummen och andra små komponenter. Dessa har bedömts ha så liten påverkan på slutresultatet att LCI-data kunnat användas i denna studie.

Funktionell enhet är 1 m^2 glasyta med 4 mm tjocklek. LCA:n beskriver miljöpåverkan från vaggan till graven, glasets livslängd antas vara >25 år. Allokeringsprincip finns ej redovisad. Data skall inte vara specifik för en viss anläggning, utan generella medelvärden för europeiskt glas. Data är relativt gamla, LCA:n är från 1998 (men publicerad 2000), men är det bästa som kunnat hittats och beskriver en mogen teknik som inte utvecklas så snabbt.

Den använda LCA:n ger inte detaljinformation utan uttrycker endast resultaten i miljöeffektkategorier som GWP och POCP.

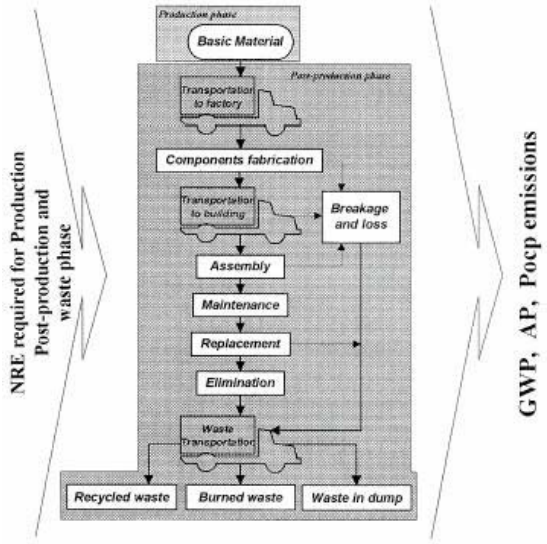

Fig 2.3. Processchema för fönstren som studeras i LCA:n som utnyttjas i denna studie[18].

[18] Citherlet m fl, 2000

2.2.4. Receiver

Solcellerna monteras på en aluminiumprofil, som sätts fast runt kopparrören. Två identiska profiler används, som sätts fast på var sida av kopparrören. Aluminiumprofilen och celler kallas tillsammans för en receiver. Alumiumprofilen tillverkas av Sapa i Vetlanda[19]. Profilen väger 1.256 kg/löpmeter och två profiler löper utmed hela trågets längd, vilket ger att totalvikten är 15 kg/FE.

LCI-data baseras till stor del på en LCA för aluminium[20]. Data avser endast tillverkningen av själva aluminiumet, från vagga till grind, och inte tillverkningen av själva profilen. LCI-data som är mer uppdaterad och även avser profiltillverkning har fåtts från SkanAluminium, men inte hunnit bearbetas i tid för slutförande av denna LCA.

Återvinningsgraden för aluminiumet är svårt att uppskatta innan systemet börjar tillverkas skorskaligt. I denna LCA görs en uppskattning på 85%, vilket är strax under återvinningsgraden för aluminiumburkar idag[21]. Ännu högre återvinningsgrader borde inte vara omöjligt.

Som referens till de resultat som erhållits från Sunérs LCA, så har även en EPD från SkanAluminium avseende aluminiumprofiler använts. Detta redovisas i kap 6.2.

2.2.5. Kopparrör

Kopparrören är av vanlig typ för varmvatten (15 mm) och köps in från grossist, som inte närmare specificerats[22]. För miljödata används LCA för koppar (vagga till grind)[23]. LCI-data för tillverkningsfasen av själva rören har inte kunnat hittas.

[19] Karlsson, 2005

[20] SkanAluminium

[21] Returpack, 2003

[22] Karlsson, 2005

[23] Sunér, 1996

Kopparrören har ytterdiameter 15 mm och innerdiameter 12 mm. Tvärsnittsarean är följaktligen $2.55 \cdot 10^{-4}$ m^2. Rören går dubbelt längs hela trågets längd och sticker ut uppskattningsvis 20 cm på varje sida. Med längden $2 \cdot 6$ m + $4 \cdot 0.2$ m, och med densiteten 8900 kg/m^3 så blir vikten för rören 28 kg/FE.

Koppar tillverkas endast på ett ställe i Sverige och det är på Bolidens smältverk Rönnskär, Skellehamn. Smältverket hanterar även bly och en del andra metaller/metallföreningar i små mängder. I de fall många produkter hanteras i samma smältverk så har man i studien gjort en ekonomisk allokering. Tillräcklig information om tillverkningsprocessen har inte funnits för att göra en god fysikalisk allokering, därför används resultaten oförändrade.
Eftersom användningen av utländsk el är liten (<1%) i jämförelse med den andel som är svensk medelel (största delen av utländska elen är norsk medelel, som är jämförbar med svensk med stor andel vattenkraft), så approximeras i följande beräkningar att elförbrukningen är enbart svensk medelel. Att ha uppdaterad data på (enbart) svensk medelel antas ge säkrare resultat, än att ha gamla data på den verkliga elmixen.

Andelen återvunnen råvara i kopparrören antas vara ca 30%.

2.2.6. Teflonfilm

Runt receivern sitter en film av teflon som förmodas tillverkas av Du-Pont. Filmen står för en liten massandel av tråget, uppskattningsvis inte mer än någon procent. På grund av detta och svårigheter att hitta LCI-data, görs enbart en kvalitativ analys av produktens toxicitet och liknande egenskaper, och ingen kvantitativ analys av effekter såsom utsläpp av växthusgaser.

Fig 2.4. Teflontält över receiver. Källa: Helgesson m fl, 2003

2.2.7. Betongstativ

Två olika monteringsanordningar kan användas för trågen. Om de är markmonterade används betongstativ, för takmontering rekommenderas EPS-fötter klädda med standardplåt[24]

För ett tråg behövs två betongstativ (se figur 2.5) som väger ca 100 kg var, dvs 200 kg betong går åt per FE[25]. För att uppskatta stativens miljöpåverkan användes en LCA för betong från 2005[26]. LCA:n sträcker sig från vaggan till graven, men inkluderar ej bruksfas (antas ha försumbar miljöpåverkan). Data för produktion är från 2002 och specifik för tillverkning i företaget Cementa AB, som har moderna anläggningar. Övrig viktig LCI-data är från 2000-tal eller sent 1990-tal och avser relativt moderna processer. Allokeringsprincip redovisas inte tydligt. Inte heller anges någon livslängd. Här antas att stativen har en livslängd som är (minst) lika lång som trågets, och att fundamenten rivs när tråget demonteras.

Betong görs av en blandning av cement, ballast, bindemedel och vatten[27]. Cement tillverkas av $CaCO_3$ som bränns till CaCO och koldioxid (här uppstår alltså betydande CO_2-utsläpp). Ballast görs av grus och krossad sten (makadam). Utöver detta ingår vatten, och ett kemiskt bindemedel (*superplasticizers*) som minskar vattenbehovet och därmed ger ökad styrka. Innehållet i en kubikmeter betong anges i tabell 2.1.

	kg/m^3	%
Cement	295	13
Macadam	749	32
Gravel	1093	47
Bindemedel	1.51	0.06
Vatten	202	8.6

Tabell 2.1. Innehållsförteckning för betong (C20/25 16 S4), innehåll per m^3 betong[28].

[24] Karlsson, 2005 (1)

[25] Karlsson, 2005 (2)

[26] Sjunnesson, 2005

[27] Sjunnesson, 2005

[28] Sjunnesson, 2005

2.3. Restprodukthantering och återvinning

Tråget antas bli slutbehandlat på Ragn-Sells avfallsstation i Bromölla (den som är närmast Malmö), och så långt som möjligt skall ingående delar återvinnas. Detta torde vara möjligt i mycket hög grad för metallkomponenter och glas.

För vissa komponenter, såsom koppar och stål, så ingår återvinning till viss del i beräkningarna av materialproduktion. För dessa komponenter har samma återvinningsgrader använts som i de använda studierna, i de fall återvinning beräknats med i tillverkning, för att kunna använda data från tillverkningen. Data över återvinningsgrader för de olika materialen redovisas i tabell 1.1 (avsnitt 1.4.3).

Betong kan inte återvinnas, men däremot ofta återanvändas[29]. Det körs till en återvinningsstation där man tar bort ev. armeringsjärn och krossar betongen till lämplig storlek. Den krossade betongen kan användas i fyllningsarbeten mm. Solceller är en relativt ny teknik och inga uppgifter finns om återvinning, därför förutsätts deponi. Detta bör kunna komma att förändras i framtiden.

Eftersom någon data för återvinning av planglas inte kunnat hittas så antas i detta fall 100% deponi. Detta bör ses som ett ”worst case” och har viss negativ påverkan på trågets miljödata.

3. Inventering

I detta kapitel presenteras resultat av inventering för miljöpåverkan av tråget under dess livscykel. Värden redovisas per FE. En sammanvägning av miljöpåverkan i kategorier redovisas i kapitel 4.

3.1. Tillverkning

Tillverkning innefattar miljöpåverkan för komponenterna, från vaggan till det att tråget står monterat.

[29] Sjunnesson, 2005

3.1.1. Solceller

LCI-data för tillverkning av solceller visas i tabell 3.1. Detaljerad information om miljöpåverkan återfinns i Appendix B.

Betydande resurs-förbrukning	**Förbrukning, (kg/FE)**	***Utsläpp till luft***	**Utsläpp, (kg/FE)**
Silver	0.0085	CO_2	186 000
Kol	51	SO_2	770
Koppar	0.034	CH_4	540
Råolja	9.0	Partiklar	76
Brunkol	36	NO_x	390
Naturgas	27	Halog. kolväten, klorfluorkarboner	$3.0 \cdot 10^{-02}$
Platinum	3.0 E-09	NH_3	1.1
Kisel (*Silicon*)	2.5	Halog. kolväten, bromerade	$1.9 \cdot 10^{-03}$
Uranium	0.0031	Halog. kolväten, klorväteflourkarboner	$1.9 \cdot 10^{-02}$
		Metan, tetrakloro-, CFC-10	$3.1 \cdot 10^{-02}$
Utsläpp till vatten	**Utsläpp, (g/FE)**	***Utsläpp till mark***	**Utsläpp, (g/FE)**
NH_3	3.1	As	$2.9 \cdot 10^{-04}$
COD	5.0	Cd	$6.4 \cdot 10^{-06}$
N (aq)	7.2 E-04	Cr	$3.7 \cdot 10^{-03}$
Phosphate	4.8	Pb	$3.7 \cdot 10^{-03}$
		Miner.oljor. ospec	0.20

Tabell 3.1. LCI-data för tillverkning av solceller.

Värt att notera är att vid tillverkning av celler till 1 FE släpps det ur Radon-222 i omfattningen 172 000 kBq!

3.1.2. Reflektor och gavlar

Data finns för den färdiglaminerade Dobel-plåten, exkl film, med 20% återvinning från stålskrot. Huvudsaklig miljöpåverkan visas i tabell 3.2. Mer detaljer finns i Appendix A + B.

	Förbr/FE	*Utsläpp till atmosfär*	Utsläpp, (g/FE)
El (svensk medel~)	21.18 MJ	CO_2	4600
Järnmalm	66 kg	Total HC	9.9
Kol	17.4 kg	NO_x	3.9
Kalksten	3.12 kg	Partiklar	0.103
LP-gas	49.8 MJ	CO	0.81
Energi – fossil	13 MJ	SO_2	0.23
Energi-tillvaratagande	**Tillv/FE**	***Utsläpp till vatten***	**Utsläpp, (mg/FE)**
Varmvatten	2.7 MJ	Fasta partiklar	33
		Fluorin	75
		Metaller	12

Tabell 3.2. Miljöbelastning för Dobel-plåt till receiver, vagga till grind.

3.1.3. Glas

I LCA för glas så anges miljödata endast direkt i miljöpåverkanskategorier. Mer detaljerad data än vad som redovisas här har inte kunnat fås tag på, därför presenteras *inte* någon ytterligare information i Appendix. Livscykeldata vagga till grav:

Kategori:	Miljöpåv. per m^2 glas	Miljöpåv. per FE
Växthuseffektpåv. (GWP)	16 500 g eq. $CO_2/(m^2)$	**24 000** g eq.CO_2
Försurningspåv. (AP)	60 g eq. $SO_x/(m^2)$	**220** g eq. SO_x
Fotokem. oxid. (POCP)	6.0 g eq. $C_2H_4/(m^2)$	**22** g eq. C_2H_4
Icke-förnybar energi (NRE)	240 MJ/(m^2)	**890** MJ

Tabell 3.3. Miljöpåverkansdata för glas under hela livscykeln[30].

3.1.4. Receiver

Nedan finns data för produktion av aluminium från jungfrulig råvara. Räknar med endast 15% nyframställning av aluminium enligt nedanstående data (p g a 85% återvinning). Utsläpp per tråg är alltså utsläpp associerade till 15% av receiverns vikt, d v s 2,25 kg.

[30] Citherlet m fl, 2000

Detaljerad data finns i appendix B.

Energiförbrukning	**Förbr, (MJ/FE)**		***Resursanvändning***	**Förbr, (g/FE)**
El (norsk medel~)	117,45		Bauxit	11070
El (UCPTE)	5,3325		Kalksten	1986,75
Råolja	47,925		Råolja	1167,75
Energi - fossil	10.2			
Diesel (båt)	20,52		***Utsläpp till atmosfär***	**Utsläpp, (g/FE)**
Kol	7,11		CO_2	10500
Utsläpp till vatten	**Utsläpp, (g/FE)**		SO_2	54,4
COD	83,7		NO_x	31.1
SO_2 (aq)	18,675		CO	4.41
Tot-F (aq)	3,7125		HC	4.2
BOD	3,555		Partiklar	63,7
TOT-N	0,0234		Tot-F	0,9675
			CH_4	0,25
			PAH	0,135225
			SO_x	0,0144
			N_2O	0,0036675
			VOC	0,0027
			HCl	0,0006525
			NH_4NO_3	0,000216675
			NH_3	0,00015975

Tabell 3.4. LCI-data för tillverkning av aluminium från jungfrulig råvara.

3.1.5. Kopparrör

Data för huvudsaklig miljöpåverkan av koppartillverkning, med ca 30% återvinning av koppar från skrot står i tabell 3.6. Mer detaljerade uppgifter finns i Appendix B.

Resursförbrukning	**Förbr, (g/FE) alt (MJ/FE)**		***Utsläpp till atmosfär***	**Utsläpp, (g/FE)**
El (svensk medel~)	1010 MJ		CO_2	18 700
Diesel	149 MJ		SO_2	450
Vatten	171 000		NO_x	230
Cu	24 000		CO	48
Calcit	7 400		HC	34
Naturgas	2000 MJ		Partiklar	28
Bauxit	690		CH_4	10.8
Råolja	290 MJ		NH_4NO_3	2.4
Fossil energi	25 MJ		SO_x	1.69
			NH_3	1.4
Utsläpp till vatten	**Utsläpp, (g/FE)**		N_2O	0.72
NH_4NO_3	8.6		Dioxin (TCDD-ekv)	$3.5 \cdot 10^{-6}$
NO_3-N	6.5			
NH_4-N	5.8			
Tot-N	$1.86 \cdot 10^{-3}$			
HNO_3 (aq)	0.118			
NH_3 (aq)	0.062			
COD	0.026			

Tabell 3.6. LCI-data för tillverkning av koppar till rör.

3.1.6. Teflonfilm

Teflon PFA-film består till 100% av polymeren Tetrafluoretylen-Perfluor(Propyl Vinyl Eter) [31] . Teflon är inert vid normala rumsförhållanden. Vid förbränning kan farliga ångor uppkomma, alla är inte närmare specificerade. Vid ofullständig förbränning bildas kolmonoxid och vätefluorid. Förbränningsångor kan ge polymerfeber hos människor. Produkten har inga kända ekotoxikologiska effekter.

Att förbränna eller deponera Teflonfilmen rekommenderas inte. Filmen går att återvinna. Om återvinning inte är lämpligt bör den i första hand deponeras.

[31] Du Pont, 2001

3.1.7. Betongstativ

Data för huvudsaklig miljöpåverkan av tillverkning av betongstativ finns i tabell 3.7. Mer detaljerade uppgifter finns i Appendix B.

Resursförbrukning	**Förbr, (MJ/FE)**		***Utsläpp till luft***	**Utsläpp, (g/FE)**
Kol	48		CO2	25 600
Koks	12.9		CO	7.4
Diesel	2.0		NO_x	83
Olja	1.38		SO_x	3.4
Naturgas	1.06		SO_2	1.84
Bildäck	12.6		CH_4	66
El	15.6		HC	6.9
Energi - fossil	122		Partiklar	2.6
			NH_3	0.71
Utsläpp till vatten	**Utsläpp, (g/FE)**		N2O	$7.8 \cdot 10^{-3}$
Tot-N	$9.6 \cdot 10^{-5}$		halon-1301	$1.0 \cdot 10^{-6}$
Tot-P	$1.1 \cdot 10^{-5}$			
COD	$9.1 \cdot 10^{-5}$			
PAH	$3.0 \cdot 10^{-6}$			

Tabell 3.7. LCI-data för betongstativ till ett tråg.

3.1.8. Elproduktion

Användning av el, för de komponentsystem där elanvändning ej beaktats i LCI-data, redovisas i tabell 3.8.

Tillverkning:	**Elförbrukning (MJ/FE)**	**Elsort**
Kopparproduktion (rör)	1010	Svensk medelel
Aluminiumprod (reciever)	*122.8*	*Elmix, främst Norsk medelel*
Reflektor&gavlar	21.18	Svensk medelel
Återvinning:		
Aluminiumåtervinning	11.5	Svensk medelel

Tabell 3.8. Användning av el fördelad på komponent

Utsläpp från förbrukning av svensk medelel redovisas i tabell 3.9.

	Per 1 MJ[32]	*Kopparrör*	*Refl&gavlar*	*Alum. återv.*
Resursanv	**Anv/ MJ**	**Anv/FE**	**Anv/FE**	**Anv/FE**
Tot. Resursanv (MJ)	0.032	32	0.68	0.37
Uranmalm 0.3% U, (g)	0.71	720	15	8.2
Uranmalm 1.6% U, (g)	0.084	85	1.78	1.0
Utsläpp till luft	**Utsläpp, (g/FE)**	**Utsläpp, (g/FE)**	**Utsläpp, (g/FE)**	**Utsläpp, (g/FE)**
NO_x	0.015	15.2	0.32	0.173
SO_x	0.013	13	0.28	0.150
CO	0.018	18.2	0.38	0.21
HC	$2.9 \cdot 10^{-3}$	2.9	0.061	0.033
CO_2	7.8	7900	166	90
N_2O	$7.1 \cdot 10^{-4}$	0.72	0.015	$8.2 \cdot 10^{-3}$
CH_4	0.049	49	1.038	0.56
Partiklar	$2.5 \cdot 10^{-3}$	2.5	0.053	0.029
NH_3	0.22	220	4.7	2.5

Tabell 3.9. Utsläpp från elförbrukning (svensk medelel) för olika komponenter.

Utsläpp från förbrukning av norsk medelel mm, avseende endast aluminiumproduktion, redovisas i tabell 3.10.

[32] IVL, 2001

Resursanv	**Förbr, (g/FE) alt (MJ/FE)**		***Utsläpp till luft***	**Utsläpp, (g/FE)**
Kol	159		CO2	780
vattenkraft	118 MJ		SO2	4.3
Olja	37		HC	3.3
Naturgas	31		NO_x	2.1
Förnybar energi	0.052		CO	0.54
Torv	$9.41 \cdot 10^{-3}$		Partiklar	0.34
Uran	$2.27 \cdot 10^{-3}$		N_2O	0.110
			Aldehyder	$4.1 \cdot 10^{-3}$
			NH_3	$8.0 \cdot 10^{-4}$
			Fluorider	$1.55 \cdot 10^{-5}$
			CH_4	$3.1 \cdot 10^{-6}$

Tabell 3.10. Utsläpp från elproduktion, för tillverkning av aluminium[33].

3.2. Användarfas

För att systemet skall vara ekonomiskt skall underhåll under driftsfasen vara minimal och tråget mer eller mindre sköta sig självt. Negativa miljöeffekter av driftsfasen har därför försummats. ”Positiva” miljöeffekter redovisas i kap 4.4.

3.3. Resthantering och återvinning

3.3.1. Hantering av tråget

Tråget körs i ”base case” till Ragn-Sells avfallsstation i Bromölla för nedmontering. LCI-data för miljöpåverkan av denna transport finns i tabell 3.11. Se Appendix A för detaljer.

[33] Sunér, 1996

Resursanvändning:	**Anv/FE**	
Energi – fossil	82	MJ
Utsläpp till atmosfär:	**Utsläpp per FE**	
fossil CO_2	4 900	g
NOx	44	g
HC	4.3	g
PM	0.69	g
CO	4.72	g
SO_2	1.23	g

Tabell 3.11. Miljöpåverkan av transport av helt tråg till avfallsstation, Bromölla.

3.3.2. Solceller

Miljöpåverkan för sluthantering av solceller finns i tabell 3.12. Detaljerad data finns i Appendix C.

Resursförbrukning	**förbrukn, (kg/FE) resp (Nm3/FE)**
Kol	0,00116
Råolja	0,05545
Brunkol	0,00093
Naturgas	0,000154818 Nm3
Uranium	6,40E-08
Utsläpp till vatten	**Utsläpp, (g/FE)**
NH3	5,95E-03
COD	1,06E-02
PAH	3,63E-05

Utsläpp till atmosfär	**Utsläpp, (g/FE)**
CO2, fossil	191,52
SO2	0,14
NH3	1,50E-05
Nox	3,14
CH4, fossil	0,22
Partiklar	6,00E-02

Fig 3.12. Miljödata för sluthantering av solceller.

3.3.3. Aluminium

LCI-data finns i tabell 3.13 och avser återvinning av aluminium motsvarande 85% av receiverns aluminiumprofil, dvs 12.75 kg. Detaljerade data återfinns i Appendix C.

Energianvändning	**Användn. (MJ/FE)**		***Resursförbrukning***	**Förbr, (g/FE)**
El (svensk medel~)	11.5		Cybernit	2100
El (Tysk medel~)	0.62			
Brännolja (Eo1)	63		***Utsläpp till atmosfär***	**Utsläpp (g/FE)**
Diesel	6.4		CO_2	5900
Naturgas	0.05		SO_2	12.9
Propan	1.3		NO_x	9
Råolja	0.0138		CO	2
			HC	1.95
Utsläpp till vatten	**Utsläpp (g/FE)**		Partiklar	3.38
Sludge	340			
Saltavfall	3200		CH_4	0.25
Avfall	420		SO_x	0.166
			N_2O	0.029

Tabell 3.13. Data för återvinning av aluminium[34].

3.3.4. Betong

Miljöpåverkan för rivning av betong finns i tabell 3.14.

	per kg	per FE
Diesel (MJ)	$7.0 \cdot 10^{-3}$	1.4
CO2	0.54	108
CO	$9.0 \cdot 10^{-5}$	0.018
NOx	$5.3 \cdot 10^{-3}$	1.06
SOx	$2.8 \cdot 10^{-4}$	0.056
CH4	$1.0 \cdot 10^{-5}$	$2 \cdot 10^{-3}$
HC	$3.1 \cdot 10^{-4}$	0.062

Tabell 3.14. Resursåtgång och miljöutsläpp vid rivning av 1 kg / 1 FE betong (=2400 kg/m^3)[35].

[34] Sjunnesson, 2005

[35] Sjunnesson, 2005

4. Miljöpåverkansbedömning och resultat

4.1. Karaktärisering

Utsläpp/användning av ämnen/resurser vägs samman till ett fåtal miljöpåverkanskategorier (se nästa rubrik). För att beräkna ett ämnes bidrag i en viss kategori multipliceras mängden med nyckeltal, enligt bestämda Tabelleller. Använder i denna LCA tabeller från ”The Hitch Hiker's Guide to LCA”[36].

Energiresurser som angivits i vikt eller Nm^3 måste räknas om till MJ. För detta används Tabellellsamling[37] över värmevärden. Värden som använts redovisas tabell 4.1. Energiresurser som använts i icke-energiändamål (exempelvis kol i stålframställning) redovisas som energianvändning.

Energiresurs	Värmevärde, (MJ/kg)
Naturgas	50 (43 MJ/Nm^3)*
Stenkol	34
Brunkol	18.9
Olja	42**
Eldningsolja	42
Diesel	42**
Torv	15.5
Bensin	44

Tabell 4.1. Värmevärden för fossila bränslen.

* Uppgift från ”Energigasteknik”[38]
**Uppskattat

4.2. Miljöpåverkanskategorier

Miljöpåverkan av trågets livscykel har bedömts utifrån följande miljöpåverkanskategorier:

Energi

[36] Baumann & Tillman, 2004

[37] Mörtstedt&Hellsten, 2003

[38] Näslund, 2003

Anger hur mycket energi (både förnyelsebart och icke-förnyelsebart) som använts för produktion, transport osv. Anges i **MJ**.

GWP – Global Warming Potential
Visar utsläpp av gaser som har klimatpåverkan genom ökning av växthuseffekt. Olika gaser har olika klimateffekt beroende av vilken tidshorisont man har, d v s hur långt framåt i tiden man räknar. Exempelvis har vissa gaser en väldigt kraftig växthuseffekt men kort livslängd, och ger därför högre värden för korta tidshorisonter, medan andra kan vara allvarliga klimatgaser p g a sin persistens. Här används 100-årigt scenario. Anges som **kg CO_2**-ekvivalenter.

POCP – Photochemical Ozone Creation Potential
Visar utsläpp av ämnen som kan bidra till bildning av marknära ozon. För effekten har närvaron av NO_x betydelse. Här antas hög bakgrundskoncentration av NO_x. Anges som
g C_2H_2-ekvivalenter

EP – Eutrophication Potential
Visar utsläpp till luft och vatten som har övergödande verkan på hav och sjöar. Anges som
g PO_4^{3-}-ekvivalenter.

AP – Acidification Potential
Visar utsläpp till luft och vatten som har försurande verkan på mark, vattendrag och sjöar. Anges som **g SO_2**-ekvivalenter.

Utsläppen av ozonförstörande gaser anges sällan/otydligt i källor och kategorisering i ODP görs ej. Effekter av markanvändning och toxicitet studeras inte.

4.3. Sammanställning miljöpåverkan

I tabell 4.1 redovisas trågets sammanlagda miljöpåverkan, i de fem studerade kategorierna, uppdelat i de olika komponentsystemen. Högsta värdena per kategori är fetmarkerade.

	Celler		Receiver		Reflektor	Rör	Betong		Glas	Tråg	
	Tillv	*Slut-beh*	*Jungfr råvara*	*Återv*	*Stål-plåt*	*Koppar*	*Tillv*	*Slut-beh*	*Livsc*	*Slut-beh*	
Ener.	**4200**	2.4	210	70	710	3500	220	1.40	890	82	MJ
GWP	**197**	0.196	11.3	6.0	5.0	28	27	0.108	24	4.9	kg ekv CO_2
POCP	**40**	0.008	3.0	0.69	0.057	24	0.69	0.0005	22	0.19	g ekv C_2H_2
EP	57	0.41	6.2	2.1	2.2	**114**	11	0.138	-	5.7	g ekv PO_4^{3-}
AP	**1050**	2.3	100	24	12.0	**1050**	62	0.74	220	32	g ekv SO_2

Tabell 4.1. Trågets miljöpåverkan indelat i miljöeffektkategorier, per komponentsystem.

*Exkl. uran

Tabellellen nedan visar trågets totala miljöbelastning i de fem studerade kategorierna. Som referens visas miljöpåverkan av ett plant system (dubbla cellarean) som ger samma mängd el (men ingen värme):

	MaReCo	Plan PV	
Energi	9900	8500	MJ
GWP	304	390	kg ekv CO_2
POCP	90	80	g ekv C_2H_2
EP	199	114	g ekv PO_4^{3-}
AP	2500	2100	g ekv SO_2

Tabell 4.2. Miljöpåverkan av tråget, samt referenssystem (plan PV), indelat i miljöeffektkategorier.

För tråget finns under driftsfasen en ”positiv” miljöeffekt , nämligen att tråget omvandlar solstrålar till nyttig energi. Det årliga utbytet för MaReCo är som tidigare nämnt 186 kWh el och 539 kWh värme (se kap 1.3.2). Med 25 års livslängd så ger tråget 4650 kWh el och 13 500 kWh värme, vilket motsvarar ca **16 700** MJ **el** och **48 500** MJ **värme**.

Med energianvändningen 9900 MJ för tillverkning och energiomvandling enligt ovan så är trågets energi-”payback”-tid ca 3.8 år

4.4. Resultat

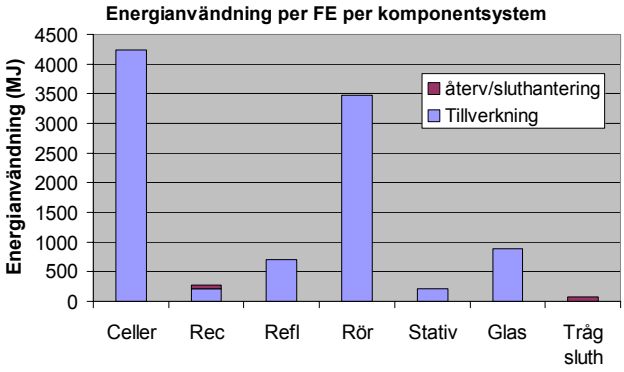

Fig 5.1. Energianvändning under trågets livscykel, uppdelat per komponent-system.

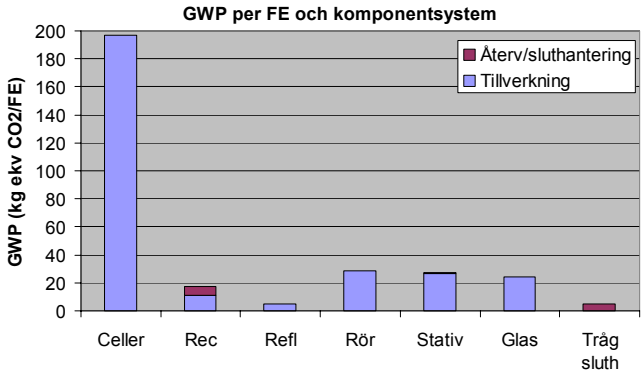

Fig 5.2. Växthuseffektpåverkan av tråget under livscykeln, uppdelat per komponentsystem.

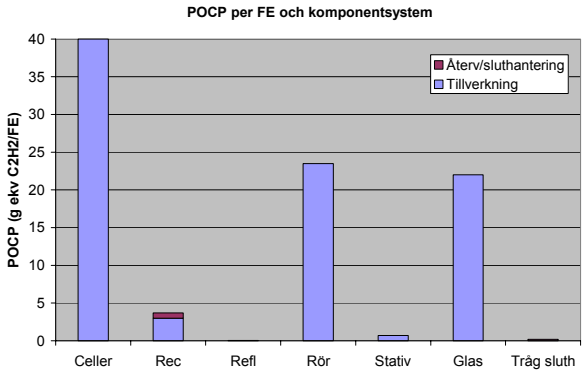

Fig 5.3. Potential att bilda marknära ozon under trågets livscykel, uppdelat per komponentsystem.

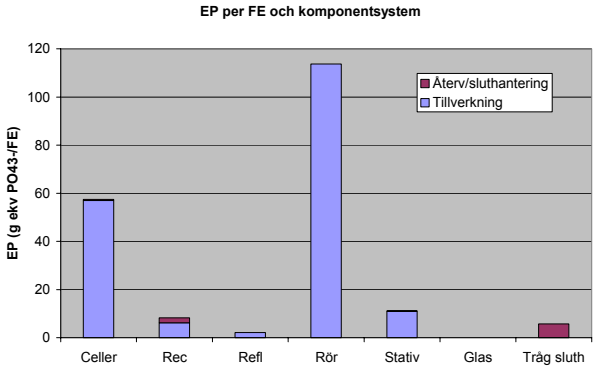

Fig 5.4. Eutrofierings-påverkan av tråget under livscykeln, uppdelat per komponentsystem.

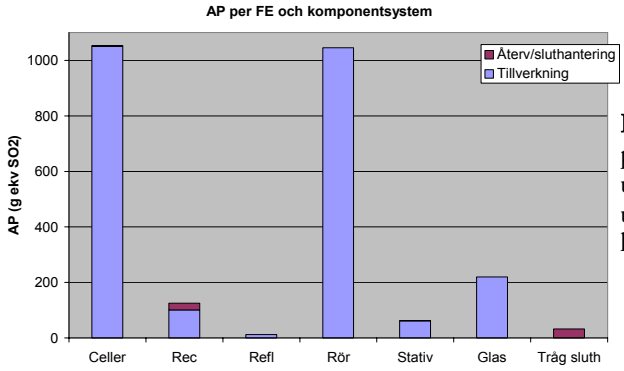

Fig 5.5. Försurnings-påverkan av tråget under livscykeln, uppdelat per komponentsystem.

6. Tolkning

6.1. Datakvalitet och dataluckor

Datakvaliteten i denna studie varierar. För vissa komponenter har relativt bra data hittats, för andra är data äldre, mindre specifik och/eller mindre fullständig.

LCI-data för glas är relativt osäker och den LCA som gjorts för glas är inte särskilt transparent. Den är inte specifik för den process som skall användas, och är relativt gammal (>5 år). LCI-data för koppar, aluminium och stål är ännu äldre, men däremot bättre, mer specifik för denna studie och är mer transparent utförd.

Data saknas för PET-Al filmen som lamineras på reflektor-stålplåten. Filmen utgör en ganska liten del av tråget (< 1%) och borde inte ha så stor betydelse på slutresultatet.

Data saknas för tillverkningsfasen av aluminiumreceivern och kopparrören. Framställningen av själva aluminiumet antas ha betydligt större miljöpåverkan är bearbetning till färdig profil, i synnerhet energimässigt, men sannolikt är inte profiltillverkningsdelen helt försumbar. Samma antas gälla för kopparrören.

6.2. Jämförelse med alternativa data

För aluminium finns alternativa miljödata att tillgå, i en EPD från SkanAluminium[39]. Till skillnad från den LCA som använts i denna studie, så är metod inte tydligt redovisad i EPD:n utan endast resultat. Däremot har den en fördel gentemot Sunérs LCA genom att den täcker hela livscykeln från vagga till grav (dvs även inkluderar profiltillverkning etc) och är mer uppdaterad. Värdena är allmänna för aluminiumbranschen, men SAPA är medlemsföretag i SkanAluminium så värdena borde vara relativt representativa för detta företag. Resultat av jämförelse mellan Sunérs och SkanAluminiums data finns i figur 6.1.

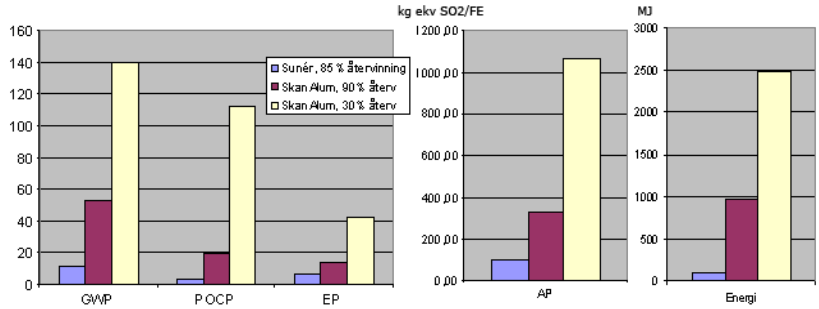

Figur 6.1. Jämförelse mellan resultat från Sunérs LCA och SkanAluminiums EPD.

Tydligen finns en stor skillnad mellan de båda studiernas resultat. De är dock svåra att jämföra rakt av, eftersom det är osäkert hur EPD:n är utförd. Därför har också Sunérs resultat använts i denna studie. Man kan antaga att sanningen ligger någonstans mitt emellan, men det viktigaste slutsats som kan dras är ändå att osäkerheten är mycket stor.

[39] SkanAluminium, 2000

6.3. Gränsdragningar och avvikelser

Komponenter som finns i liten mängd i tråget, ex kablar, skruvar mm har försummats.

Underhåll under driftsfasen, såsom glasputs, har försummats. Likaså har störningar, som t ex förstörelse av glas eller brand i celler, inte medräknats eftersom osäkerheten kring störningsfrekvens är mycket stor.

För kopparrör frångås principen om fysikalisk allokering. Detta eftersom ekonomisk allokering använts i för att få fram LCI-data och tillräcklig kunskap om processen inte funnit för att göra annan allokering och räkna om resultaten. Samma gäller för solceller.

På grund av tids- och databrist beräknas inte utsläpp från alla transporter. Detta gäller transport av komponenter under 15 kg, som inte beaktas inom studerade LCA, samt transport till deponi och återanvändning.

6.4. Osäkerhetsanalys

I tabell 6.1. visas kvalitativ uppskattning över osäkerhet i LCI-data för de olika komponentsystemen.

Komponentsystem	Osäkerhet	Känslighet
Solceller	Medel	Stor
Receiver	Stor	Stor
Reflektor och gavlar	Medel	Liten
Kopparrör	Stor	Stor
Betong	Liten	Medel
Glas	Stor	Medel
Sluthantering av tråg	Medel	Liten

Tabell 6.1. Analys av osäkerhet och känslighet i LCI-data för varje komponentsystem.

Osäkerheter beror i fallet med rör och receiver på att data saknas för delar av livscykeln, samt att källorna är gamla. För glas är huvudproblemet att den studerade analysen har dålig transparens och inte redovisar detaljerade resultat, utan endast visar resultat som grafisk

presentation i miljöeffektkategorier. För solceller är data mycket exakta, men viss osäkerhet ligger i den snabbt skiftande teknikutvecklingen, samt de många olika alternativen vid val av celler.

6.5. Känslighetsanalys

I följande känslighetsanalys uppskattas hur stor påverkan förändringar i ett enskilt komponentsystem har på trågets totala miljöpåverkan (se tabell 6.1.).

Solcellerna svarar för en stor del av miljöpåverkan, och förändringar här slår igenom tydligt. I ett framtidsscenario för enkristallina solceller, med bland annat bättre intern kiselåtervinning och bättre verkningsgrader, bedömer man att utsläppen drastisk kan minska[40]. Bland annat kan utsläppen av växthusgaser minskas med ca 50%. Med en halvering av GWP för solcellerna, så skulle trågets totala GWP minska med ca 33%.

I tabell 6.2 kan man se effekter av minskad miljöpåverkan från enskilda komponentsystem på trågets totala påverkan i miljöpåverkanskategorier. Minskningen av komponentsystemens påverkan baseras på grova antaganden och skall bara ses som exempel.

	Minskn (%)	**Minskn av energi (%)**	**Minskn av GWP (%)**	**Minskn av POCP (%)**	**Minskn av EP (%)**	**Minskn av AP (%)**
Celler	*50*	21	32	22	14.4	21
Koppar-rör	*60*	21	4.5	15.6	34	25
Alumin-ium	*10*	0.28	0.57	0.40	0.41	0.49
Stativ	*50*	1.25	4.5	0.39	2.8	1.22
Reflekto r	*40*	2.87	0.62	0.025	0.44	0.19
Glas	*50*	4.5	3.9	12.2	-	4.3

Tabell 6.2. Effekter av procentuell minskning av miljöpåverkan i varje komponentsystem.

[40] Frankl m fl, 2004

7. Diskussion och slutsats

Att göra denna LCA för MaReCo har visat sig vara en stor uppgift. Det har inte funnits tid och/eller möjlighet att studera alla aspekter i detalj och vissa dataluckor i de ingående komponenternas livscykler har inte kunnat fyllas. Därför är det viktigt att än en gång påpeka att denna LCA främst bör ses som en vägledning i miljömässig utveckling av MaReCo, för att peka ut betydande *hot spots* och vara en grund för kommande studier av samma eller liknande system.

Det ingår och bildas potentiellt farliga metaller och kemikalier i de processer som är inkluderas i denna studie, de flesta i små mängder, men bland annat radon-222 bildas i betydande mängd vid solcellstillverkning. Därför skulle det vara intressant att också närmare studera den toxiska påverkan av produkten under dess livscykel. Detta har dock, på grund av studiens begränsningar i omfattning, inte kunnat göras.

Att aluminiumtillverkning ser ut att ha liten energianvändning beror på att mycket norsk vattenkraft används, vilket inte syns i energianvändning eller utsläpp av växthusgaser (GWP). Att koppar har större miljöpåverkan än aluminium beror till del på antagandet om mycket högre återvinningsgrad på aluminium. Resultat för aluminium beror dock mycket på vilken studie som används, och osäkerheten är mycket stor.

MaReCo har ungefär dubbelt så högt elutbyte per cellyta, relativt en cell som står rakt mot solen. Miljöpåverkan mellan de två systemen är jämförbara när de ger samma mängd el, men eftersom MaReCo dessutom ger tredubbla mängden värme (relativt el), så förefaller MaReCo ge mer nyttig energi för samma miljöpåverkan, och därmed vara ett bättre val ur energi- och miljösynpunkt.

Sammanfattningsvis är det tydligaste resultatet att komponentsystemet solceller ger störst miljöpåverkan i nästan alla kategorier och bevisligen har mycket stor påverkan på trågets totala miljöpåverkan. Det syns även tydligt att kopparrör har stor miljöpåverkan, men detta är troligen delvis på grund av låg återvinningsgrad. Aluminiumreceiver, betongstativ och glas har medelhög påverkan, medan stålreflektorn och sluthantering av tråget har mycket liten påverkan.

Tråget har en positiv energibalans, d v s det ger mer energi än det använder för framställning. Dock kommer det ta nästan 4 år innan det når "energinollpunkten".

MaReCo förefaller ha en miljömässig fördel gentemot vanliga plana PV-system.

8. Förbättringsanalys och rekommendationer

Den största miljöpåverkan på MaReCo-systemet har solcellerna, därför är det av stort intresse att bevaka möjligheter att minska på cellarean eller använda mindre resurskrävande celler. En möjlighet är att använda mer högkoncentrerande system, d v s minska cellytan och förändra reflektorkoncentrationen så att mer ljus infaller per cellarea. Detta arbete pågår redan, bland annat med solföljande system som *Solar8*. Andra lösningar är att cellindustrin satsar på miljön och gör energieffektivare tillverkning, samt att man påbörjar/ökar återanvändning och återvinning av celler. Trots allt är cellers miljövänlighet en faktor som blir allt viktigare för ökad användning.

Kopparrör är i flera fall den högsta eller näst högsta källan till den totala miljöpåverkan. Alternativ bör prövas men kan vara svåra att hitta. En bra lösning är att tillse hög återvinningsgrad av rören. Man kan även fundera över möjligheten att ha klenare dimensioner (större innerdiam.), om detta är tekniskt möjligt borde det även kunna vara ekonomiskt sunt. Hög återvinningsgrad uppskattas vara av stor betydelse även för glas, och har bevisligen stor påverkan på miljöpåverkan av aluminiumreceivern.

Betong är den tredje största utsläppsposten för systemet vad gäller GWP och EP. Man kan överväga att inte använda betongstativ för montering och istället ställa trågen på hustak och använda enbart stålfötter (så slipper man ockupera mer mark också).

10. Referenser

Referenser gäller även bilagorna.

10.1. Dokument, böcker mm

Baumann, H., Tillman, A.M.; 2004; "The Hitch Hiker's Guide to LCA"; *Studielitteratur;* Studentlitteratur, Lund.

Citherlet, S., Di Guglielmo, F., Gay, J-B.; 2000; "Window and advanced glazing systems life cycle assessment"; *LCA i artikelform*; Elsevier 32, sid 225-234

Du Pont; 2004-06-24; "SäkerhetsdaTabelllad enligt EU-Direktiv 2001/58/EG, PFA Film"; *SäkerhetsdaTabelllad*

Frankl, P., Corrado, A., Lombardelli, S.; jan 2004; "Photovoltaic (PV) Systems, Final Report"; *LCA*; ECLIPSE

Helgesson, A., Hedberg, J., Karlsson, B.; 2003-09-03; "Mareco för stora fält"; *Rapport inom FUD-program;* Vattenfall Utveckling AB.

IVL; 2001; "MiljöfakTabellok för bränslen"; *Main Report IVL report B1334A-2 and Technical Appendix IVL report B1334B-2*

Mörtstedt, S-E., Hellsten, G.; 2003; "Data och Diagram, Energi- och kemitekniska Tabelleller"; *Tabellellsamling*; Liber förlag; ISBN 91-47-00805-9

Näslund, M.; 2003; "Energigasteknik"; *Kurslitteratur*; LTH

Returpack; 2003; "Statistik för 2003"

Sjunnesson, Jeanette; 2005; "Life Cycle Assessment of Concrete"; *Examensarbete;* Avdelningen för Energi och Miljösystem, LTH

SkanAluminium, sept 2000, *EPD för Aluminium*

SSAB; 1999; ”Environmental specification for film-laminated steel sheet”; *miljödatablad;* SSAB tunnplåt (1)

SSAB; aug 2005; ”Dobel SOLAR”; *miljödatablad;* SSAB Tunnplåt (2)

Sunér, Maria; maj 1996; ”Life Cycle Assessment of Aluminium, Copper and Steel”; *examensarbete;* Chalmers Tekniska Högskola; ISSN 1400-9560

10.2. Personliga kontakter

Byström, Joakim; Logosol; 2005-10-15; *Mail*

Karlsson, Björn; LTH/Vattenfall; 2005-11-11; *Mail* (1)

Karlsson, Björn; LTH/Vattenfall; 2005-11-17; *Intervju* (2)

Larsson, Fredrik; SSAB; 2005-11-25; M*ail*

10.3. Internetreferenser

Map24, 2005-12-05, www.se.map24.com

Sunarc, 2005-10-20, www.sunarc.net

Appendix A - Transportberäkningar

Transportavstånd och fordonsval

Extra transportsträckor som inte finns med i tillverkningsdata behöver beräknas. För transporten av betong till slutanvändare är avståndet längre i vårt ”base case”, än vad som anges i LCA, och mellanskillnaden beräknas som en ny transportsträcka. Distanser hämtas från Map24[41]. Antar att lastbilar tar snabbaste vägen med normal motorvägsanvändning (ger samma resultat som maximal motorvägsanvändning). Beräknar endast tranporter för vikter •15 kg.

Resultaten från beräkningar av transport innan slutanvändning finns medräknade i LCI för tillverkning och presenteras inte separat utanför Appendix.

Andra tranporter (som ej ingår i LCA för produkten):

Transporterat gods	Fordon	Avst. (km)	(kg) per tråg
Betong (betongfabrik – Malmö) *	Medeltung lastbil, Euro 2	370-100**	200
Receiver (Sapa, Vetlanda – Malmö)	Medeltung lastbil, Euro 2	300	15
Koppar (Boliden - Malmö) (eg. måste koppar via rörtillv)	Tung lastbil, Euro 3	1400	28
Reflektor+gavlar (SSAB, Ronneby - Malmö)	Lätt lastbil, Euro 3	180	30

Tabell A.1. Transportsträckor före slutanvändning, transport •15 kg.

*Transportsträcka utöver det som presenteras i LCA
**Sträckan som beräknas utifrån i LCA är 100 km, i vårt ”base case” är sträckan 370 km.

Återvinning:

Transporterat gods	Fordon	Avst. (km)	(kg) per tråg
Tråg t. avfallsstation (Malmö–Bromölla)	Medeltung lastbil, Euro 2	130	279

Tabell A.2. Sträckor, fordon och lastvikter för transporter till återvinning/resthantering.

[41] Map24, 2005

Fordon miljödata

Lastbilstransport				
Fordonstyp	**Lätt**	**Medeltung**	**Tung**	
Miljöklass	Euro 3	Euro 2	Euro 3	
Nyttolast(max) / totalvikt	8.5/14	14/24	40/60	
	Totalt	*Totalt*	*Totalt*	
Energibehov	**kWh(LCI)/tkm**	**kWh(LCI)/tkm**	**kWh(LCI)/tkm**	
Energi - fossil	0,67	0,63	0,18	
	Totalt	*Totalt*	*Totalt*	
Emissioner till luft	**g(LCI)/ton·km**	**g(LCI)/ton·km**	**g(LCI)/ton·km**	
fossil CO_2	176	136	48	*(medel)*
NOx	1,1	1,2	0,30	*(medel)*
HC	0,16	0,12	0,043	*(medel)*
PM	0,019	0,019	0,0052	*(medel)*
CO	0,15	0,13	0,041	*(medel)*
SO_2	0,043	0,034	0,01	*(medel)*

Tabell A.3. LCI data för transport med olika lastbilstyper[42].

Resultat av transportberäkningar:

Resursförbrukning:

	Betong	**Rec**	**Koppar**	**Reflektor**	**Tråg slut**	
Energi - fossil	122	10.2	25	13.0	82	MJ
Utsläpp till atmosfär:						
fossil CO_2	7300	610	1880	950	4900	g
NOx	65	5.4	11.8	5.9	44	g
HC	6.5	0.54	1.69	0.86	4.3	g
PM	1.03	0.086	0.20	0.103	0.69	g
CO	7.0	0.59	1.61	0.81	4.72	g
SO_2	1.84	0.153	0.39	0.23	1.23	g

Tabell A.4. Miljöpåverkan för transporter.

[42] NTM, 2005

Appendix B - *Detaljerade LCI-data för komponenter*

Solceller

Resursförbrukning	**Förbr/FE (kg) alt (Nm3 där anges)**	***Utsläpp till mark***	**Utsläpp/FE (kg)**
Silver	0.0085	As	2.9 E-07
Aluminium	10.4	Cd	6.4 E-09
Bentonitlera	0.048	Cr	3.7 E-06
Krom	0.0029	Pb	3.7 E-06
Kol	51	Miner.oljor. ospec	0.00020
Koppar	0.034		
Råolja	9.0		
Grus	12.9		
Järn	0.69		
Brunkol	36		
Kalcit	0.41		
Mangan	0.00064		
Naturgas	27		
Nickel	0.0020		
Platinum	3.0 E-09		
Kisel (*Silicon*)	2.5		
Sn	1.4 E-05		
Uranium	0.0031		
Trä	0.37		
Zink	0.00022		

Utsläpp till luft	**Utsläpp/FE (kg) alt (kBq där anges)**	***Utsläpp till vatten***	**Utsläpp/FE (kg) alt (kBq där anges)**
Arsenik	6.0 E-06	NH_3	0.0031
Metan, tetrakloro-, CFC-10	3.1 E-05	Arsenik (aq)	0.00015
Kadmium	1.9 E-06	Barium (aq)	0.0064
Halog. kolväten, klorfluorkarboner	3.0 E-05	Kadmium (aq)	5.1 E-06
Metan, fossil	0.54	Klorid (aq)	0.024
CO_2, fossil	186	COD	0.0050
CO_2, biologisk	3.1	Cr (aq)	0.00074
Krom	1.0 E-05	Cu (aq)	0.000368843
Koppar	2.9 E-05	Kol-14 (aq)	0.16 kBq

Kol-14	1.9 kBq	Fe (aq)	0.076394369
Halog. kolväten, bromerade	1.9 E-06	Flourid	0.006027254
Halog. kolväten, klorväteflourkarboner	1.9 E-05	N (aq)	7.2 E-07
Väteflourid	0.47	*Sodium*	0.557935402
Mg	1.1 E-05	Ni	0.000367607
NH_3	0.0011	Miner.oljor. ospec	0.002750026
Ni	3.7 E-05	P (aq)	8.0 E-09
NMVOC	0.075	PAH	4.22114 E-05
Nox	0.39	Pb	0.000431383
PAH	5.4 E-06	Fenol	3.62515E-05
Partiklar	0.076	Phosphate	0.004775929
Pb	2.33E-05	Se (aq)	0.000371322
Radon-222	172000 kBq	Sulfate	0.747075176
Selenium	1.86E-05		5.43755E-06
SO2	0.768695	V (aq)	0.000390074
Vanadium	9.4E-05	Zn (aq)	0.000760566
Zn	7.25E-05		

Tabell B.1. Miljödata för solceller, vagga till grind.

Koppar(rör)

Energiförbrukning	**Förbrukning/ kg koppar (MJ)**		**Resursanvändning**	**Förbrukning/kg koppar (g)**
El (svensk medel~)	35.9		Vatten	6110
El (norsk medel~)	0.263		Cu	863
El (UCPTE)	$67.4 \cdot 10^{-3}$		Calcit	265
El (Fransk medel~)	$4.61 \cdot 10^{-3}$		Naturgas	71.3
Diesel	5.32		Bauxit	24.8
Gas	0.884		Råolja	10.2
Råolja	0.539		Kalksten	4.45
Brännolja (Eo1)	0.279		Na_2SO_4	2.80
Diesel (båt)	0.112		Sand	0.879
Kol	$15 \cdot 10^{-3}$		*Kalk*	0.153
			Portland soda	0.126
Utsläpp till atmosfär	**Utsläpp/kg koppar (g)**		*Solvey soda*	0.126
CO_2	601		Dolomit	0.107
SO_2	16.2		Feltspat	0.0796
NO_x	7.97			
CO	1.67		***Utsläpp till vatten***	**Utsläpp/kg koppar (mg)**
HC	1.16		NH_4NO_3	309
Partiklar	1.00		NO_3-N	232
CH_4	0.385		NH_4-N	207
NH_4NO_3	$84.3 \cdot 10^{-3}$		Tot-N	66.6
SO_x	$60.2 \cdot 10^{-3}$		Zn (aq)	20.1
NH_3	$50.0 \cdot 10^{-3}$		NaCl (aq)	13.3
Pb	$37.6 \cdot 10^{-3}$		As (aq)	7.78
Cu	$32.2 \cdot 10^{-3}$		Cu (aq)	6.87
N_2O	$25.8 \cdot 10^{-3}$		HNO_3 (aq)	4.23
Zn	$5.71 \cdot 10^{-3}$		Olja (aq)	2.48
As	$4.08 \cdot 10^{-3}$		NH_3 (aq)	2.20
Cd	$7.81 \cdot 10^{-3}$		Ni (aq)	9.73
Cl	$0.134 \cdot 10^{-3}$		COD	0.923
Hg	$39.2 \cdot 10^{-6}$		Pb (aq)	0.516
Flourider	$34.7 \cdot 10^{-6}$		Cd (aq)	0.350
Cr	$7.54 \cdot 10^{-6}$		Hg (aq)	0.195
Dioxin (TCDD-ekv)	$0.124 \cdot 10^{-6}$		Susp.	$71.0 \cdot 10^{-3}$
			Fenol	$34.8 \cdot 10^{-3}$

Tabellell B.2. LCI-data för kopparproduktion[43].

[43] Sunér, 1996

Aluminium (receiver)

Energiförbrukning	**Förbr/kg alum. (MJ)**		***Resursanvändning***	**Förbr/kg alum. (g)**
El (norsk medel~)	52.2		Bauxit	4920
El (UCPTE)	2.37		Kalksten	883
El (svensk medel~)	$9.74 \cdot 10^{-3}$		Råolja	519
El (kolkondens)	$4.14 \cdot 10^{-3}$		*Rocksand.*	74.2
El (Fransk medel~)	$5.26 \cdot 10^{-6}$		CaF_2	48.5
Diesel	0.282		Vatten	17.9
Bensin	$0.018 \cdot 10^{-3}$		Järnmalm	14.7
Naturgas	0.660		Kol	13.8
Blast Furnace Gas	0.012		Olivin	0.320
Propan	$0.2 \cdot 10^{-3}$		*Caliche*	0.303
Råolja	21.3		Naturgas	$81.4 \cdot 10^{-3}$
Brännolja (Eo1)	$8.37 \cdot 10^{-6}$		Legeringsmaterial	$65.4 \cdot 10^{-3}$
Brännolja (Eo5)	$0.777 \cdot 10^{-3}$		Bentonit	$50.4 \cdot 10^{-3}$
50 Diesel (båt)	9.12		Na_2SO_4	$3.20 \cdot 10^{-3}$
Kol	3.16		Sand	$1.00 \cdot 10^{-3}$
			Kalk	$0.175 \cdot 10^{-3}$
Utsläpp till atmosfär	**Utsläpp/kg alum. (g)**		*Solvey soda*	$0.143 \cdot 10^{-3}$
CO_2	4390		*Portland soda*	$0.143 \cdot 10^{-3}$
SO_2	24.1		Bolomit	$0.123 \cdot 10^{-3}$
NO_x	11.4		Feltspat	$90.8 \cdot 10^{-6}$
CO	1.7			
HC	1.63		**Utsläpp till vatten**	**Utsläpp/kg alum. (mg)**
Partiklar	28.3		COD	37.2
Tot-F	0.430		SO_2 (aq)	8.30
Tar	0.310		Tot-F (aq)	1.65
Radon-222 (kBq)	0.165		BOD	1.58
THC	0.115		Susp.	0.460
CH_4	0.113		Olja (aq)	$20.4 \cdot 10^{-3}$
TOC	$80 \cdot 10^{-3}$		TOT-N	$10.4 \cdot 10^{-3}$
PAH	$60.1 \cdot 10^{-3}$		SO_4^{2-} (aq)	$6.91 \cdot 10^{-3}$
Cl_2	$42.3 \cdot 10^{-3}$		Cl^- (aq)	$4.83 \cdot 10^{-3}$
SO_x	$6.41 \cdot 10^{-3}$		NH_4-N	$0.540 \cdot 10^{-3}$
N_2O	$1.63 \cdot 10^{-3}$		NH_4NO_3 (aq)	$0.352 \cdot 10^{-3}$
VOC	$1.20 \cdot 10^{-3}$		Fenol	$0.292 \cdot 10^{-3}$
Fe	$1.05 \cdot 10^{-3}$		NO_3-N	$0.275 \cdot 10^{-3}$
HF	$0.389 \cdot 10^{-3}$		Pb (aq)	$0.210 \cdot 10^{-3}$
HCl	$0.290 \cdot 10^{-3}$		Fe (aq)	$0.138 \cdot 10^{-3}$
Cd	$73.7 \cdot 10^{-9}$		Sr (aq)	$0.138 \cdot 10^{-3}$
Co	$46.1 \cdot 10^{-9}$		Mn (aq)	$26.3 \cdot 10^{-6}$
Hg	$0.577 \cdot 10^{-9}$		NaCl	$15.2 \cdot 10^{-6}$
NH_4NO_3	$96.3 \cdot 10^{-6}$		Al (aq)	$13.8 \cdot 10^{-6}$
NH_3	$71.0 \cdot 10^{-6}$		Tot-P	$8.54 \cdot 10^{-6}$
Zn	$28.9 \cdot 10^{-6}$		Tot-CN	$6.56 \cdot 10^{-6}$
Pb	$3.54 \cdot 10^{-6}$		HNO_3 (aq)	$4.84 \cdot 10^{-6}$
Cr	$3.34 \cdot 10^{-6}$		NO_2-N	$3.25 \cdot 10^{-6}$
Cu	$3.21 \cdot 10^{-6}$		NH_3 (aq)	$2.52 \cdot 10^{-6}$
V	$2.89 \cdot 10^{-6}$		Ni (aq)	$1.76 \cdot 10^{-6}$

As	$1.68 \cdot 10^{-6}$		Zn (aq)	$1.64 \cdot 10^{-6}$
Ni	$1.44 \cdot 10^{-6}$		Cu (aq)	$1.08 \cdot 10^{-6}$
Mn	$0.173 \cdot 10^{-6}$		Cr (aq)	$0.478 \cdot 10^{-6}$
			As (aq)	$61.5 \cdot 10^{-9}$
			Co (aq)	$22.5 \cdot 10^{-9}$
			Cd (aq)	$0.308 \cdot 10^{-9}$

Tabellell B.3. LCI-data för aluminiumproduktion, vagga till port[44].

Stålplåt (reflektorplåt)

Råmaterialförbr:	**Utsläpp/anv per kg prod Dobel**	**Utsläpp/anv per FE**
Järnmalm	2200 g*	66 kg *
Kol	580 g*	17.4 kg *
Kalksten	104 g*	3.12 kg *
Energiförbrukning		
LP-gas	1.66 MJ	49.8 MJ
Elektrisk energi	0.706 MJ	21.18 MJ
Energitillvaratagande		
Varmvatten	90 kJ	2.7 MJ
Utsläpp till atmosfär		
CO_2	120 g	3600 g
Total HC	0.3 g	9 g
NO_x	0.1 g	3 g
Utsläpp till vatten		
Fasta partiklar	1.1 mg	33 mg
Flourin	2.5 mg	75 mg
Metaller	0.4 mg	12 mg
Restprodukter		
Totalt	34 g	1020 g
av vilket återvinns	31 g	930 g
av vilket deponeras	3 g	90 g

Tabell B.4. LCI-data för stålplåtsproduktion[45,46].
* Beräknad användning med 80% jungfrulig råvara.

[44] Sunér, 1996

[45] SSAB, 1999 (1)

[46] Sunér, 1996

Nedan följer LCI för betongkomponenter:

Per prod av 1 kg:	**Cement**	**Makadam**	**Grus**	**Bindemedel**	**Per FE:**
Resurs-förbrukning:					
Kol (MJ)	1.9		$9.6 \cdot 10^{-5}$	1.7	**48**
Råolja (MJ)				3.2	**0.42**
Koks (MJ)	0.51				**12.9**
Diesel (MJ)	0.03	0.02			**2.1**
Olja (MJ)			$1.0 \cdot 10^{-3}$		**0.094**
Naturgas (MJ)			$2.2 \cdot 10^{-5}$	8.2	**1.06**
Torv (MJ)			$1.1 \cdot 10^{-5}$		**1.03** $\cdot 10^{-3}$
Biomassa (MJ)			$1.1 \cdot 10^{-4}$		**0.0103**
Bildäck (MJ)	0.42	0.03			**13**
Bone meal(MJ)	0.01				**0.25**
El (MJ)	0.48		$2.4 \cdot 10^{-3}$	2.9	**12.8**
Utsläpp till luft:					
CO2 (g)	710	1.6	70	690	**18 200**
CO (g)	$2.7 \cdot 10^{-3}$	$8.1 \cdot 10^{-4}$	$0.07 \cdot 10^{-3}$	2.1	**0.34**
NOx (g)	0.7	0.014	$0.60 \cdot 10^{-3}$	3.5	**18.2**
SOx (g)	0.09	$7.8 \cdot 10^{-4}$	$5.0 \cdot 10^{-5}$	6.6	**3.2**
CH4 (g)	2.6	$1.7 \cdot 10^{-3}$	$0.38 \cdot 10^{-6}$	1.2	**66**
HC (g)	$1.3 \cdot 10^{-3}$	$9.0 \cdot 10^{-4}$	$4.0 \cdot 10^{-5}$	2.2	**0.35**
Partiklar (g)	0,063	$2.9 \cdot 10^{-4}$			**1.60**
NH3 (g)	0,010	$7.1 \cdot 10^{-3}$			**0.71**
N2O (g)	$1.07 \cdot 10^{-4}$	$7.6 \cdot 10^{-5}$	$2.3 \cdot 10^{-6}$		**7.8** $\cdot 10^{-3}$
Metanol (g)				1.1	**0.14**
Bensen (g)				$2.6 \cdot 10^{-3}$	**3.4** $\cdot 10^{-4}$
Tungmetaller (g)				$2.6 \cdot 10^{-4}$	**3.4** $\cdot 10^{-6}$
Hg (g)				$1.0 \cdot 10^{-5}$	**1.3** $\cdot 10^{-6}$
Cd (g)				$9.1 \cdot 10^{-6}$	**1.18** $\cdot 10^{-6}$
Halon-1301 (g)				$8 \cdot 10^{-6}$	**1.04** $\cdot 10^{-6}$
Utsläpp till vatten:					
Olja (aq) (g)	$1.25 \cdot 10^{-4}$	$8.8 \cdot 10^{-5}$	$3.22 \cdot 10^{-7}$		**8.9** $\cdot 10^{-3}$
Fenol (aq) (g)	$1.67 \cdot 10^{-8}$		$4.59 \cdot 10^{-7}$		**4.35** $\cdot 10^{-5}$
Tot-N (g)	$9.51 \cdot 10^{-8}$	$1.23 \cdot 10^{-6}$	$1.53 \cdot 10^{-7}$		**9.58** $\cdot 10^{-5}$
Tot-P (g)		$1.76 \cdot 10^{-7}$			**1.13** $\cdot 10^{-5}$
COD (g)	$9.51 \cdot 10^{-9}$		$9.67 \cdot 10^{-7}$		**9.1** $\cdot 10^{-5}$
Formaldehyd (g)				0.09	**0.012**
Ni (aq) (g)				0.00028	**3.63** $\cdot 10^{-5}$
PAH (g)				0.000023	**2.98** $\cdot 10^{-6}$
Ba (g)				0.0088	**1.1** $\cdot 10^{-3}$

Tabell B.5. Resursåtgång och miljöutsläpp vid produktion av ingredienser till betong[47].

[47] Sjunnesson, 2005

Betongproduktion

	Per m^3 tillv. betong	Per FE
Olja (MJ)	15	1.29
El (MJ)	33	2.8
CO2 (g)	1500	129
CO (g)	0.86	0.074
NOx (g)	2.3	0.197
SOx (g)	3.3	0.28
CH4 (g)	1.7	0.146
HC (g)	0.32	0.027

Tabell B.6. Resursåtgång och miljöutsläpp vid produktion av 1 m^3 betong (exkl påverkan från ingredienser)[48].

[48] Sjunnesson, 2005

Appendix C - *Detaljerade data för slutbehandling/återvinning*

Resursförbrukning	**Resursförbrukn/ FE (kg) resp (Nm3)**	**Utsläpp till vatten**	**Utsläpp/FE (kg) resp (kQq där anges)**
Silver	1.7E-07	NH3	5.95076E-06
Aluminium	1.6E-05	Arsenik (aq)	6.25006E-09
Bentonitlera	2.1E-05	Barium (aq)	7.1675E-06
Krom	8.3E-07	Kadmium (aq)	5.79134E-09
Kol	0.00116	COD	1.05506E-05
Koppar	2.1E-06	Cr (aq)	4.4269E-08
Råolja	0.05545	Cu (aq)	1.53098E-08
Grus	0.00509	Kol-14 (aq)	0.000003285582 kBq
Järn	0.00041	Fe (aq)	3.19957E-06
Brunkol	0.00093	Flourid	3.77871E-07
Mangan	3.1E-07	*Sodium*	0.000934642
Naturgas	0.000154818 Nm3	Ni	1.77754E-08
Nickel	4.8E-07	PAH	3.62962E-08
Platinum	6.1E-12	Pb	2.20759E-08
Sn	9.7E-08	Fenol	3.44613E-07
Uranium	6.4E-08	Phosphate	1.51951E-07
Zink	8.1E-08	Se (aq)	1.17547E-08
		Sulfate	0.000071675
		V (aq)	1.20414E-08
		Zn (aq)	9.63312E-08
Utsläpp till atmosfär	**Utsläpp/FE (kg) resp (kQq där anges)**	***Utsläpp till mark***	**Utsläpp/FE (kg)**
Arsenik	2E-09	As	1.27868E-09
Metan, tetrakloro-, CFC-10	3.7E-11	Cd	5.90602E-11
Kadmium	2.3E-09	Cr	1.59405E-08
Halogenerade kolväten, klorfluorkarboner	2.3E-09	Pb	1.59405E-08
Metan, fossil	0.00022	Miner.oljor. ospec	2.39108E-06
CO2, fossil	0.19152		
Krom	1.9E-09		
Koppar	1.5E-08		
Kol-14	0.00003962194 kBq		
Halogenerade kolväten, bromerade	2.1E-08		

Halogenerade kolväten, klorväteflourkarboner	1.1E-08
Väteflourid	8.7E-08
Mg	3.8E-10
NH3	1.5E-08
Ni	5.8E-08
NMVOC	0.00042
Nox	0.00314
PAH	5.6E-10
Partiklar	6E-05
Pb	1.5E-08
Radon-222	3.5244031 kBq
Selenium	2.4E-09
SO2	0.00014
Vanadium	2E-07
Zink	1E-07

Tabell C.1. Miljödata för sluthantering av solceller

Aluminium

Data för återvinning av aluminium.

Energianvändning	**Användn./kg alum. (MJ)**		***Resursförbrukning***	**Förbr/kg alum. (g)**
El (svensk medel~)	0.904		Cybernit	164
El (Tysk medel~)	0.049		Vatten	1.73
Brännolja (Eo1)	4.92		NaCl	0.970
Diesel	0.50		sandsten	$15.2 \cdot 10^{-3}$
Naturgas	0.00395		Järnmalm	$5.51 \cdot 10^{-4}$
Propan	0.102		Sand	$1.82 \cdot 10^{-4}$
Råolja	0.00108			
Utsläpp till atmosfär	**Utsläpp/kg alum. (g)**		***Utsläpp till vatten***	**Utsläpp/kg alum. (g)**
CO_2	464		*Sludge*	26.9
SO_2	1.01		Saltavfall	253
NO_x	0.708		Avfall	32.6
CO	0.156		Avfall (industriellt)	$9.08 \cdot 10^{-4}$
HC	0.153		Avfall (mineraler)	0.0618
Partiklar	0.265		Avfall (slagg&aska)	0.0114
Smuts/damm	3.09		Avfall (inerta kemikalier)	0.0106
CH_4	0.0192		Avfall (reglerade kemik.)	$1.8 \cdot 10^{-5}$
SO_x	0.013			
N_2O	0.00228			
Metaller	$1.82 \cdot 10^{-6}$			

Tabell C.2. Data för återvinning av aluminium från skrot[49].

[49] Sunér, 1996